

1970

Polarization reversal in "Ferrielectric" bismuth titanate

James Edward Lucas
Iowa State University

Follow this and additional works at: <https://lib.dr.iastate.edu/rtd>

 Part of the [Electrical and Electronics Commons](#)

Recommended Citation

Lucas, James Edward, "Polarization reversal in "Ferrielectric" bismuth titanate " (1970). *Retrospective Theses and Dissertations*. 4245.
<https://lib.dr.iastate.edu/rtd/4245>

This Dissertation is brought to you for free and open access by the Iowa State University Capstones, Theses and Dissertations at Iowa State University Digital Repository. It has been accepted for inclusion in Retrospective Theses and Dissertations by an authorized administrator of Iowa State University Digital Repository. For more information, please contact digirep@iastate.edu.

70-25,802

LUCAS, James Edward, 1938-
POLARIZATION REVERSAL IN "FERRIELECTRIC"
BISMUTH TITANATE.

Iowa State University, Ph.D., 1970
Engineering, electrical

University Microfilms, A XEROX Company, Ann Arbor, Michigan

**POLARIZATION REVERSAL IN "FERRIELECTRIC"
BISMUTH TITANATE**

by

James Edward Lucas

**A Dissertation Submitted to the
Graduate Faculty in Partial Fulfillment of
The Requirements for the Degree of
DOCTOR OF PHILOSOPHY**

Major Subject: Electrical Engineering

Approved:

Signature was redacted for privacy.

In Charge of Major Work

Signature was redacted for privacy.

Head of Major Department

Signature was redacted for privacy.

Dean of Graduate College

**Iowa State University
Ames, Iowa**

1970

TABLE OF CONTENTS

	Page
INTRODUCTION	1
FERROELECTRICITY	3
FERRIELECTRICITY	8
PURPOSE OF INVESTIGATION	22
INVESTIGATION OF SWITCHING TRANSIENTS OF MBO CRYSTALS	23
INVESTIGATION OF THE THRESHOLD FIELD EFFECT IN $\text{Bi}_4\text{Ti}_3\text{O}_{12}$ SINGLE CRYSTALS	34
INTERNAL FIELD SOURCE INVESTIGATION	83
DOMAIN DYNAMICS	95
COMMENTS	117
BIBLIOGRAPHY	118
ACKNOWLEDGMENTS	122
APPENDIX A: GROWTH TECHNIQUES FOR BISMUTH TITANATE SINGLE CRYSTALS	123
APPENDIX B: HYSTERESIS LOOP ANALYSIS OF FERROELECTRICS	136

INTRODUCTION

Materials possessing hysteresis loop characteristics have potential application as memory elements. Remanent capabilities allow storage of " 1 " and " 0 " information. For example, the B-H loop characteristic of a magnetic material and its remanent magnetization feature make it useful for memory application.

In recent years there has been a widespread search for additional materials possessing hysteresis loop characteristics with remanence capabilities, and this search has prompted investigators to consider the possible use of ferroelectric crystals as storage or memory devices. Ferroelectric crystals exhibit a hysteresis loop (polarization P versus applied field E), and they possess a spontaneous polarization feature so that storage of " 1 " and " 0 " information is possible. However, there is one very serious limitation to the use of ferroelectric crystals as memory elements. Fields much smaller than the coercive field as determined from the hysteresis loop are capable of switching the crystal if one waits a sufficient period of time. This property is described by saying that ferroelectrics do not possess a true coercive field feature. This means that there is no threshold field for the switching of a ferroelectric crystal.

For applications in memory devices it is desirable to have a ferroelectric which possesses a true coercive field so that switching will not occur for fields below this value regardless of the time of application of the field, but switching will occur for values above this

coercive field. Recently it has been reported that a new class of materials possesses a feature of this nature. These materials have been classified as "ferrielectrics". These are really ferroelectrics which possess a threshold switching field and are given the classification "ferrielectrics" through an analogy with ferrimagnetics.

This investigation will be concerned with the subject of polarization reversal in these "ferrielectrics". Since these materials are ferroelectric in nature, it would be advantageous at this point to present a general discussion of ferroelectrics and of polarization reversal in this class of materials, and then to present similar information concerning polarization reversal in this new class of materials. The actual goals of this investigation will be outlined after the presentation of this essential introductory material.

FERROELECTRICITY

General Comments On Ferroelectricity

Until 1950, only three ferroelectric materials had been investigated in any great detail. These were Rochelle salt, potassium dihydrogen phosphate, and barium titanate. Since this time, investigators have examined numerous other ferroelectric materials in search of characteristics that might lead to potential device applications for the materials. As a result of this increased interest in ferroelectrics, the extant literature on the subject is extensive. References (1-8) are general texts that treat the subject comprehensively. For a more current treatment referring to state-of-the-art, fabrication technique, and applications, references (9-11) are useful. For the purpose of this thesis it will suffice to focus attention upon the process of polarization reversal which is treated in some detail in the next section.

Polarization Reversal In Ferroelectrics

The process of polarization by means of an externally applied electric field is one of the primary concerns in any investigation of a ferroelectric material. Both optical and electrical techniques are used to study the reversal of polarization in ferroelectrics. Optical techniques¹ relate to the direct observation of the motion of domain

¹Optical techniques can only be used with ferroelectrics with visible domains. Also, a study of high speed switching is not practical with optical techniques.

walls during polarization reversal. Electrical techniques² relate to the measurement of switching transients that result when polarization is reversed.

Switching transients that result from electrical techniques of study are of interest in this investigation. The conventional technique utilized in a switching transient study is discussed in articles by Merz (12) and Fatuzzo and Merz (13). Generally a small resistance is placed in series with the crystal to be tested. Then the combination is pulsed with an electrical pulse of one polarity so as to align the dipoles in one direction, and then a second pulse of the opposite polarity is applied. The change in polarization with time, or the switching current, is measured with the aid of an oscilloscope connected across the series resistance.

A sketch of a typical current waveform resulting from reversal of polarization by a square pulse is shown in Figure 1. The initial peak is simply the transient current connected with the charging of the ferroelectric capacitor. Two of the most important parameters resulting from a transient study are (a) i_m , the maximum current achieved and (b) t_s , the time it takes to switch the crystal. The switching time is defined as the time required for the current to drop to $.05 i_m$. The variables, i_m and t_s , are functions of the geometry of the crystal, its

²High speed switching can be studied with electrical techniques for almost all ferroelectric materials. Results of electrical techniques of study do though require a great deal of interpretation.

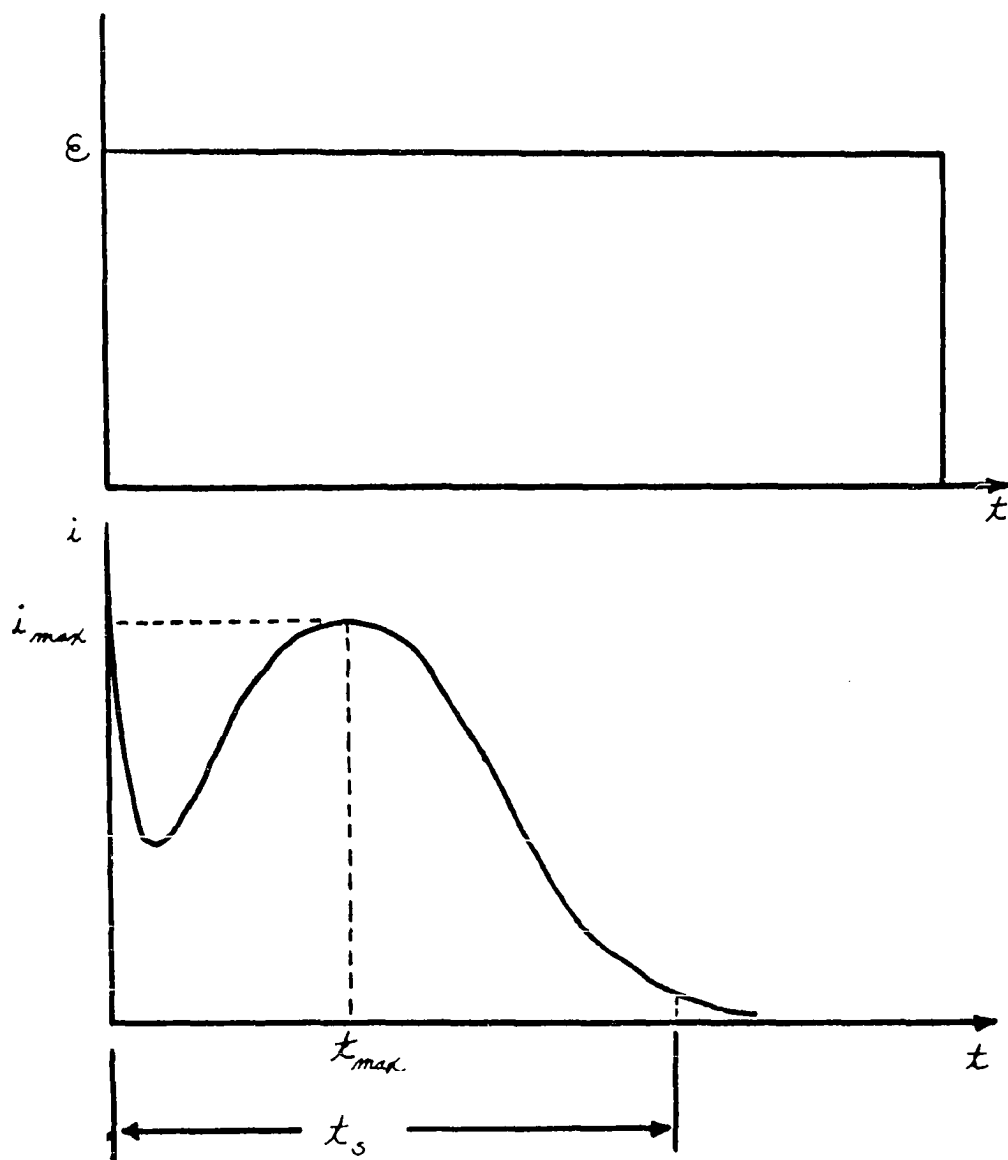


Figure 1. Applied field and sketch of a typical current transient resulting from polarization reversal in a ferroelectric crystal.

past history, the temperature, and the switching field. Experimentally it has been found that the maximum switching current, i_m , for a given crystal at a fixed temperature increases with an increasing applied field. The results that are often reported concerning a switching transient study of a ferroelectric generally include a plot of the maximum current and the switching time as a function of the applied switching field.

For low applied fields, an exponential variation of maximum current with applied field has been noted. To date, ferroelectric research has revealed that polarization reversal under the condition of low fields follows an exponential law, i.e.

$$i_{\max} \propto e^{-\alpha/\mathcal{E}} \quad (1)$$

where

i_m = peak current during switching,

α = nucleation constant,

\mathcal{E} = applied field.

Jona and Shirane (10) state that this exponential variation has been validated for numerous ferroelectrics under the condition of a low externally applied field. Research on the ferroelectric colemanite drew Wieder (14, 15) to postulate a variation of the form

$$i_{\max} \propto \frac{\mathcal{E}}{\alpha} e^{-\alpha/\mathcal{E}} \quad (2)$$

Pulvari (16) stated that this type of variation applies generally for any ferroelectric. Regardless of the exact form of the equation, the most significant point to be made is that polarization reversal varies exponentially with the applied field for low values of field. This indicates that switching occurs immediately upon the application of an externally applied electric field.

Summary

In ordinary ferroelectrics, the reversal of polarization at low fields varies exponentially with applied field. Because of this dependence, it can be concluded that ordinary ferroelectrics do not possess a threshold field feature, i.e. ordinary ferroelectrics do not exhibit a true coercive force. The coercive force is in fact field dependent, and is not a material constant.

To date, it has been accepted that no ordinary ferroelectric possesses a true threshold field that must be overcome before reversal can occur. The question then arises as to whether it would be possible to find or develop a material that would possess this feature of a true threshold field. This then leads to the introduction of the new class of materials that reportedly exhibit the previously mentioned feature.

FERRIELECTRICITY

Literature Survey Of The Ferrielectric $\text{Na}(\text{Nb}_{1-x}\text{V}_x)\text{O}_3$

In 1960 Pulvari (17) reported a study of the characteristics of mixed crystals of sodium-vanadate-niobate. For the $\text{Na}(\text{Nb}_{1-x}\text{V}_x)\text{O}_3$ crystals he found the onset of the ferroelectric state to be a function of the applied electric field. Pulvari assumed this phenomenon to be the result of a strong transverse dipole-dipole interaction in this material which was composed of two antiferroelectrics with unequal dipoles. This phenomenon is not present in ordinary ferroelectrics since they possess a weak dipole-dipole interaction perpendicular to the polarization. In his investigation of the switching characteristics of this material he observed two important items which are listed below:

- a) Tested samples indicated that the opening of a hysteresis loop required a higher field than the coercive field measured on the hysteresis loop.
- b) Switching transients did not appear continuously with increasing field as is the case with ordinary ferroelectrics. Transients appeared when the applied field exceed a certain threshold level. In general this threshold field was higher in magnitude than the coercive field determined from loop measurements.

Because of the analogy with ferrimagnetic materials, Pulvari suggested that this new group of materials with ferroelectric properties be named "ferrielectrics". The term ferrielectric has also been

used by Cross (18), Kanzig (19) and Goldsmith and White (20). Cross used it to denote a particular phase of ferroelectric and anti-ferroelectric mixed crystals; Kanzig used it to describe crystals that exhibit ferroelectric properties along one axis and anti-ferroelectric properties along another axis; Goldsmith and White used the term to describe an uncompensated anti-dipole structure which they found in thiourea.

Miller, et al. (21) also investigated the $\text{Na}(\text{Nb}_{1-x}\text{V}_x)\text{O}_3$ system and its "ferrielectric" properties. They did find on occasion a threshold field effect in the vanadium-doped material. However, their experimental data indicated no evidence of a "ferrielectric" structure (that is, an unbalanced antidipole configuration), as was reported by Pulvari. The general use of the term "ferrielectricity" is obviously a controversial point. However, Shuvalov and Sonin (22) commenting on this issue, indicated the use of the term "ferrielectricity" to describe this situation was much to be preferred just for the sake of brevity. Henceforth, the use of the term "ferrielectricity" in this discussion will correspond to the suggested title by Pulvari which was proposed on the basis of an analogy to ferrimagnetics.

From a practical standpoint there was one major limitation associated with the previously described material and other similar materials. The limiting factor in this situation was the magnitude of applied field required to initiate switching. A typical value of threshold field was indicated by Pulvari (16) to be 10 KV/cm. For an extensive description of the "ferrielectric" phenomenon in sodium-vanadate-niobate reference is made to the article by Pulvari (23).

Literature Survey Of The Ferrielectric $\text{Bi}_4\text{Ti}_3\text{O}_{12}$

Since the discovery of "ferrielectric" properties in sodium-vanadate-niobate, many investigators have searched for materials similar in structure which might also possess similar properties, but which would exhibit a lower threshold field. This would make them more attractive for practical applications. Because of a similarity in structure, a family of so called "multilayer interstitial compounds" of the general formula,



have been investigated in great detail. The compound with bismuth as the A element and titanium as the B element with a value of $x = 3$ becomes



or more commonly,



This compound is referred to as a Mixed Bismuth Oxide or MBO and its chemical title is bismuth titanate.

In the interest of clarity and brevity, pertinent literature related to this specific compound and the discovery of its "ferrielectric" prop-

erties will be presented in outline form.³ Therefore, the major contributions of each author are listed in chronological order as follows:

1958 Aurivillius (24) determined the basic crystal structure of $\text{Bi}_4\text{Ti}_3\text{O}_{12}$. According to Aurivillius, the structure is comprised of a stacking of Bi_2O_2 and perovskite-like $\text{Bi}_2\text{Ti}_3\text{O}_{10}$ layers along a pseudotetragonal c axis.

1961 Subbarao (25) established $\text{Bi}_4\text{Ti}_3\text{O}_{12}$ as a ferroelectric on the basis of dielectric studies on poly-crystalline specimens. He established that the Curie temperature of the material was 675°C and that at room temperature the symmetry is orthorhombic. He suggested that the polar axis was probably the orthorhombic b.

Van Uitert and Egerton (26) reported on the ferroelectric properties of single crystals of $\text{Bi}_4\text{Ti}_3\text{O}_{12}$. A growing technique for single crystals was presented. (For a description of this technique, reference is made to

³In reading through these references, the reader will find that various authors have referred to the structure of bismuth titanate as "pseudotetragonal", orthorhombic, tetragonal, and monoclinic. This situation is due to a lack of precision in terminology that is regrettably wide spread in this field. The actual structure of bismuth titanate is monoclinic m, but the tilt of the monoclinic axis is so slight, that it is almost orthorhombic. Further, the difference between the a and b dimensions is so slight that it is almost tetragonal. To add to the confusion, it really is tetragonal above the Curie temperature. Finally, a multi-domain crystal below the Curie temperature can exhibit macroscopic properties that are consistent with tetragonal symmetry.

Appendix A). Measurements were made on various electrical properties such as the d-c resistivity, the dielectric constant at a frequency of 1000 hertz, and the loss tangent at a frequency of 1000 hertz. Asymmetric hysteresis loops were noted, but the loops became more symmetrical after long cycling. A saturation polarization of $P_s = 3.5 \mu$ coulombs/cm² was established. The Curie temperature was noted to be 643°C.

1962 Fang and Fatuzzo (27) reported on the switching properties in ferroelectrics of the family $\text{Bi}_4\text{Ba}_{m-2}\text{Ti}_{m+1}\text{O}_{3(m+2)}$. For this new class of ferroelectrics, the crystal structure was described as being made up of perovskite layers consisting of doubly negatively charged $\text{Bi}_2\text{Ba}_{m-2}\text{Ti}_{m+1}\text{O}_{3m+4}$ interrupted by one layer of $\text{Bi}_2\text{O}_2^{2+}$ along the c axis. The ferroelectric axis was reported to be the c axis. Switching time measurements were made for various applied fields. For fields above 6KV/cm the switching time was found to be given by

$$t_s = .4 \times 10^{-6} \exp\left(\frac{41 \text{ KV/cm}}{E}\right). \quad (6)$$

For decreasing fields it was noticed that t_s approached infinity quite rapidly. The authors attributed this either to poor samples or to a distinctive coercive field for the onset of ferroelectricity.

Fang, Robbins, and Aurivillius (28) reported the compound $\text{Bi}_4\text{Ti}_3\text{O}_{12}$ to be ferroelectric. Hysteresis loops were observed for both polycrystalline ceramics and single crystals. Through x-ray studies, the polar axis was established to be the orthorhombic c axis. The authors did not rule out that the b axis might also be a polar axis as was reported by Subbarao (25). The authors noted a dielectric maximum occurred at 675°C for increasing temperature and at 670°C for decreasing temperature.

1963 McDonnell (29) for a dissertation performed a very detailed study of the domain dynamics and the threshold switching field phenomena for $\text{Bi}_4\text{Ti}_3\text{O}_{12}$. He discussed the general properties of a ferroelectric, and he examined two materials which fit this description - namely $\text{Na}(\text{Nb}_{1-x}\text{V}_x)\text{O}_3$ and $\text{Bi}_4\text{Ti}_3\text{O}_{12}$. A detailed discussion was given on the optical properties, the dielectric constant, the conductivity, and the electrical characteristics of $\text{Bi}_4\text{Ti}_3\text{O}_{12}$ ferroelectric. Switching characteristics were analyzed and the threshold field effect was examined. Domain dynamic studies were performed through direct observation of the domains and through measurement of switching transients and electrical properties.

1964 Pulvari (30) discussed the basic properties of ferroelectrics and examined specifically the characteristics of $\text{Bi}_4\text{Ti}_3\text{O}_{12}$. The utilization of this ferroelectric material in a

Transpolarizer⁴ application was discussed and analyzed. Other possible applications utilizing the unique storage, switching, and control properties of the Transpolarizer were examined with special emphasis on use as adaptive control devices involving pattern recognition and/or learning.

Tambovtsev, Skorikov, and Zheludev (31) described a method of production of $\text{Bi}_4\text{Ti}_3\text{O}_{12}$ single crystals. (For a description of this technique, reference is made to Appendix A.) The temperature dependence of the spontaneous polarization, the coercive field, the coefficient of non-linearity, and resistivity of this material were studied. The dependence of the maximum reversal switching as a function of applied electric field was examined.

Pulvari (32) reported on mixed bismuth oxide on MBO type ferroelectrics and their switching characteristics. For the mixed bismuth oxide $\text{Bi}_4\text{Ti}_3\text{O}_{12}$ he reported that it possessed ferroelectric properties in one direction and anti-ferroelectric properties in a perpendicular direction.

⁴C. F. Pulvari - U. S. Patent No. 2884617, September 1953. The Transpolarizer is an electrostatically controlled circuit impedance with stored settings. Through polarization control, it is possible to use this device for storing and gating electrical signals or to use it as a controlling circuit impedance.

He described a modified flux technique utilized in growing single crystals of $\text{Bi}_4\text{Ti}_3\text{O}_{12}$. (For a description of this technique, reference is made to Appendix A.)

Cummins (33) reported on the effect of constant d-c fields on the hysteresis loops of ferroelectric $\text{Bi}_4\text{Ti}_3\text{O}_{12}$ single crystals. He found that reverse bias fields applied to poled samples for a period of time caused a reduction in the hysteresis loop height and that if high d-c fields were applied for a sufficiently long period of time in the proper direction that there was a change in the field axis bias. He noted that bias to be stable in its new state, and he observed that after bias modification occurred that the hysteresis loops suffered a loss of squareness. He presented several possible explanations in order to account for the reduction in loop height which corresponds to a reduction in polarization.

1965 Cummins (34) studied the switching behavior of single crystal ferroelectric $\text{Bi}_4\text{Ti}_3\text{O}_{12}$ at room temperature for various ranges of applied fields. His finds are outlined below:

- a) For fields between 4 KV/cm and 14 KV/cm
the switching time was found to be

$$t_s = 1.32 \times 10^{-3} \exp \left(\frac{61.6 \text{ KV/cm}}{E} \right) \quad (7)$$

- b) For fields between 3 KV/cm and 4 KV/cm only partial switching occurred.
- c) For fields below 3 KV/cm switching did not occur.

The low field behavior was established through use of S curves.⁵ These curves converged upon a threshold level of 3 KV/cm. He explained the threshold field effect in this material in terms of a rapidly changing internal bias field. Relaxation times ranging from 5×10^{-3} seconds to several minutes were noted for the bias field effect.

1966 Pulvari and de la Paz (35) presented a phenomenological theory of polarization reversal in ferroelectric single crystals. The format was much like the work presented by Pulvari and Kuebler (36) on BaTiO_3 single crystals. A mathematical description of polarization reversal was developed. This work related the switching current, the switching field E , and the time of switching in an expression of the form $i = f(E, t)$. Derivation of the switching current i , switching time t_s , switching resistance R_s , and the polarization P at a given tem-

⁵The fraction of polarization which is reversed from an initially saturated state is measured as a function of pulse amplitude for a constant pulse width. The measurement is repeated for a number of pulse widths thus producing S shaped curves much like those used in characterizing magnetic materials.

perature was accomplished through the equation that described the time rate of change in current. The existence of a threshold field was experimentally verified.

Cummins (37) described a technique utilized in observing ferroelectric domains in $\text{Bi}_4\text{Ti}_3\text{O}_{12}$. He applied electric fields to test crystals through transparent liquid electrodes, and he observed the domain patterns through a polarizing microscope with crossed polarizer and analyzer.

1967 Cummins and Cross (38) found the symmetry of $\text{Bi}_4\text{Ti}_3\text{O}_{12}$ to be monoclinic point group m . From their investigation they found the spontaneous polarization to be in the monoclinic a - c plane at an angle of approximately 7° with respect to the major crystal surface. The magnitude of the polarization was estimated to be greater than $30 \mu\text{c}/\text{cm}^2$. They found switching to occur through a unique change in the monoclinic tilt resulting in a change of sign of polarization in the c direction but with no change of sign of polarization in the b direction. The authors concluded that the complex domain structure and the twinning in the crystals were the result of the four possible spontaneous polarization directions present in the virgin crystals. The authors reporting on switching

along the b axis found a high coercive force of 50 KV/cm at a frequency of 60 hertz.

Cummins (39) discussed the possible use of $\text{Bi}_4\text{Ti}_3\text{O}_{12}$ single crystals as memory cell elements which could be read optically. He utilized the unique switching properties of $\text{Bi}_4\text{Ti}_3\text{O}_{12}$ a rocking of the polarization through approximately 10° - and the subsequent large difference in extinction directions between opposite domains as the basis of operation for a continuously read non-destructive memory cell.

Cummins (40) utilized the switching and optical properties of $\text{Bi}_4\text{Ti}_3\text{O}_{12}$ single crystals described in the previous paragraph as the basis of operation of a bi-stable light gate. He discussed the possible use of this method of electrical gating of a light beam as the basic principle of operation of such devices as display systems, optical modulators, and optical computer logic gates.

Hamilton (41) utilized a novel x-ray technique to determine if a true threshold field exists in $\text{Bi}_4\text{Ti}_3\text{O}_{12}$. By detection of small changes in the Bragg diffraction angle of a diffracted x-ray beam, he was able to show the existence of a true threshold field. He established the polarization threshold level to be 3 KV/cm.

1968 Cummins and Cross (42) presented an extension of the work on $\text{Bi}_4\text{Ti}_3\text{O}_{12}$ which was discussed under Cummins and Cross (38). This presentation was much more detailed, and it reiterated many of the points made in the earlier article. There was one significant change reported by the authors. They found the polarization at room temperature to be $50 \pm 10 \mu\text{c}/\text{cm}^2$ and the polarization to be in the monoclinic a-c plane at an angle of less than 5° from the plane of the crystal. At room temperature the spontaneous polarization along the c axis was reported to be $4\mu\text{c}/\text{cm}^2$.

Cross and Pohanka (43) derived a simple elastic Gibbs function for ferroelectric crystals with point group symmetry $4/\text{mmm}$ in the paraelectric phase. Expressions for the polarization, dielectric constant, and free energy in the seven possible ferroelectric states were derived. The optical data of Cummins and Cross (38) was used in determining the absolute orientation and the temperature dependence of the spontaneous polarization. At room temperature the components were given as $P_x = 50/\sqrt{2} \mu\text{c}/\text{cm}^2$ and $P_z = 4 \mu\text{c}/\text{cm}^2$. P_z showed a slight decrease with increasing temperature while the decrease in P_x was much more significant.

Summary of $\text{Bi}_4\text{Ti}_3\text{O}_{12}$ Characteristics

In the previous section, the research contributions of several of the investigators of the $\text{Bi}_4\text{Ti}_3\text{O}_{12}$ system, were outlined and presented in their chronological order of appearance in the literature. Considering their reported finds, this author has summarized the most important features of the $\text{Bi}_4\text{Ti}_3\text{O}_{12}$ system below:

- a) $\text{Bi}_4\text{Ti}_3\text{O}_{12}$ or bismuth titanate is definitely a ferroelectric.
- b) The Curie temperature for this material is 675°C which is unusually high for a ferroelectric.
- c) The crystal structure (along the c axis) consists of a stacking of two perovskite - like $\text{Bi}_2\text{Ti}_3\text{O}_{10}$ layers interrupted by one layer of Bi_2O_2 .
- d) The symmetry is monoclinic point group m - an allowed derivative of the point symmetry of the paraelectric phase $4/mmm$. At room temperature $\text{Bi}_4\text{Ti}_3\text{O}_{12}$ corresponds to a classification of $F4/mmm(4)AZ$ - one of the five possible ferroelectric species which according to Aizu (44) may be derived from the paraelectric symmetry $4/mmm$.
- e) The main polarization, P_s lies in the monoclinic a-c plane at a slight angle. The best estimates of the components of P_s at room temperature are $P_z = 4 \mu\text{c}/\text{cm}^2$ and $P_x = 50/\sqrt{2} \mu\text{c}/\text{cm}^2$. (There are four possible spontaneous polarization directions in the virgin crystal.)
- f) The components of the polarization, P_s , are temperature

dependent. Both P_z and P_x decrease with increasing temperature; the P_x component exhibits a large change while the P_z component decreases just slightly. (The P_z component corresponds to the saturation polarization which Pulvari and de la Paz (35) and McDonnell (29) reported as being temperature independent.

- g) Switching for fields along the c axis occurs through an unusual "rocking" of the polarization vector P_s through a small angle. This switching behavior requires a change in the monoclinic tilt.
- h) There is a threshold field for the onset of ferroelectricity, and the best value reported is 3 KV/cm. Above this threshold, the switching follows an exponential dependence with an extremely large nucleation constant α . (Two reported values for this constant were 41 KV/cm and 61.6 KV/cm).
- i) D. C. fields applied for long periods of time in the reverse direction to previously poled $\text{Bi}_4\text{Ti}_3\text{O}_{12}$ samples can modify the internal bias as well as the reversible polarization.

PURPOSE OF INVESTIGATION

The ultimate goal from an engineering standpoint is to utilize any attractive features that a material might possess in some practical device application. For example, in the case of $\text{Bi}_4\text{Ti}_3\text{O}_{12}$ two attractive features are (a) the unusual electrical property of a threshold switching field, and (b) the unique optical property of extinction that occurs on polarization reversal. In the previous chapter, mention was made of these features in connection with application of this material in various devices.

However, successful device application depends to a large extent on a thorough understanding of the basic properties of the ferroelectric. Although a considerable amount of research has already been conducted on $\text{Bi}_4\text{Ti}_3\text{O}_{12}$, a number of yet unanswered questions concerning the material properties still remain. Therefore the purpose of this investigation is to make a contribution which might add to the understanding of the basic properties. To achieve this purpose, this author intends in the following chapters to (a) perform an original investigation of polarization reversal in this material, (b) examine in detail the threshold field phenomenon, (c) determine any limitations that might hamper device applications and (d) examine the mechanism associated with polarization reversal.

INVESTIGATION OF SWITCHING TRANSIENTS OF MBO CRYSTALS

Test Equipment

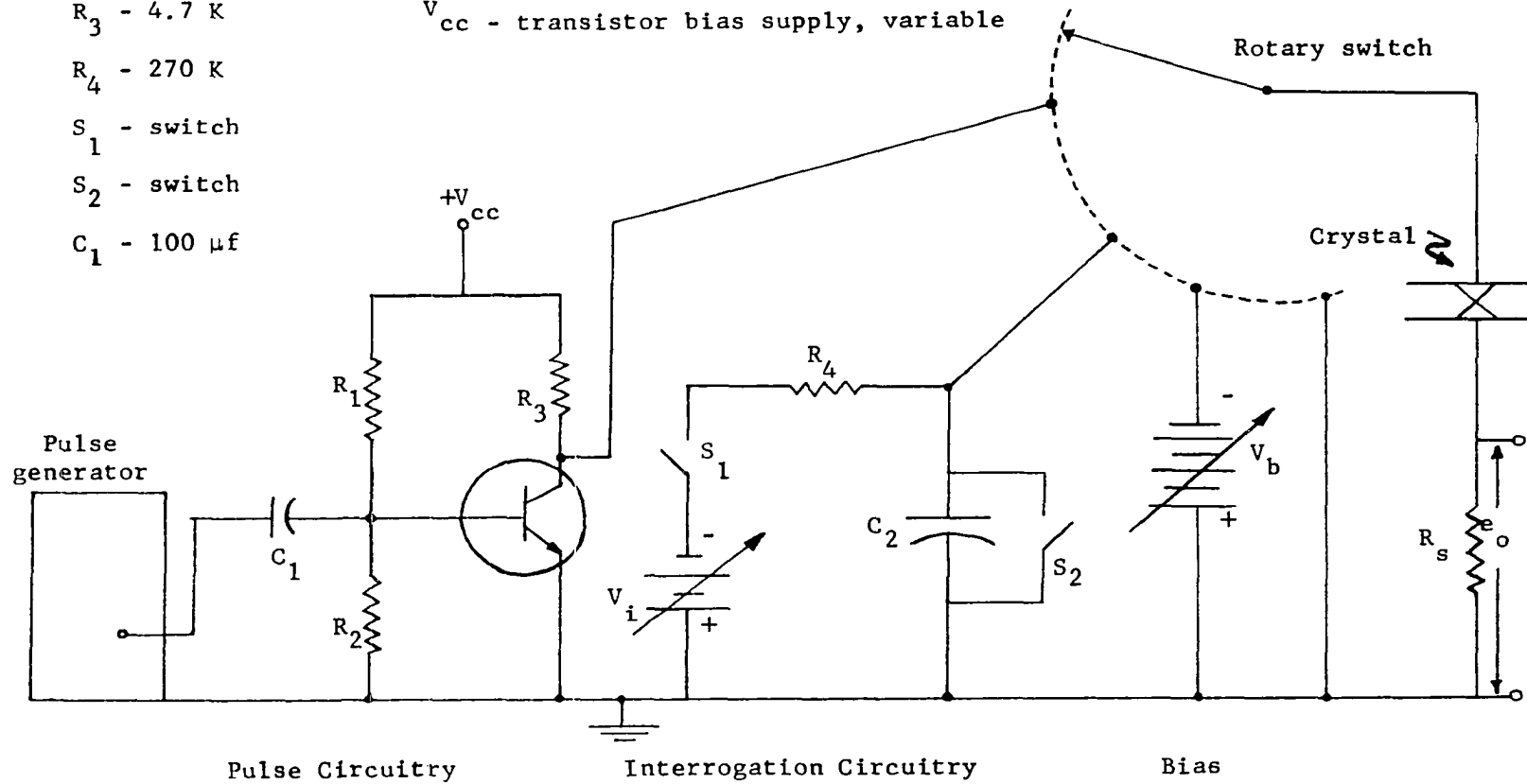
The test equipment developed by this author for the purpose of examining the polarization reversal in these MBO crystals utilizes a switching arrangement that allows the application of three separate types of voltages to the crystals under test. The schematic of this arrangement is shown in Figure 2. A description of these voltages and their waveforms is given below:

- a) There is a rapid rise time, positive pulse available for setting the polarization of the crystal. This pulse is obtained from a simple transistor switch which is driven by a single pulse from a Rutherford B2 pulse generator. The transistor switch was included in order to adjust pulse level. This output level can be adjusted by changing the bias on the switch. Pulse duration can be varied through controls on the pulse generator.
- b) There is a slow rise time, exponential voltage available for interrogation of the poled crystal. Its polarity can be made either positive or negative thus allowing interrogation in either direction. The time constant of this voltage was measured and was found to be .84 seconds. By controlling the interrogation power supply, the maximum voltage level can be adjusted to any desired level.
- c) The third voltage is a variable voltage source that can

Figure 2. Circuitry of test equipment.

- C_2 - 4 μ f
- R_1 - 68 K
- R_2 - 30 K
- R_3 - 4.7 K
- R_4 - 270 K
- S_1 - switch
- S_2 - switch
- C_1 - 100 μ f

- V_i - interrogation supply, variable
- V_b - external bias supply, variable
- R_s - 10 K
- V_{cc} - transistor bias supply, variable



be used to bias the test crystal at any level between 1 and 10 volts with either a positive or negative polarity.

Operational Analysis

With the test equipment described in the previous section, an operator can set the polarization of a crystal in one direction with the single pulse, and then reverse this polarization with the application of the interrogation voltage. This reversal gives rise to a current which can be measured on an oscilloscope by measurement of the voltage developed across the resistance in series with the test crystal. The form of the response can be determined by examining the flux density D in the crystal, which is given by

$$D = \epsilon_0 \mathcal{E} + P , \quad (8)$$

and by utilizing the fact that

$$i = A \frac{\partial D}{\partial t} . \quad (9)$$

A partial derivative of D yields

$$\frac{\partial D}{\partial t} = \epsilon_0 \frac{\partial \mathcal{E}}{\partial t} + \frac{\partial P}{\partial t} , \quad (10)$$

which when multiplied by the area, can be written as

$$i = A \frac{D}{t} = \epsilon_0 A \frac{\partial \mathcal{E}}{\partial t} + A \frac{\partial P}{\partial t} . \quad (11)$$

The electric field is given by

$$\mathcal{E} = V/d , \quad (12)$$

so

$$i = \frac{\epsilon_0 A}{d} \frac{dV}{dt} + A \frac{\partial P}{\partial t} . \quad (13)$$

Now the interrogation voltage is given by

$$V = V_0(1 - e^{-at}) , \quad (14)$$

so that

$$\frac{dV}{dt} = a V_0 e^{-at} . \quad (15)$$

Substitution of Equation (15) into Equation (13) yields

$$i = \left(\frac{A \epsilon_0 a V_0}{d} \right) e^{-at} + A \frac{\partial P}{\partial t} . \quad (16)$$

The form of the current expression given in Equation (16) indicates that the resulting current is composed of two components - one an exponentially decreasing term and the other a term dependent upon the rate of reversal of the polarization. The second term is of utmost importance in this investigation since it yields information related to the polarization reversal phenomena.

Experimental Results

In order to obtain MBO crystals to test, a number of Transpolarizers were purchased from the Electrocrystal Corporation.⁶ The schematic for a Transpolarizer is shown in Figure 3. Due to the three electrical connections, there are two possible sections of the crystal that can be examined.

The general method of studying polarization reversal has been described in the previous sections. To be more specific, a typical test for an MBO crystal is described below:

- a) One section of the Transpolarizer crystal was placed in series with a 10 K resistor.
- b) The combination was pulsed with an 80 volt level pulse of 1×10^{-3} seconds duration thus setting the polarization to its maximum remanent level in one direction.
- c) The crystal was then interrogated in the opposite direction with the slow rise time exponential voltage with its maximum level set at 60 volts.

The resultant current waveform due to the subsequent reversal of the polarization is shown in Figure 4a while the reversing voltage is shown in Figure 4b.

A careful analysis of the photograph of the transient definitely shows the exponentially decreasing portion of the current and the

⁶C. F. Pulvari, President. 2014 Taylor St., N. E. Washington, D. C.

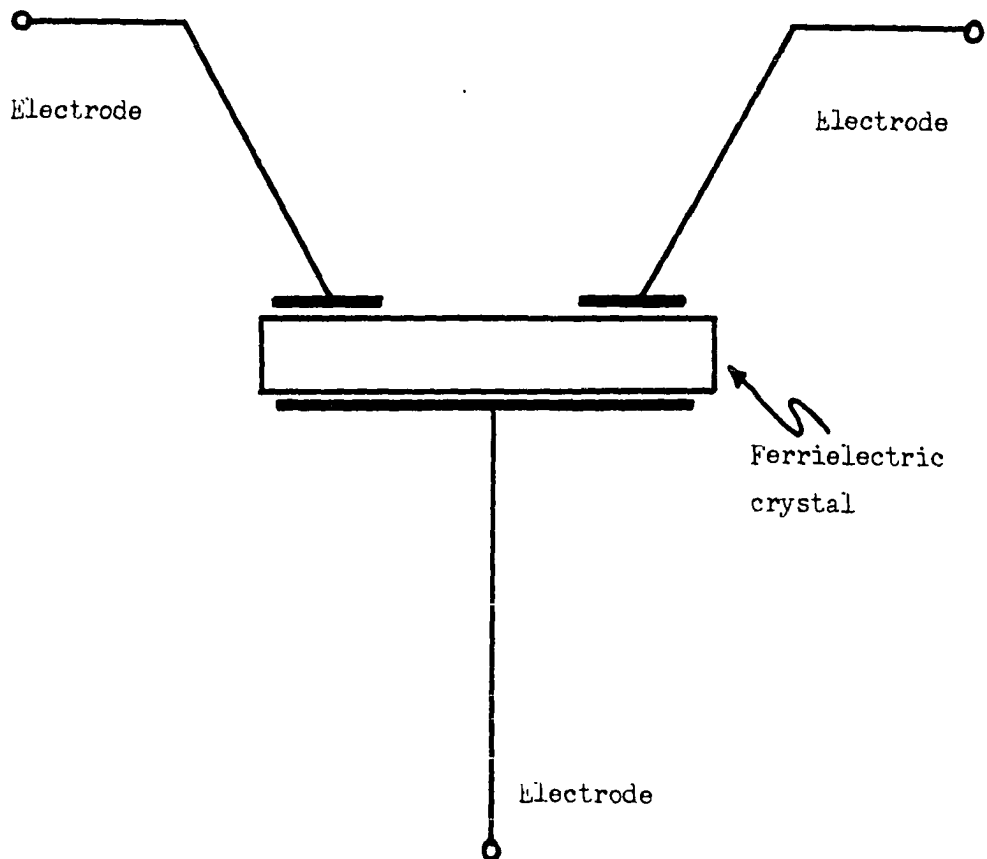


Figure 3. Schematic of a Transpolarizer.

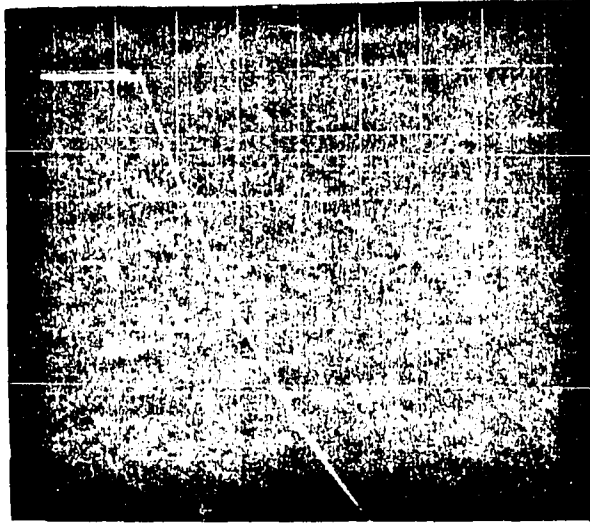


Figure 4a. Interrogation voltage. Scale: 5 volts/cm.

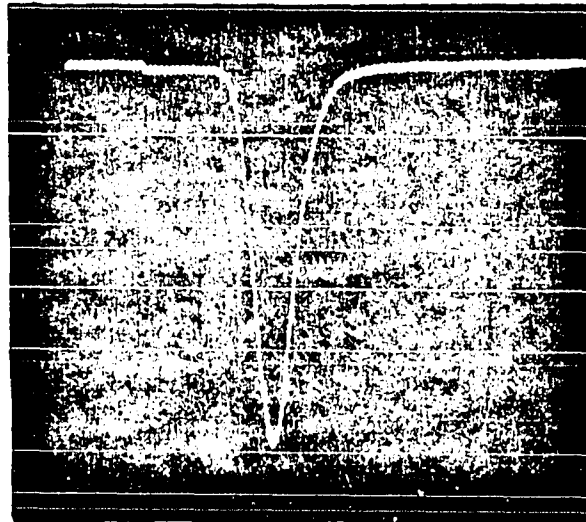


Figure 4b. Switching transient due to application of interrogation voltage to a $\text{Bi}_4\text{Tl}_3\text{O}_{12}$ single crystal. Scales: Time - .2 seconds/cm; Current - 5×10^{-8} amps/cm; Interrogation voltage - 10 volts/cm.

component due to the actual reversal of the polarization. It can be noted that the portion due to the reversal does not take place until a certain threshold level of the interrogation waveform is reached. This test was repeated on a number of MBO crystals and in each case a threshold level of some degree was noted. It is possible to examine this threshold more closely, if on the oscilloscope the resulting current is traced as a function of voltage. The threshold level is quite evident from this type of response as can be seen in Figure 5a. The corresponding current versus time curve is shown in Figure 5b.

Conclusions

The results described in the previous section indicate that there definitely is a "threshold field" effect in these bismuth titanate crystals. The exact value of the threshold field was difficult to determine from these experiments since it was impossible to measure the thickness of each crystal as they were enclosed in transistor cases. However, Pulvari⁷ did indicate that the approximate thickness of the crystals utilized in the Transpolarizers was 1×10^{-3} inches. Assuming then that $d = 2.54 \times 10^{-3}$ cm and using typical measured threshold levels from the transient responses of 6 to 13 volts, the apparent threshold range appears to be between 2.4 KV/cm and 5.1 KV/cm. This range as determined from transient measurements compares favorably with

⁷C. F. Pulvari, 2014 Taylor St. N. E., Washington, D. C.
Crystal data. 1965.

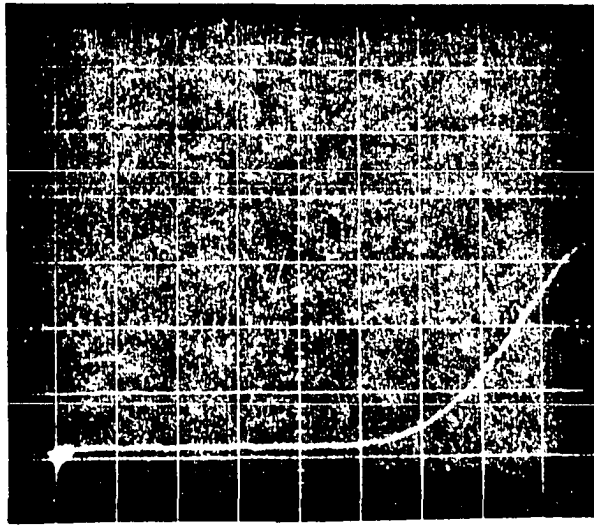


Figure 5a. Switching current for a $\text{Bi}_4\text{Ti}_3\text{O}_{12}$ single crystal versus interrogation voltage. Scales: Current - 10×10^{-8} amps/cm; Voltage - 2 volts/cm.

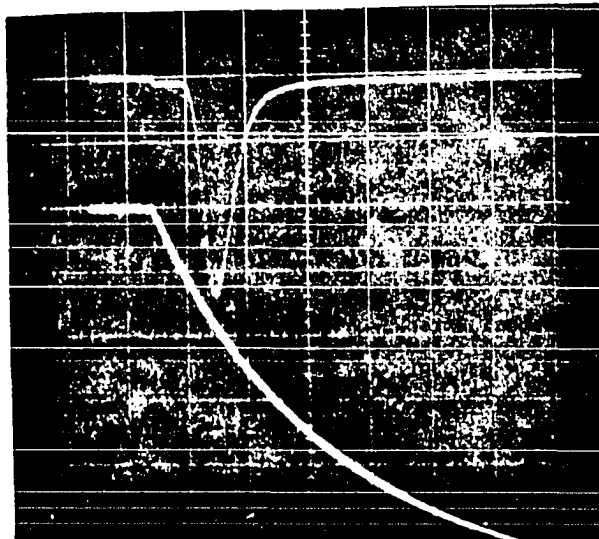


Figure 5b. Switching transient due to application of interrogation voltage to a $\text{Bi}_4\text{Ti}_3\text{O}_{12}$ single crystal. Scales: Time - .2 seconds/cm; Current - 10×10^{-8} amps/cm; Voltage - 10 volts/cm.

the values previously reported in the literature which are as follows:

- a) A 5 KV/cm threshold level which was obtained from a modified Sawyer and Tower experimental circuit employed by McDonnell (29).
- b) A 3 KV/cm threshold level which was obtained from S curve techniques employed by Cummins (34).
- c) A 3.3 KV/cm threshold level which was obtained from opening of loop measurements by Pulvari and de la Paz (35).
- d) A 3 KV/cm threshold level which was obtained from x-ray techniques employed by Hamilton (41).

INVESTIGATION OF THE THRESHOLD FIELD EFFECT IN $\text{Bi}_4\text{Ti}_3\text{O}_{12}$ SINGLE CRYSTALS

Introduction

The test equipment discussed in the previous chapter was developed for the purpose of studying the threshold field. It was anticipated that if a true threshold does exist, the charge switched upon interrogation would not be altered by a reverse bias disturbance field. For an apparent threshold field, the charge switched upon interrogation would be affected appreciably by the magnitude and the time application of a disturbance field.

With this concept in mind, this author developed the test procedure outlined below:

- a) Set the polarization in a saturation state with a positive voltage pulse.
- b) Select a negative bias voltage of magnitude less than the threshold level as determined from a typical switching response.
- c) Apply the negative bias voltage to the crystal for an extended length of time.
- d) Remove the bias and interrogate the crystal with a slow rise time exponential voltage of negative polarity.
- e) Photograph the scope trace of either current versus time or current versus applied voltage.

Subsequently, it became necessary to modify this procedure. Since this procedure did provide useful information, it is necessary to present

the experimental data resulting from its application in order to show the rationale for the modification. The next section is labeled "Preliminary Experiments" to draw a clear distinction between data obtained from this procedure and that obtained later from a refined procedure.

Preliminary Experiments

Original test

One half of a Transpolarizer device was placed in series with a 10K resistor. The combination was pulsed in the positive sense with an 80 volt, 1×10^{-3} seconds duration pulse. A reverse bias of approximately 2 volts was then placed on the combination for a period of 24 hours. The bias was then removed, and the crystal was interrogated with the slow rise time exponential voltage. The resulting switching transient along with the interrogation voltage waveform is shown in Figure 6a. The waveform for the zero bias case is shown in Figure 6b.

The area under the current versus time response corresponds to the amount of charge switched. A planimeter was used to determine the area under (a) the current response shown in Figure 6a and (b) the current response shown in Figure 6b. There was no significant difference in area which indicates that the amount of charge switched in each case was approximately the same. Either no polarization was reversed by the application of the reverse bias or the amount reversed for this bias level was too small to detect by comparing the respective areas. A more significant point to note from comparing the two curves of this original test is that

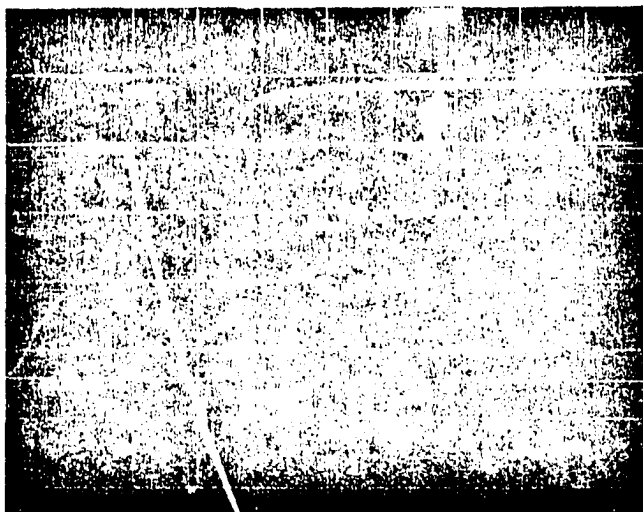


Figure 6a. Switching transient due to application of the interrogation voltage to a $\text{Bi}_4\text{Ti}_3\text{O}_{12}$ single crystal for the case of zero bias. Scales: Time - .2 seconds/div.; Current - 5×10^{-8} amps/cm; Voltage - 5 volts/cm.

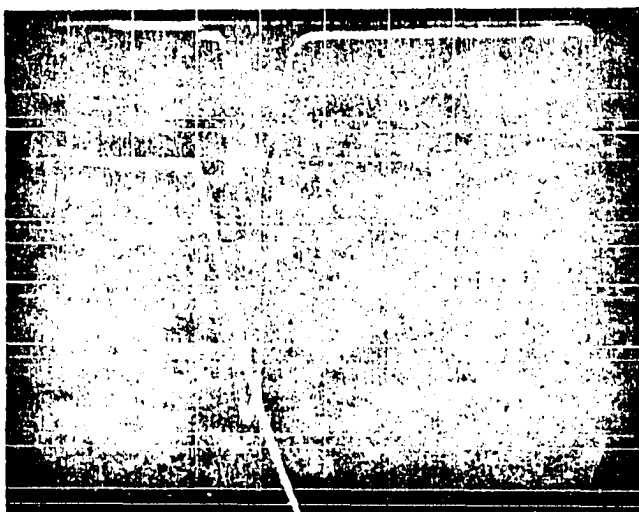


Figure 6b. Switching transient due to application of the interrogation voltage to a $\text{Bi}_4\text{Ti}_3\text{O}_{12}$ single crystal but following a 2 volt reverse bias applied for a period of 24 hours. Scales: Same as for Figure 6a.

the threshold voltage level has increased from its zero bias value with the application of the reverse bias for the extended length of time.

Test for relative time dependence of the field

To determine the approximate time required for the apparent change in threshold field to occur, a similar test was repeated on one half of a Transpolarizer device with a reverse bias of 4 volts applied for a period of 30 minutes. The resulting switching transient is shown in Figure 7a, and the waveform for the zero bias case is shown in Figure 7b. Again the threshold level was increased by the application of the bias voltage, but it appears as though this change took place, not in a matter of hours, but in a matter of minutes. The current transient for the zero bias case when compared to the zero bias case shows a steeper rise when reversal begins, a higher peak value, and a broader tail as reversal subsides. As before the area under each curve was determined with a planimeter. There was no significant difference in area which indicates that the charge switched in each case was approximately the same.

Trend of field with time for various bias levels

From the previous test it was established that the threshold field change occurs in a matter of minutes. To establish the rate of change of this field, the standard test was repeated for a fixed bias level that was applied for various lengths of time. Since the interest here was with the threshold field and not the charge switched, current versus applied voltage data was taken. This form of response shows the voltage

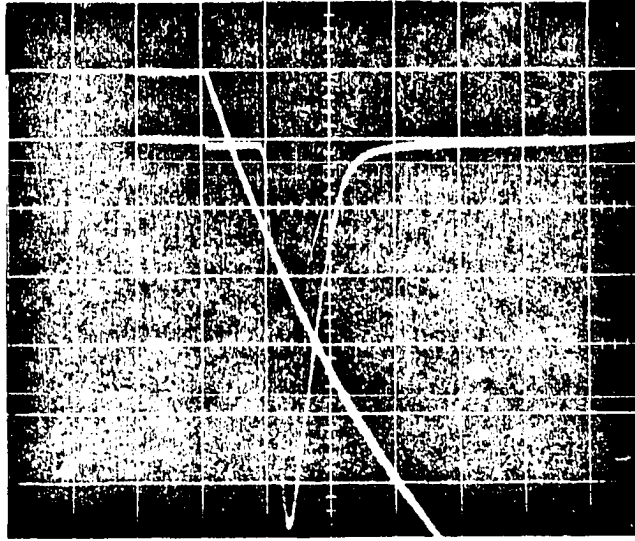


Figure 7a. Switching transient due to application of the interrogation voltage to a $\text{Bi}_4\text{Ti}_3\text{O}_{12}$ single crystal but following a 4 volt reverse bias applied for a period of 30 minutes. Scales: Time - .2 seconds/div.; Current - 5×10^{-8} amps/cm; Voltage - 5 volts/cm.

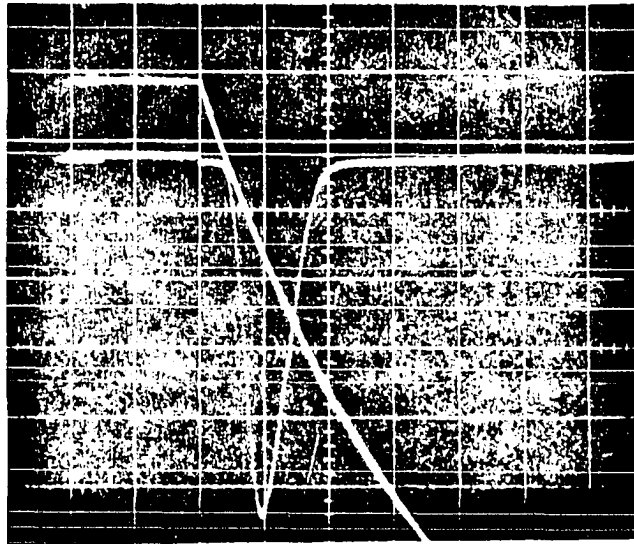


Figure 7b. Switching transient due to the application of the interrogation voltage to a $\text{Bi}_4\text{Ti}_3\text{O}_{12}$ single crystal for the case of zero bias. Scales: Same as for Figure 7a.

threshold more clearly than does the current versus time response.

For the crystal selected for this test the threshold level was established to be approximately 6.2 volts for the zero bias response. A bias level of 4 volts was selected, and it was applied for time increments of 30 seconds, 60 seconds, 300 seconds, 600 seconds, and 1800 seconds. The resulting switching transients for these time applications of the 4 volt bias are shown in Figures 8a - 8f. From each of these traces the threshold level was determined. These threshold levels for each bias level and the time for which it was applied are listed in Table 1. The test was repeated for levels of 6 volts, 5 volts, and 3 volts. Similar transients occurred, and the resulting threshold levels that were obtained are also listed in Table 1. A graph of this data results in a family of curves which are shown in Figure 9.

A similar test was repeated on another crystal, but in this case the data was taken from the response curves of current versus time rather than from the response curves of current versus applied voltage. In this test a 5 volt reverse bias was applied to a poled crystal for various lengths of time, and the threshold level for each time application was determined from the resulting transient response. To demonstrate the form of the response for this crystal, the resulting transients for the 5 volt case are shown in Figure 10a-f. A similar test was conducted on the crystal with an 8 volt reverse bias. The corresponding threshold levels as determined for each bias voltage and its time application are listed in Table 2. Plots of the threshold level as a function of the time application of each bias level are shown in Figure 11.

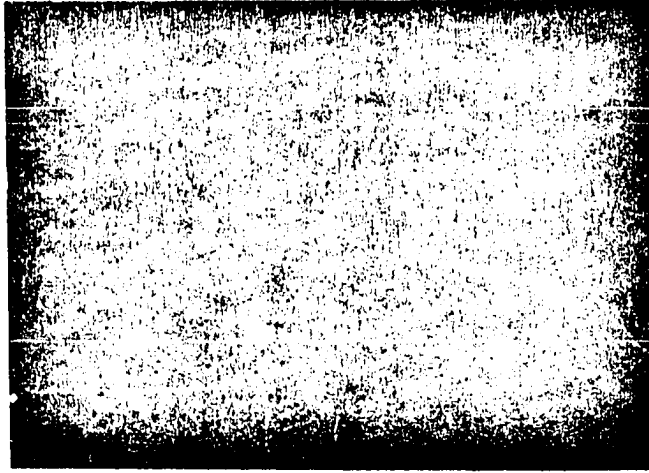


Figure 8a. Switching current for a $\text{Bi}_4\text{Ti}_3\text{O}_{12}$ single crystal versus interrogation voltage for the case of zero bias. Scales: Current - 5×10^{-8} amps/cm; Voltage - 2 volts/cm.



Figure 8b. Switching current for a $\text{Bi}_4\text{Ti}_3\text{O}_{12}$ single crystal versus interrogation voltage following the application of a 4 volt reverse bias for 30 seconds. Scales: Same as for Figure 8a.

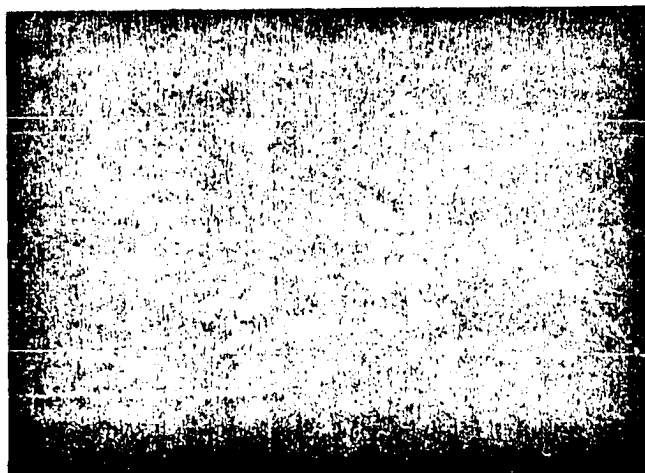


Figure 8c. Switching current for a $\text{Bi}_4\text{Ti}_3\text{O}_{12}$ single crystal versus interrogation voltage following the application of a 4 volt reverse bias for 60 seconds. Scales: Same as for Figure 8a.



Figure 8d. Switching current for a $\text{Bi}_4\text{Ti}_3\text{O}_{12}$ single crystal versus interrogation voltage following the application of a 4 volt reverse bias for 300 seconds. Scales: Same as for Figure 8a.



Figure 8e. Switching current for a $\text{Bi}_4\text{Ti}_3\text{O}_{12}$ single crystal versus interrogation voltage following the application of a 4 volt reverse bias for 600 seconds. Scales: Same as for Figure 8a.

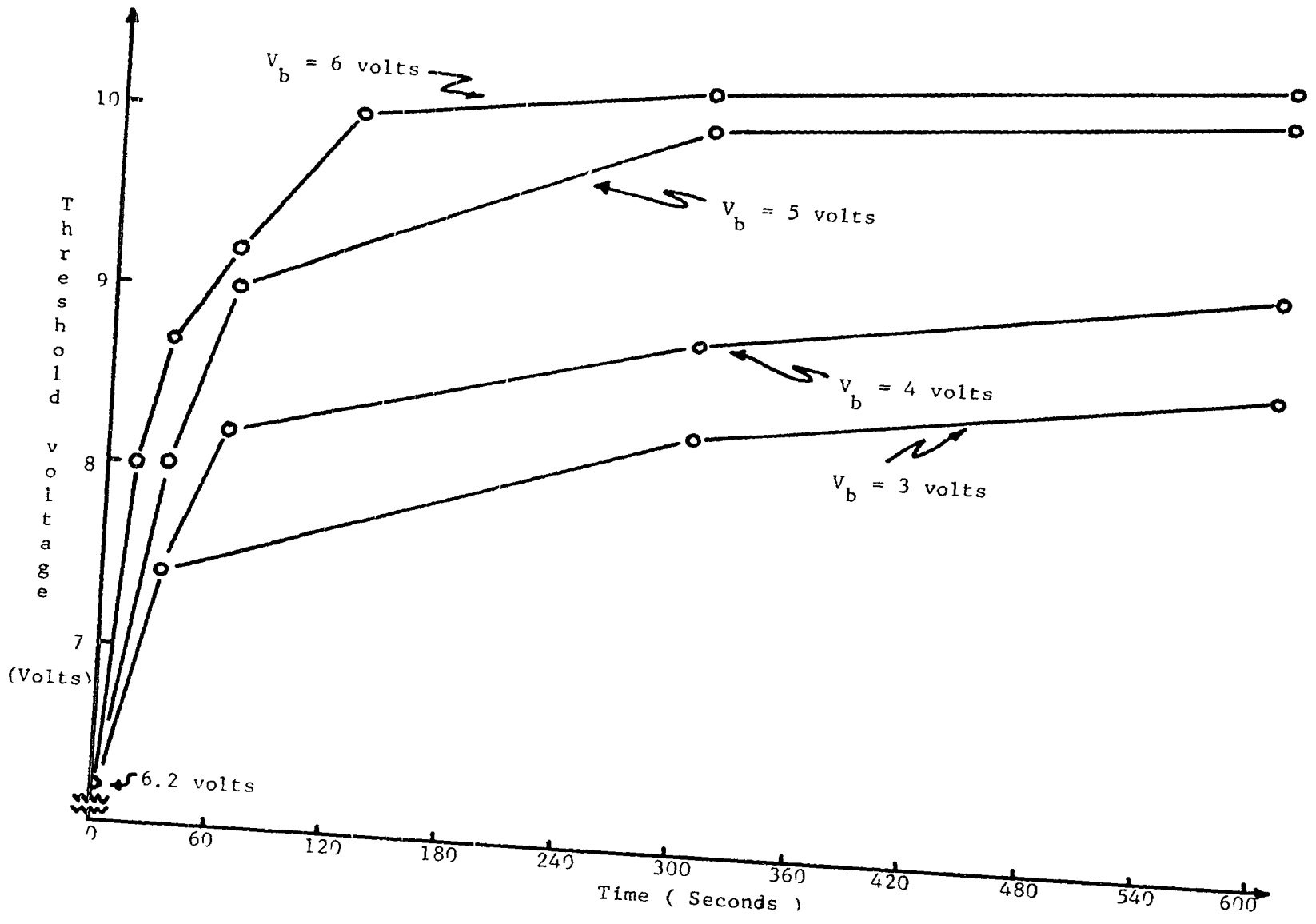


Figure 8f. Switching current for a $\text{Bi}_4\text{Ti}_3\text{O}_{12}$ single crystal versus interrogation voltage following the application of a 4 volt reverse bias for 1800 seconds. Scales: Same as for Figure 8a.

Table 1. Threshold level for selected bias voltages applied to a poled $\text{Bi}_4\text{Ti}_3\text{O}_{12}$ crystal for various periods of time.

Time (seconds)	Threshold (volts) @ $V_B = 6$	Threshold (volts) @ $V_B = 5$	Threshold (volts) @ $V_B = 4$	Threshold (volts) @ $V_B = 3$
0	6.2	6.2	6.2	6.2
15	8.0	-	-	-
30	8.75	8.0	7.4	7.4
60	9.2	9.0	8.2	8.0
120	10	-	-	-
300	10.2	10	8.8	8.3
600	10.4	10.2	9.22	8.75
1200	-	10.4	-	-
1800	-	-	10	9.4

Figure 9. Threshold voltage as a function of the application time of selected reverse bias voltages to a poled $\text{Bi}_4\text{Ti}_3\text{O}_{12}$ single crystal.



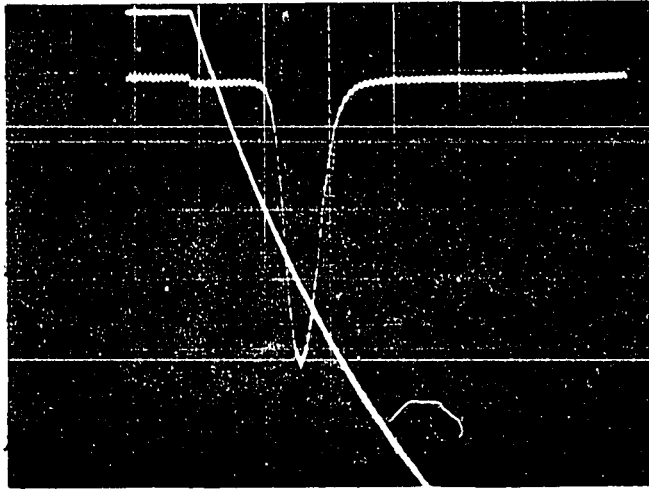


Figure 10a. Switching transient due to the application of the interrogation voltage to a $\text{Bi}_4\text{Ti}_3\text{O}_{12}$ single crystal for the case of zero bias. Scales: Current - 5×10^{-8} amps/div.; Voltage - 5 volts/cm.

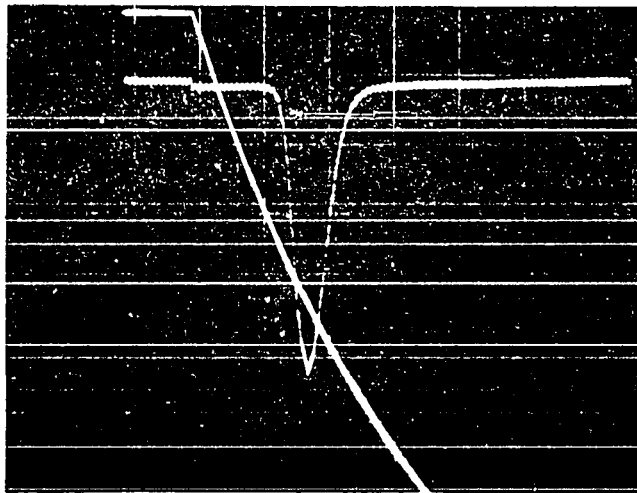


Figure 10b. Switching transient due to the application of the interrogation voltage to a $\text{Bi}_4\text{Ti}_3\text{O}_{12}$ single crystal but following a 5 volt reverse bias applied for 15 seconds. Scales: Same as for Figure 10a.

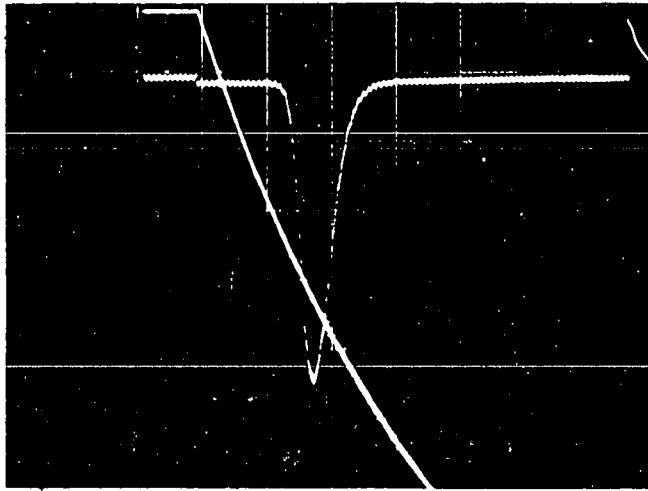


Figure 10c. Switching transient due to the application of the interrogation voltage to a $\text{Bi}_4\text{Ti}_3\text{O}_{12}$ single crystal but following a 5 volt reverse bias applied for 30 seconds. Scales: Same as for Figure 10a.

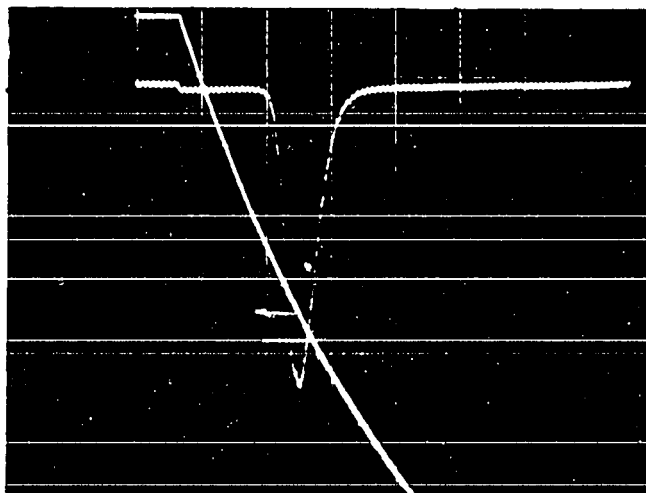


Figure 10d. Switching transient due to the application of the interrogation voltage to a $\text{Bi}_4\text{Ti}_3\text{O}_{12}$ single crystal but following a 5 volt reverse bias applied for 120 seconds. Scales: Same as for Figure 10a.

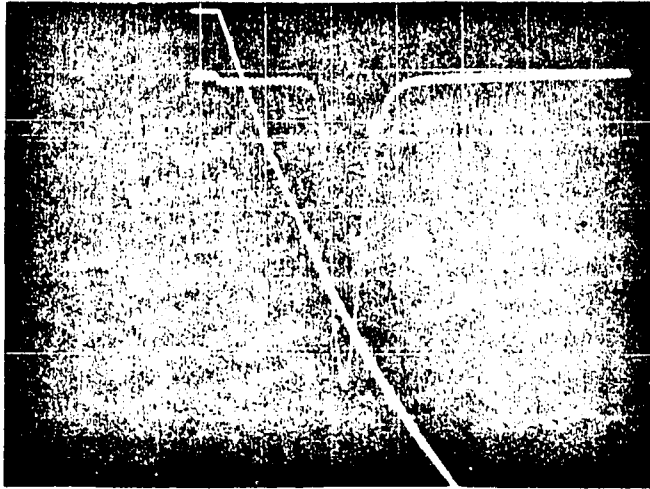


Figure 10e. Switching transient due to the application of the interrogation voltage to a $\text{Bi}_4\text{Ti}_3\text{O}_{12}$ single crystal but following a 5 volt reverse bias applied for 300 seconds. Scales: Same as for Figure 10a.

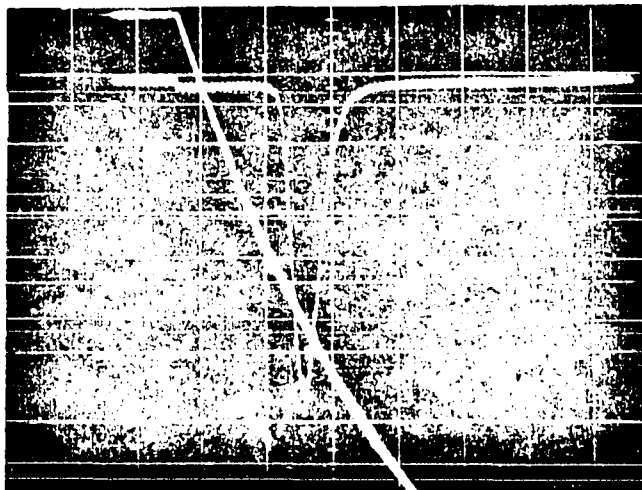
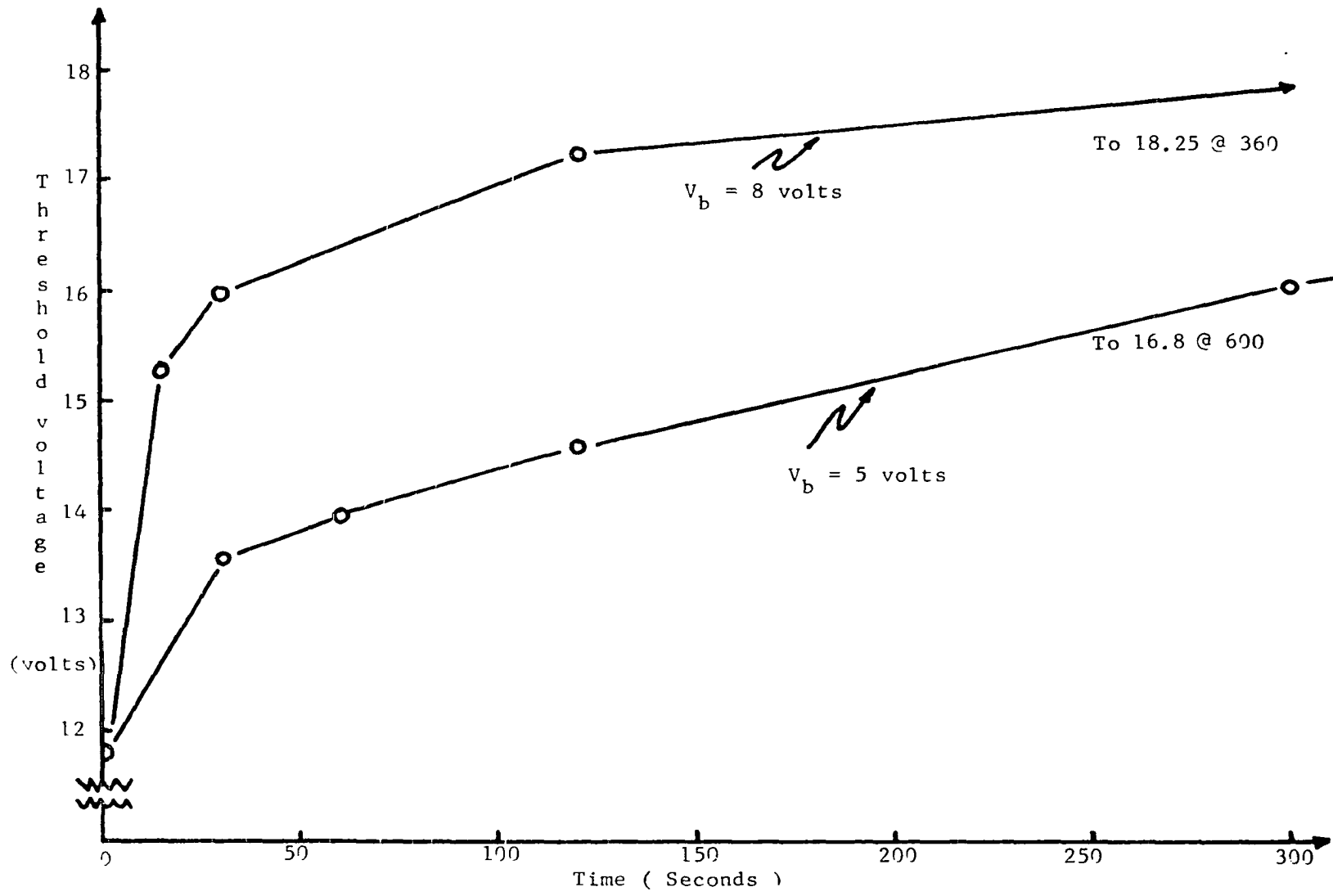


Figure 10f. Switching transient due to the application of the interrogation voltage to a $\text{Bi}_4\text{Ti}_3\text{O}_{12}$ single crystal but following a 5 volt reverse bias applied for 600 seconds. Scales: Same as for Figure 10a.

Table 2. Threshold level for 5 and 8 volt bias voltages applied to a poled $\text{Bi}_4\text{Ti}_3\text{O}_{12}$ single crystal for various periods of time.

Time (seconds)	Threshold (volts) @ $V_B = 5$	Threshold (volts) @ $V_B = 8$
0	11.9	11.8
15	13.6	15.25
30	13.9	16
120	14.6	17.3
300	16	-
360	-	18.25
600	16.8	-

Figure 11. Threshold voltage as a function of the application time of a 5 volt and an 8 volt reverse bias to a poled $\text{Bi}_4\text{Ti}_3\text{O}_{12}$ single crystal.



It appears from the curves of Figure 9 and Figure 11 that (a) the effect is bias field dependent, i.e. the threshold field growth occurs much faster at the higher fields and (b) the threshold field approaches a limiting value as time increases. This limiting value appears to be equal to the sum of the reference threshold voltage and the selected bias level, i.e.

$$V_{T_{\text{new}}} = V_{T_{\text{ref}}} + V_{\text{bias}} \quad (17)$$

Charge reduction through the application of a d.c. bias

The threshold field effect was examined for a number of crystals. In some cases the application of the reverse bias field caused a reduction in the total charge switched. To demonstrate this, the results of a standard test on one of the devices exhibiting this characteristic are shown in Figures 12a-b. The response in Figure 12a of current versus voltage is for the situation in which prior to interrogation a bias level of 6 volts was applied to the crystal for a period of 24 hours. Following the interrogation for the situation described above, the crystal was poled and then immediately interrogated. This interrogation resulted in the reference response shown in Figure 12b. To obtain the amount of charge reversed for each case it was necessary to transform the current versus voltage information into current versus time information. The functional dependence of the voltage on time as given in Equation 14 was used in making a point by point transformation. Integration of the transformed current versus time information was achieved through the application of

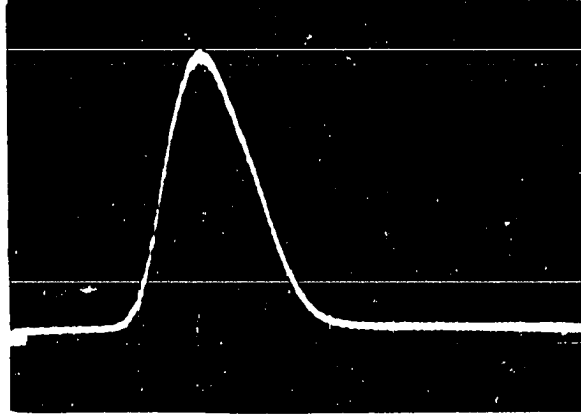


Figure 12a. Switching current for a $\text{Bi}_4\text{Ti}_3\text{O}_{12}$ single crystal versus interrogation voltage for the case of zero bias. Scales: Current - 5×10^{-8} amps/cm; Voltage - 5 volts/cm.

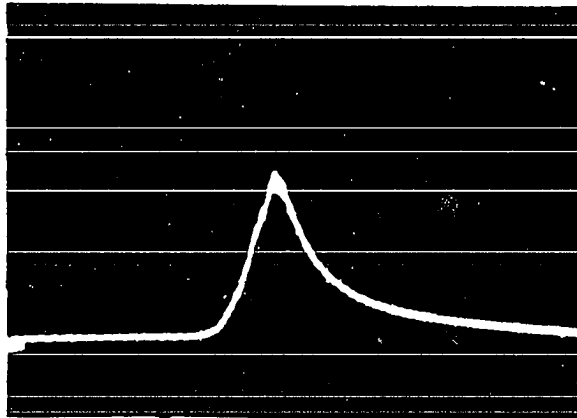


Figure 12b. Switching current for a $\text{Bi}_4\text{Ti}_3\text{O}_{12}$ single crystal versus interrogation voltage but following a 6 volt reverse bias applied for a period of 24 hours. Scales: Same as for Figure 12a.

the trapezoidal rule. The charge switched for the reference case was found to be 31.9×10^{-9} coulombs while for the 6 volt bias case the charge switched was found to be 27.6×10^{-9} coulombs.

The decrease in the amount of charge switched indicates that the polarization was reduced from its saturation value. It is possible that the reduction in polarization resulted from nucleation of oppositely polarized domains. However, it is also possible that the reduction in polarization resulted from some decay mechanism. This author wishes to pursue the latter possibility and to present related information.

In general, decay or fatigue effects for ferroelectric single crystals are not discussed in any great detail in the literature. However, Fatuzzo and Merz (11) do present a detailed discussion of the decay effects in ferroelectric BaTiO_3 single crystals. In their summary, they note the following:

- a) Repeated switching of a sample with a square wave or a sine wave does not cause a change in the spontaneous polarization.
- b) Repeated switching of a sample with pulses of opposite polarity - spaced such that no field is applied for a considerable part of the time - does cause a reduction in the spontaneous polarization.
- c) Generally, decay is characterized by a decrease in the spontaneous polarization and an increase in the coercive field.
- d) Two distinct types of decay exist.

- e) Type I decay is characterized by a rapid decrease in polarization. Recovery from this type of decay is achieved by applying a d.c. potential of appropriate polarity or by cycling the sample with a low-frequency sine wave.
- f) Type II decay is characterized by an increase in coercive field with no significant change in polarization. This decay is generally associated with switching at high frequencies. Recovery from this type of decay is not possible.

Type I decay is of interest since it is manifested by a reduction in polarization. Merz and Anderson (45) assumed Type I decay to be connected with injection of carriers into the crystal and interaction of the injected carriers with the domain walls. They indicated that injection might be enhanced by the presence of high fields near the surface of the crystal. Fatuzzo and Merz (11) indicate that Type I decay is the result of injection of charge carriers, and that it can be prevented by the use of liquid electrodes which being ionic conductors do not permit injection of charge into the crystal.

Decay in BaTiO_3 single crystals has also been noted by Williams (46) for switching with very low fields with switching times in minutes. He concluded the decay associated with slow switching was connected with motion of ionic space charge which caused back switching of domains after the removal of the field. He found (a) the room temperature conductivity was predominately ionic and (b) the depolarization of a polarized sample occurred by ferroelectric polarization reversal and by normal conduction.

This author noted that the application of a reverse bias to poled $\text{Bi}_4\text{Ti}_3\text{O}_{12}$ single crystals did not always produce a reduction in reversible polarization. In the cases where a reduction did occur, the reversing field could have caused (a) domains of opposite polarity to nucleate, (b) charge carriers to be injected into the crystals, or (c) ionic charge to move within the crystals. Each of the previously mentioned effects or possibly a combination of these effects could account for the reduction in reversible polarization.

For the $\text{Bi}_4\text{Ti}_3\text{O}_{12}$ single crystals that exhibited a decay upon the application of a d.c. bias, this author found that recovery was possible by cycling the crystal with a 60 hertz sine wave for a period of minutes. Recovery was also found possible by successive application of the positive pulse and the negative interrogation voltage. Recovery by this technique is demonstrated in the sequence of responses shown in Figures 13a-d. Figure 13a shows the interrogation response after a bias of 6 volts had been applied for 24 hours. The crystal was then pulsed, and upon interrogation the response in Figure 13b resulted. This technique was repeated two more times, and the respective interrogation responses are shown in Figure 13c and 13d.⁸ The responses are of current versus applied voltage and can be converted to current versus time curves which if integrated yield the charge switched. However, exact transformation is not necessary. An inspection of the maximum current in each case, the time at

⁸This response also represents the zero bias case since after repeated testing the same response as is shown in Figure 13d resulted.

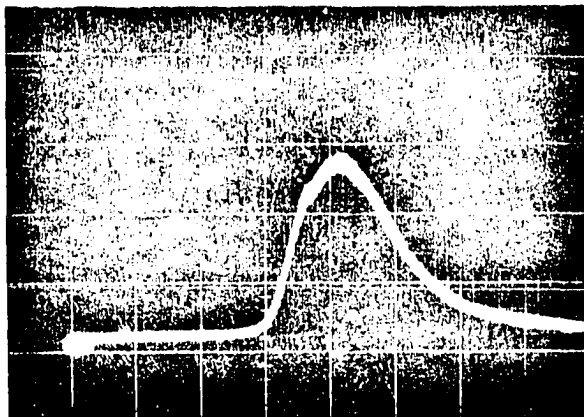


Figure 13a. Switching current for a $\text{Bi}_4\text{Ti}_3\text{O}_{12}$ single crystal versus interrogation voltage but following a 6 volt reverse bias applied for a period of 24 hours. Scales: Current - 5×10^{-8} amps/cm; Voltage - 5 volts/cm.

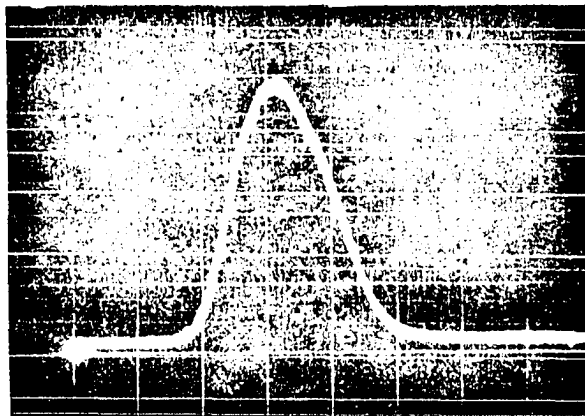


Figure 13b. Response following first application of a positive pulse and the negative interrogation voltage to the previously interrogated crystal. Scales: Same as for Figure 13a.

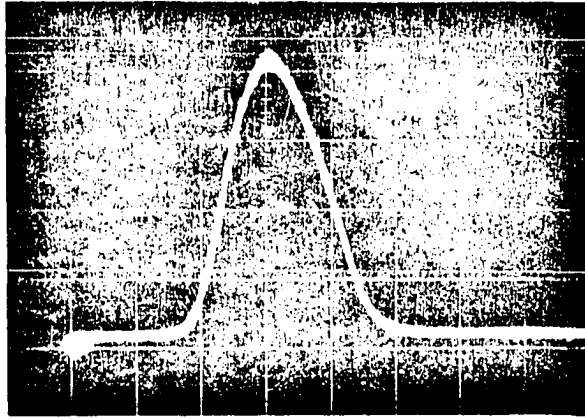


Figure 13c. Response following second application of a positive pulse and the negative interrogation voltage. Scales: Same as for Figure 13a.

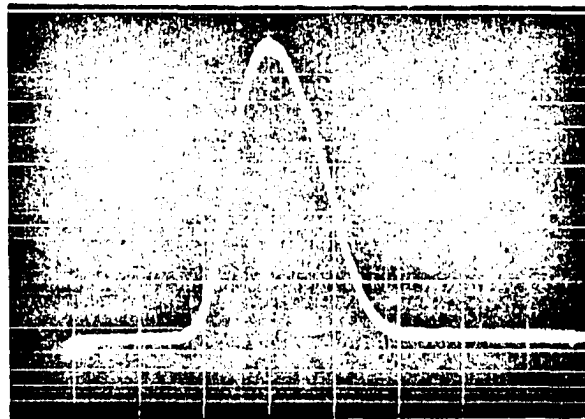


Figure 13d. Response following third application of a positive pulse and the negative interrogation voltage. Scales: Same as for Figure 13a.

which it occurs, and the general shape of the curves indicate that with each successive interrogation that the charge switched has definitely increased.

A non-recoverable decay was noted for a number of the devices after prolonged use in pulsing and interrogation experiments. Two such devices exhibiting this decay characteristic were opened, and in each case it was discovered that the single crystals were finely cracked in the electrode region. This cracking might be a product of aging, or conversely it might be the physical origin of the aging or decay.⁹ The latter assumption implies the presence of large strains in these $\text{Bi}_4\text{Ti}_3\text{O}_{12}$ single crystals. The topics of strain and microcracking and their possible relationship in these crystals will be examined in detail in the later section.

Limit on threshold

In the previous section it was suggested that a limit exists on the threshold voltage for a selected bias applied to a crystal for an extended length of time, and that limit as was proposed by Equation 17 is equal to the sum of the zero bias threshold voltage and the applied bias voltage. To test this relationship, a standard test was performed on one half of a Transpolarizer device but with a bias time application in excess of the previous 30 minute maximum limit utilized in establishing the trend of

⁹This type of explanation was offered by Taylor (47) in describing aging effects in niobium-doped ferroelectric ceramics. He established aging to be domain re-orientation resulting from strain relaxation. Sample decay was accompanied by strain decrease, and the relaxation of the strains caused microcracking.

field with time. To insure that the change in threshold would be completed, a bias time application of 90 minutes was selected.

The current versus voltage response shown in Figure 14a is for the case in which prior to interrogation a bias voltage of 4 volts was applied to the crystal for a period of 90 minutes. The threshold level was determined from this response to be 12.1 volts. The zero bias or reference response of current versus voltage is shown in Figure 14b. The reference was determined from this response to be 8.1 volts. From the results of this test, it appears that the new threshold does equal the sum of the reference threshold voltage and the bias voltage as was suggested in Equation 17.

Additional tests were performed with longer time applications of the bias, and the results of these tests substantiate this conclusion. To demonstrate this, reference is made to the responses shown in Figure 12a and Figure 12b which were utilized in exhibiting the charge reduction phenomenon. The reference threshold was determined from the response of Figure 12a to be 8 volts. The threshold level for the case in which prior to interrogation a 6 volt bias was applied for a period of 24 hours was determined from the response of Figure 12b to be 14 volts. The experimental results obtained from this one day application of the bias also validate the proposed relationship.

Summary Of Preliminary Experimental Results

The purpose of this study as was presented at the beginning of this chapter was to determine if the extended application of a reverse bias of

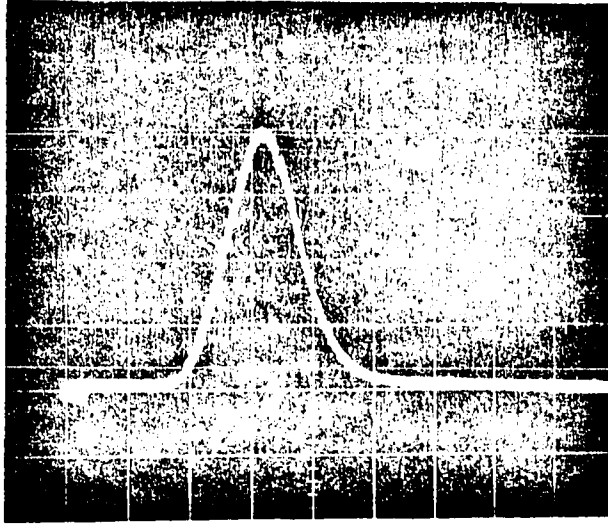


Figure 14a. Switching current for a $\text{Bi}_4\text{Ti}_3\text{O}_{12}$ single crystal versus interrogation voltage for the case of zero bias. Scales: Current - 5×10^{-8} amps/cm; Voltage - 5 volts/cm.

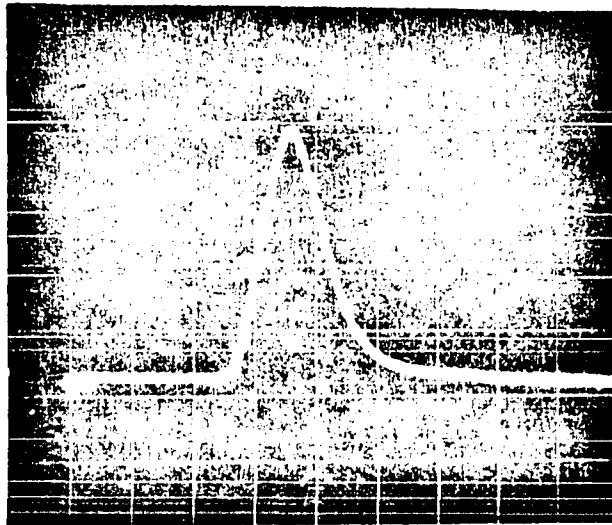


Figure 14b. Switching current for a $\text{Bi}_4\text{Ti}_3\text{O}_{12}$ single crystal versus interrogation voltage following application of a 4 volt bias for a period of 90 minutes. Scales: Same as for Figure 14a.

magnitude less than the threshold level to a poled $\text{Bi}_4\text{Ti}_3\text{O}_{12}$ single crystal could cause polarization reversal. It was originally assumed for a test of this nature that a reversal would indicate the threshold field to be an apparent threshold, while no reversal would indicate the threshold field to be a true threshold. The experiments were conducted with this purpose in mind.

From the experiments performed, three very significant effects were evident. These notable effects are as follows:

- a) For a few of the crystals tested, a reduction in the amount of reversible polarization did occur with the application of the reverse bias for an extended length of time.
- b) For all the crystals tested, an increase in the threshold level occurred as a result of the extended application of the reverse bias.
- c) A non-recoverable decay occurred in many instances after extended testing which involved the pulsing and slow-interrogation technique utilized for examination of the switching transient.

Discussion Of Preliminary Experimental Results

In part of the preceding summary section (a) it was noted that for a few of the crystals tested, the application of the reverse bias for an extended length of time did result in a reduction in the amount of reversible polarization. This was shown by a reduction in the area under

the current versus time response for the bias case as compared to the area under the reference current versus time response. This result is consistent with similar findings reported by Cummins (33). He examined hysteresis loops after a d.c. field opposing the initial polarization had been applied to a number of $\text{Bi}_4\text{Ti}_3\text{O}_{12}$ single crystals for extended lengths of time, and he discovered in some cases a reduction in loop height which indicated a reduction in reversible polarization. He also found a loss in squareness of the hysteresis loop and a shift in the field axis bias for those crystals exhibiting a reduction in reversible polarization.

He offered three possible explanations for the reduction in reversible polarization effect:

- a) The first possibility was that the effect might be similar to the decay or fatigue effect associated with barium titanate single crystals. It was noted though that the decay of barium titanate is characterized by a symmetrical reduction in loop height whereas the decay in this material is characterized by a highly asymmetrical reduction in loop height.
- b) The second possibility was that the effect might be the result of a conversion of part of the crystal to an anti-ferroelectric state or a stable anti-parallel domain structure.
- c) The third possible explanation was that the effect might be due to a slow migration of internal charge carriers

c) within the crystal. This charge could act as compensating charge for the ferroelectric polarization and would create a favorable condition for maintaining the internal field.

$\text{Bi}_4\text{Ti}_3\text{O}_{12}$ single crystals exhibit hysteresis loops which are not symmetrical with respect to the polarization axis, but which are shifted along the field axis. This type of shift is illustrated in Figure 15. This result is often referred to as a "biased hysteresis loop". The distance between the dotted center line and the polarization axis corresponds to the bias. In the literature this bias is referred to as the "intrinsic bias", the "internal bias", or the "field axis bias" - with the latter two terms being used more commonly.

In a later investigation Cummins (34) noted that the reduction in reversible polarization effect was negligible for crystals possessing low internal bias fields. However, he noted that the effect was quite significant for crystals possessing large internal bias fields. An examination by this investigator of the latter case was not possible since the devices possessing crystals that did exhibit this reduction in reversible polarization effect suffered a non-recoverable decay after extended testing. However, an examination of the former case was possible. The last group of devices ordered were described as possessing low internal bias fields. These crystals, which had not been tested to any extent, were polarized and biased in the reverse sense for an extended period of time. The crystals were then interrogated. For each crystal the charge switched was determined from current versus time response by the planimeter method. In each case, no reduction in reversible polarization was detected.

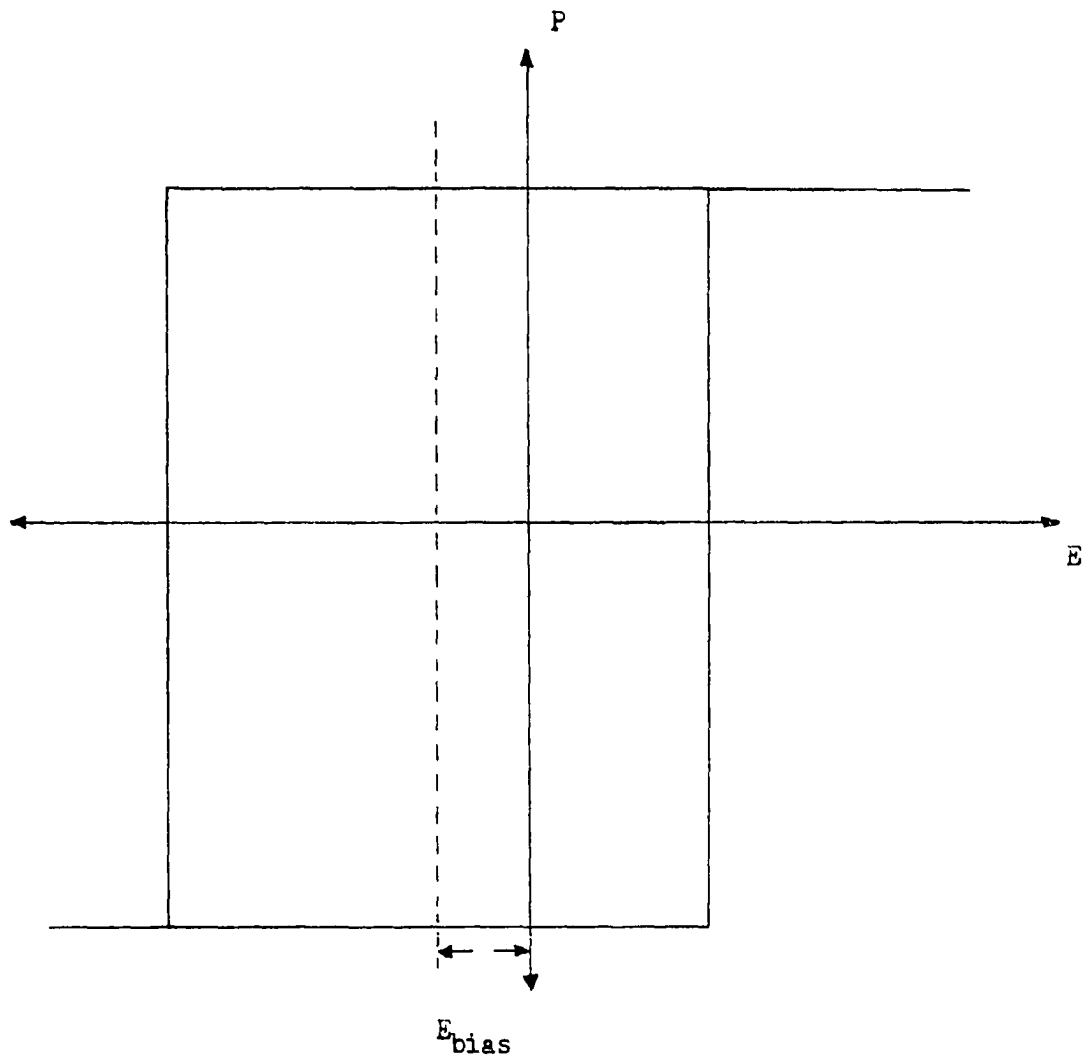


Figure 15. A biased hysteresis loop.

In part (b) of the summary section it was noted for all the crystals tested that the extended application of a reverse bias caused the threshold level to increase from its reference level. Results of this author's experiments indicate that the threshold voltage increased to a limiting value equal to the sum of the reference threshold voltage and the selected bias voltage. Interpretation of these experimental results requires the presentation of certain observations made by Cummins (33, 34).

As was previously mentioned Cummins (33) noted from a hysteresis loop examination that one effect due to the extended application of a d.c. in opposition to the initial polarization was a shift in the field axis bias. In this investigation he found that with the extended application of the d.c. the bias could even change sign and the bias was stable at its new level. Cummins (34) investigated the switching behavior of $\text{Bi}_4\text{Ti}_3\text{O}_{12}$, and he determined that the unusual switching properties could be explained in terms of a rapidly changing bias field. He found from a hysteresis loop examination that after the polarization state was established that a bias began to form quite rapidly.¹⁰ The polarity of this formed bias was always such that reversal of polarization from one saturation state to the other would not begin until the externally applied field exceeded this internal bias. He also observed that the magnitude of this bias was greater than the bias observed for the typical hysteresis loop. Although

¹⁰Cummins (34) determined that formation of the bias begins in less than .01 seconds, but required a matter of minutes to reach a final value. He also established the bias to be more stable the longer the polarization remained in that state.

he established the threshold field effect to be related to this rapidly changing bias field, he made no attempt at establishing the source of this internal bias. He indicated that the source problem could not be solved without a complete understanding of the crystal structure and the domain dynamics.

In this investigation the polarization was set in with a single, positive pulse. Polarization reversal was accomplished by interrogation of the poled $\text{Bi}_4\text{Ti}_3\text{O}_{12}$ crystal with a slow rise time exponential voltage. The resulting current versus time response showed that reversal did not begin until a certain threshold voltage was reached. Considering the observations made by Cummins (34), this observed threshold must include the internal bias that forms rapidly after the establishment of the polarization state. The positive polarization resulted in the formation of a stable negative internal bias, and therefore reversal to the negative polarization state did not begin until the negative interrogation voltage exceeded the new threshold level.

The application of the reverse bias to a poled $\text{Bi}_4\text{Ti}_3\text{O}_{12}$ single crystal for an extended length of time resulted in an increase in the threshold which implies that the internal bias must have increased due to the application of the reverse bias. Experimentally it appeared that the threshold was increased by a magnitude just equal to the value of the selected bias, and therefore the internal bias must have been increased by this value. This change in internal bias is in agreement with the observation made by Cummins (33) that the application of a d.c. opposing the initial polarization causes the field axis bias as observed from the

hysteresis loop to change. Considering these results, each curve shown in Figure 9 and Figure 11 represents the time rate of change of the internal bias due to the application of a specific reverse bias.

In part (c) of the summary section it was noted that a number of the crystals exhibited a non-recoverable decay after repeated testing, i.e. after repeated application of the pulse and slow rise time interrogation voltage the crystals exhibited a permanent reduction in reversible polarization. Breakdown of the material was considered. However, the highest fields utilized in this investigation ranged from 24,000 volts/cm to 32,000 volts/cm and the breakdown was estimated by Pulvari (30) to be at least one million volts per centimeter. Therefore, the following was assumed:

- a) The cracking might be a product of aging - a characteristic never heretofore mentioned in connection with $\text{Bi}_4\text{Ti}_3\text{O}_{12}$ single crystals, but representing a limitation with respect to application.
- b) The cracking might be the physical origin of the decay or aging - a characteristic indicating the decay to be associated with strain relaxation which in turn results in microcracking.

As a point of interest it should be noted that the non-recoverable decay of BaTiO_3 , which was classified as Type II, was associated with switching at high frequencies while for this material, reversal with a slow interrogation voltage appears to be related to this non-recoverable decay. An exact explanation of this decay phenomenon will require a study of the domain dynamics with emphasis on existing strain relationships.

Modified Experimental Technique

Comments

In one of the preceding sections it was noted that the unusual switching properties of this material could be explained in terms of a rapidly changing bias field. It was Cummins (34) who noted that an internal bias field began to form immediately after a sample was poled and that a final value for this internal bias field was not reached until several minutes had elapsed following the poling. Therefore, considering in retrospect the test procedure utilized in the preliminary experiments, it is quite obvious that a procedural error existed. Following the polarization of the test sample, ample time for complete internal bias field formation was not allowed before the crystal was disturbed by an interrogation voltage or by the application of a reverse bias voltage.

The omission of the delay step could of course lead to inaccurate experimental results and subsequently to the formation of false conclusions. Therefore, the preliminary experiments were reviewed in an attempt to determine where the omission might introduce an experimental error and correspondingly an incorrect interpretation. After this review it was concluded that neglecting to allow adequate time for internal bias formation following polarization leads to problems in determining the following items:

- a) The actual reference threshold.
- b) The manner in which the threshold changes from its reference value to its final value with the application of a reverse bias.

- c) The amount of time required for the change in (b) to occur.

In order to provide more accurate experimental results, a decision was made to repeat the tests but to do so using a modified experimental technique which included a delay step sufficient in duration to allow complete internal bias field formation. However, before proceeding with the modified tests it was necessary to conduct an internal bias field formation study.

Internal bias formation test

Through utilization of the basic test equipment described earlier, it is possible to perform a simple test which will demonstrate the change in the threshold field that occurs following poling. This change will thus indicate the growth rate of the internal bias field. The basic steps which were followed are presented below:

- a) The polarization was set in a saturation state with a positive voltage pulse.
- b) Following the polarization, a pre-determined amount of time was allowed for bias formation.
- c) Following this time delay, the crystal was interrogated with the slow rise time exponential of negative polarity.
- d) The threshold level was determined from the photograph of the response.
- e) The test was then repeated for other selected delay times.

Two crystals were tested in the previously described manner. The threshold values for various delay periods are listed in Table 3 for both

Table 3. Threshold voltage as a function of time elapsed following the polarization of two bismuth titanate single crystals.

Elapsed time (seconds)	Threshold (volts) Crystal #1	Threshold (volts) Crystal #2
5	7.1	-
15	8.55	7.3
30	9.35	7.8
45	9.8	8.6
60	-	8.9
120	10.75	-
180	11.25	-
300	-	10.0

of the crystals. These results are plotted and shown in Figure 16. The change in the threshold with time delay following poling does yield the growth rate of the internal bias. Experimentally it was found that a delay period of 10 minutes was sufficient to insure completed formation of the internal bias field.

From an examination of the resulting curves, it is noted that internal bias formation exhibits a fast growth rate period and a slow growth rate period. This suggests that possibly two mechanisms might be responsible for the manner in which the internal bias forms. An attempt to explain this variation will be presented in a later section.

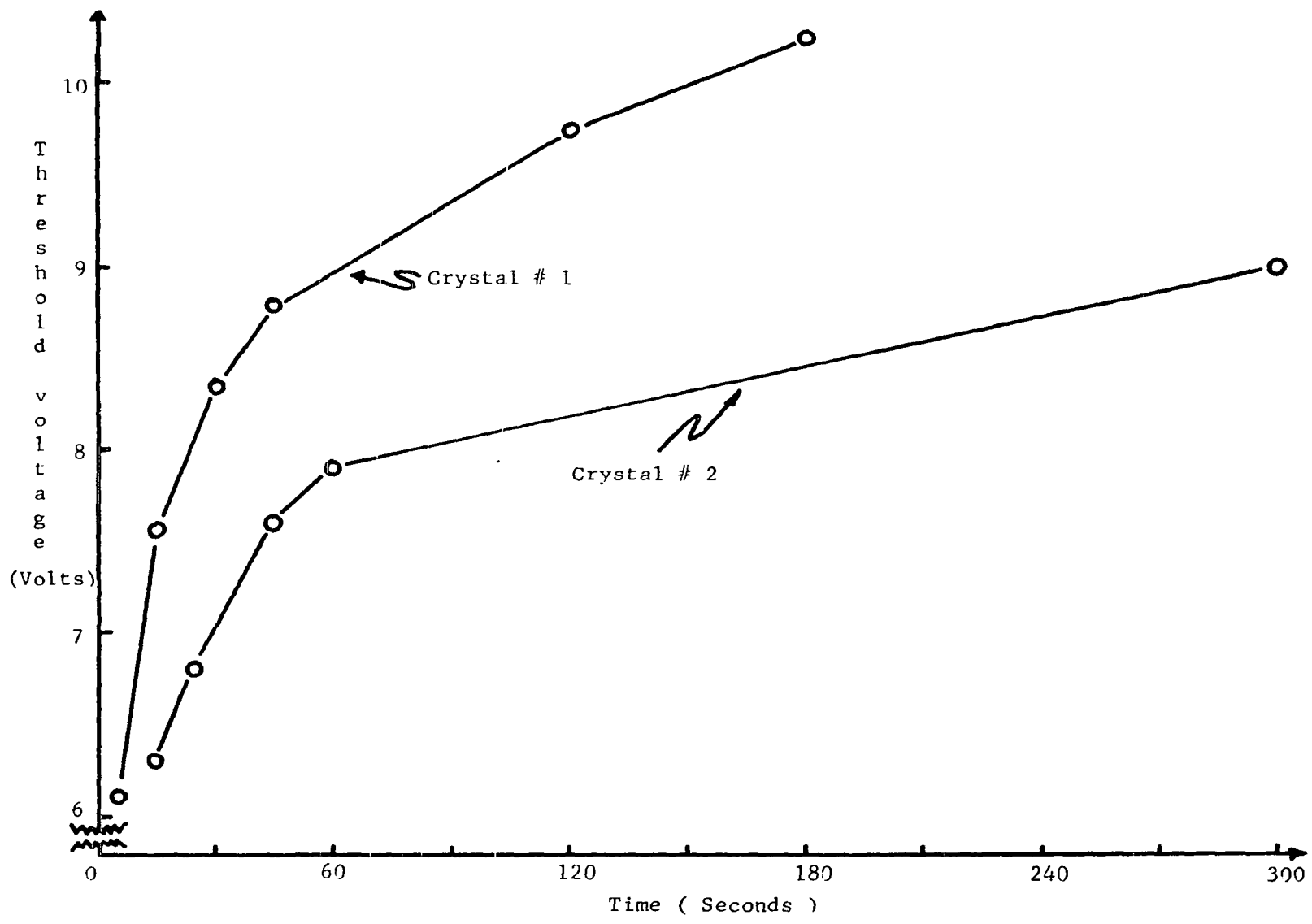
Field trend correction

In the preliminary experiments in which the variation of the threshold field with various time applications of a specific reverse bias was being examined, the reverse bias was applied to the poled crystal before the normal growth of the internal bias field was completed. As a result the curves which are shown in Figure 9 and Figure 11 do not show the true trend of the threshold field with time application of a specific reverse bias since for the low time applications the internal bias field was forming in the presence of an externally applied field.

To provide more accuracy and to correct, if necessary, the results of the preliminary experiments, it was decided that the basic test should be repeated but with the addition of a delay step. A test crystal was selected, and a modified test as is described below was conducted:

- a) The polarization was set in a saturation state with a positive voltage pulse.

Figure 16. Growth of threshold voltage for two bismuth titanate single crystals following polarization.



- b) A period of 10 minutes was allowed for internal bias formation.
- c) Following this bias formation period, a reverse bias was applied to the crystal for a selected period of time.
- d) Following this time application of this reverse bias, the crystal was interrogated with the slow rise time exponential voltage of negative polarity.
- e) The threshold level was determined from the photograph of the response.
- f) The test was then repeated for additional time applications of the reverse bias after the crystal was sine wave cycled for 10 minutes.

The preliminary experiments concerned with the effect of a reverse bias on the threshold level indicated that the threshold field growth rate was field dependent. Specifically, it was noted that the larger the value of the reverse bias, the faster the growth rate of the threshold field. Considering this field dependency, the test described above was conducted for a reverse bias level slightly less than the reference threshold level. Determination of the reference threshold level was accomplished by performing steps (a) and (b) in the procedure and then by performing the interrogation step (d). From the response the reference was determined to be approximately 14 volts. Therefore, for this representative test a 12 volt bias selected.

The modified test procedure was conducted for various time applications of the 12 volt reverse bias. The results of this test are given

in Table 4. For this specific test, the threshold levels were plotted as a function of the time application of the reverse bias. This growth rate curve is shown in Figure 17. For the purpose of comparison, it would have been desirable to obtain corrected growth rate curves on the same crystals as were examined in the preliminary experiments which yielded the growth rate curves shown in Figure 9 and Figure 11. Unfortunately, however, those two specific crystals suffered from the non-recoverable decay. Thus, for the sake of experimental accuracy a crystal which had not been extensively tested was utilized in the above test.

Threshold limit from modified test procedure

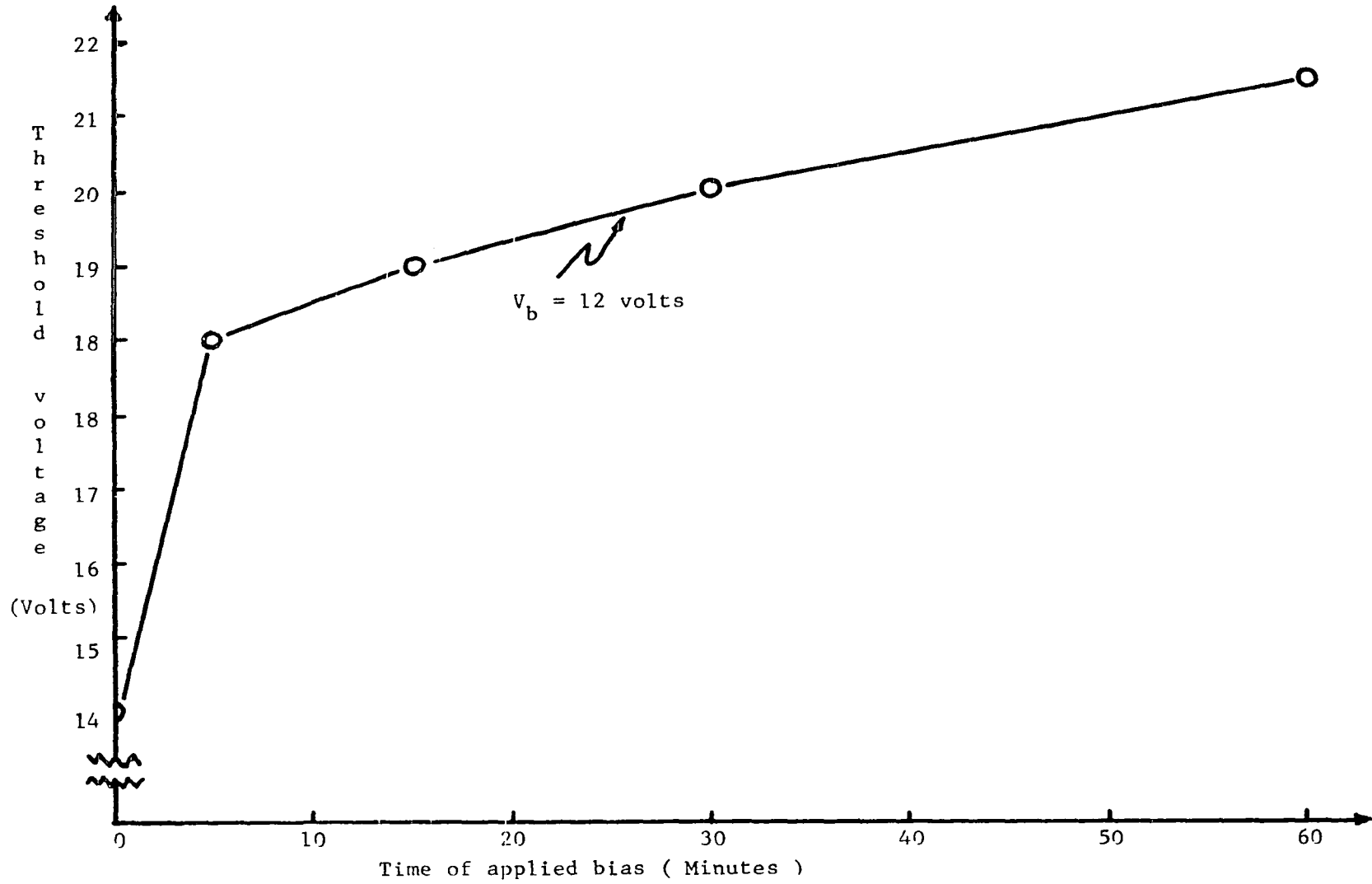
In the previous section, a reverse bias was placed on a poled crystal for selected lengths of time up to a maximum of one hour so as to establish the trend of the threshold voltage with time application of the reverse bias. In the preliminary tests conducted, it was proposed that in the limit the threshold voltage approached a value equal to the sum of the reference threshold voltage and the selected reverse bias voltage. However, in the preliminary tests time was not allowed for bias field formation and thus the reference threshold levels were in error.

To check the proposed relationship, it was decided to perform the modified test outlined in the previous section for the condition in which a reverse bias was applied for a 24 hour period prior to interrogation of the crystal. After a 10 minute internal bias formation period, a reverse bias which was measured accurately as 11.4 volts was applied to the crystal for a 24 hour period. Upon interrogation, the threshold

Table 4. Threshold voltage as a function of the time application of a 12 volt reverse bias to a crystal which was polarized and allowed a 10 minute bias stabilization period.

Bias Stabilization Time (Minutes)	Reverse Bias Application Time (Minutes)	Threshold (Volts)
10	0	14
10	5	19
10	15	20
10	30	21
10	60	22.5

Figure 17. Growth of threshold voltage from a stabilized level due to various time applications of a 12 volt reverse bias.



switching level was determined from the current versus applied voltage response to be 25.2 volts. In the previous section, the reference threshold following a 10 minute internal bias formation period was found to be 14 volts. Therefore, considering the experimental results it does appear that in the limit the threshold voltage is equal to the sum of the reference threshold (as determined after complete internal bias formation) and the selected reverse bias voltage.

Summary From Threshold Field Investigation

Considering the results of the preliminary experiments conducted by this author, the results of the modified experiments conducted by this author, the results of the experiments conducted by Cummins (33, 34), and the correlation of these findings, the following summary is presented below:

- a) Immediately following the polarization of a bismuth titanate single crystal, an internal bias field starts to form.
- b) Complete formation of the internal bias field requires a period of several minutes, e.g. in this investigation it was determined that 10 minutes was adequate for complete internal bias formation.
- c) The polarity of the formed internal bias is such that the existing polarization is made more stable.
- d) To reverse the polarization to the opposite state, the applied field must exceed a threshold level. The application for an extended length of time of a reverse bias (of

- d) magnitude less than the previously determined reference threshold level) to a poled sample causes the threshold level to increase with the limit on its final value being equal to the sum of the reference threshold and the selected bias. This change classifies the threshold field as apparent in nature. The complete change from the reference level to the final level requires the application of the reverse bias for a period of several hours.
- e) Steady state hysteresis loops indicate that some of these crystals exhibit a stable internal bias, i.e. their respective loops are shifted along the field axis. Depending upon the magnitude of the stable internal bias that each crystal possesses, the application of a reverse bias of magnitude less than the reference threshold to a poled sample can cause a reduction in the amount of reversible polarization. Crystals possessing high, stable internal bias fields exhibit this reduction while crystals possessing a low, stable internal bias field do not exhibit this reduction. The reduction in reversible polarization represents a decay, but recovery from this type of decay is possible through cycling of the crystal with a sine wave.
- f) Some crystals after repeated testing, which involved the pulsing and interrogation scheme previously described, exhibited a non-recoverable decay. Cracking of the crystals accompanied this decay. This "fatigue" represents a limitation

- f) which should be taken into account when considering the crystals in any potential device application.

INTERNAL FIELD SOURCE INVESTIGATION

Introduction

In an investigation of the ferroelectric colemanite, Wieder (15) found that the hysteresis loops were biased in many instances. He suggested that the internal bias might be the result of a space charge field which arises from the presence of non-stoichiometric impurities within the crystal lattice.¹¹ His experimental results confirmed the presence of a space charge field. He concluded that this space charge field was established by tightly bound charge carriers since the application of large fields for extended lengths of time had no effect on the space charge configuration.

In the previous chapter studies were conducted concerning (a) the formation of the internal bias field following polarization, (b) the amount of time required for this formation, (c) the alteration of the threshold field through the application of an external reverse bias, and (d) the amount of time required for the alteration of the threshold field. The experimental results obtained in the previous chapter lead to the hypothesis that a space charge field is responsible in part for the unusual switching characteristics that single crystals of bismuth titanate exhibit. The space charge field could arise from the presence of non-

¹¹ An exact correlation could not be made between the space charge field and the impurity concentration since it was discovered that crystals with small space charge fields were found to possess small concentrations of both silicon and strontium while those with large fields were found to possess large concentrations of both silicon and strontium.

stoichiometric impurities in the crystal. To explain the formation of the internal bias field following polarization and to explain the effect that an external reverse bias has on the threshold field, it would have to be assumed that the charge carriers associated with the impurities are not tightly bound in the lattice as was the case in colemanite, but are loosely bound and mobile under the influence of a field. The time required for internal bias field formation following polarization and the time required for threshold field alteration through the application of an external reverse bias seem to identify the charge carriers as ions.¹²

Theoretical Considerations

Consider the diagram in Figure 18 which represents a layered bismuth titanate crystal that has been polarized in the sense shown by a positive voltage pulse. The z component of the polarization causes the arrangement of the charges shown at the crystal surfaces and at the layer boundaries. At the layer boundaries the positive charges coincide with the negative charges and thus compensate for one another. However, at the crystal surfaces there is no compensation for the charge. These immobile, uncompensated charges produce an electric flux density and correspondingly an electric field within the material. If mobile ions of both polarities are present, then following the polarization of the crystal the depolari-

¹² As a point of interest Williams (46) found that all or part of the room temperature conductivity of BaTiO_3 is ionic. He speculated that the source of the mobile charge carriers was probably impurities or defects.

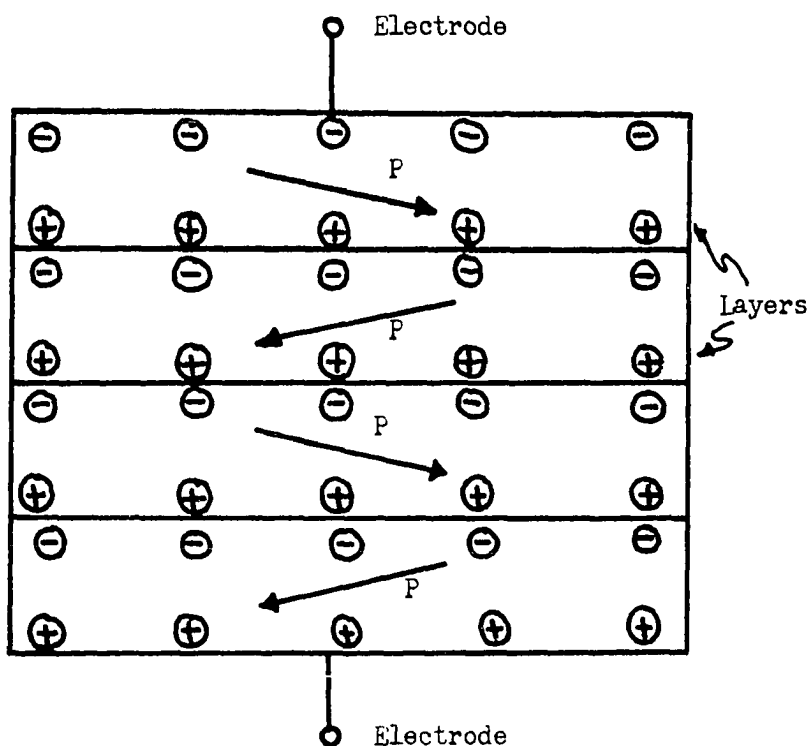


Figure 18. A simple representation of a polarized bismuth titanate single crystal showing induced charge on the electrode surfaces and the layer surfaces.

zation field will cause positive ions to migrate towards the negatively charged surface and negative ions to migrate towards the positively charged surface.¹³ It is assumed that solid electrodes block any further motion of the ions.¹⁴ Accordingly, following migration of these ions, a field would be established in opposition to the depolarization field.

To help explain some of the experimental results of the last chapter, a study of the fields in the material is necessary. For this simplified study consider first that a crystal has just been polarized and no significant ion migration has occurred. A simple representation of the polarization and the depolarization field for this situation is depicted in Figure 19a. As slow ion migration occurs, a field E_{ion} begins to develop in opposition to the depolarization field. These fields are shown in Figure 19b. Now consider at some time interval following the polarization that an interrogating field is applied in the reverse direction in order to switch the polarization. The reversing field, the depolarization field, and the field due to ion migration are all shown in Figure 19c. Considering these fields, then the field in the material is then given by

¹³In a solid which exhibits extrinsic ionic conductivity, generally ions of only one sign are mobile. Therefore, when these ions move towards the surface, they leave behind ions of the opposite sign. The net effect would be similar to the description above which was presented for the sake of simplicity.

¹⁴Williams (46) found mobile ions in single crystals of $BaTiO_3$ were blocked by solid type electrodes—specifically aluminum electrodes.

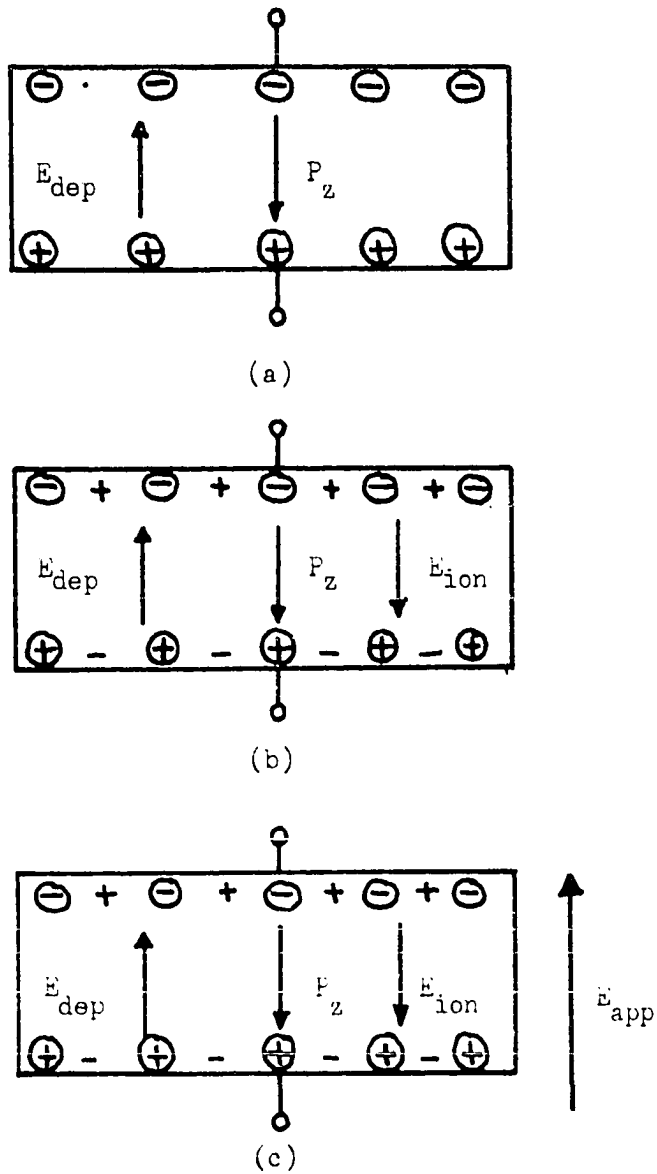


Figure 19. A simple representation of the fields for (a) the situation in which the crystal has just been polarized, (b) the situation in which an ion field appears, and (c) the situation in which a reversing field is applied.

$$E = E_{app} + E_{dep} - E_{ion} \quad (18)$$

Now assume that there definitely is a field level in the material that must be reached before polarization reversal can occur. Then reversal would begin when the field in the material was just equal to this threshold field, i.e. $E = E_t$. Thus, the applied field necessary to start reversal would be given by

$$E_{app} = E_t + E_{ion} - E_{dep} \quad (19)$$

It is evident in considering this relationship that as E_{ion} increases with time following the polarization that increasingly larger values of the applied field are necessary to produce reversal. This trend is consistent with the experimental results of the threshold field growth rate study conducted in the last chapter.

Now consider the situation in which following polarization and an internal bias field formation period, a crystal is biased in the reverse sense with a voltage of magnitude less than the magnitude of the applied voltage necessary to start reversal. The effect of the bias would be to increase the ionic field component. Now assume that after an extended application the bias voltage is removed and the crystal is interrogated. In Equation 19 if the actual threshold field and the depolarization field remain essentially constant and the ionic field increases, then in order to reverse the polarization of the crystal the applied field must reach a larger value than was necessary for reversal in the situation in which no

bias voltage was applied prior to interrogation. This trend is consistent with the experimental results obtained from the study conducted in the last chapter on the effect of a reverse bias voltage on the threshold switching level.

The assumed considerations and the simplified field study that was conducted permit an explanation of a number of the experimentally observed effects. The entire development leads to the assumption that the material might well possess a true threshold field characteristic, but due to unusual ionic effects the threshold field appears to be apparent in nature. At this point then it is necessary to determine from experimentation whether or not mobile ions are responsible for the unusual threshold field effects associated with this material.

Experimental Investigation

Ionic conductivity is, of course, temperature dependent. In the presence of a field, ions should migrate faster with increasing temperature. Therefore, if ions are responsible for the formation of the internal bias field, then a change in the ambient temperature conditions should have an effect on the threshold field growth rate that results following polarization of a crystal.

In order to check for this dependency, it was decided to perform the internal bias formation test which was described in the last chapter for two ambient temperature conditions. First, a crystal was placed in an environment of $T_a = 3^\circ\text{C}$ and was held there for a period of 20 hours. Following this holding period, the internal bias formation test was

performed. The crystal was then placed in an environment of $T_a = 26^\circ\text{C}$ and was held there for a period of 20 hours. Following the holding period, the internal bias formation test was repeated. For each test, current versus applied voltage responses were photographed. From the photos the threshold switching level was determined for each time increment following the polarization. The elapsed time following polarization and the threshold voltage level for each of the temperature conditions are listed in Table 5. A plot of the threshold voltage level versus the elapsed time following polarization for each of the ambient temperature conditions is shown in Figure 20.

For each temperature condition, a portion of the fast response and a portion of the slow response are shown. From an examination of the curves, it is evident that the threshold growth rate is slower for the lower temperature condition. As an example, note that the 13 volt level is achieved in 120 seconds for $T_a = 26^\circ\text{C}$ while the same level is achieved in 300 seconds for $T_a = 3^\circ\text{C}$.

Conclusions

In this investigation of the source of the internal bias field, the following assumptions were made:

- a) The depolarization field produced by the saturation polarization causes charge carrier motion.
- b) The charge carriers in this instance are mobile ions.
- c) The movement of the ions results in the development of a space charge field or ionic field which opposes the depolarization field.

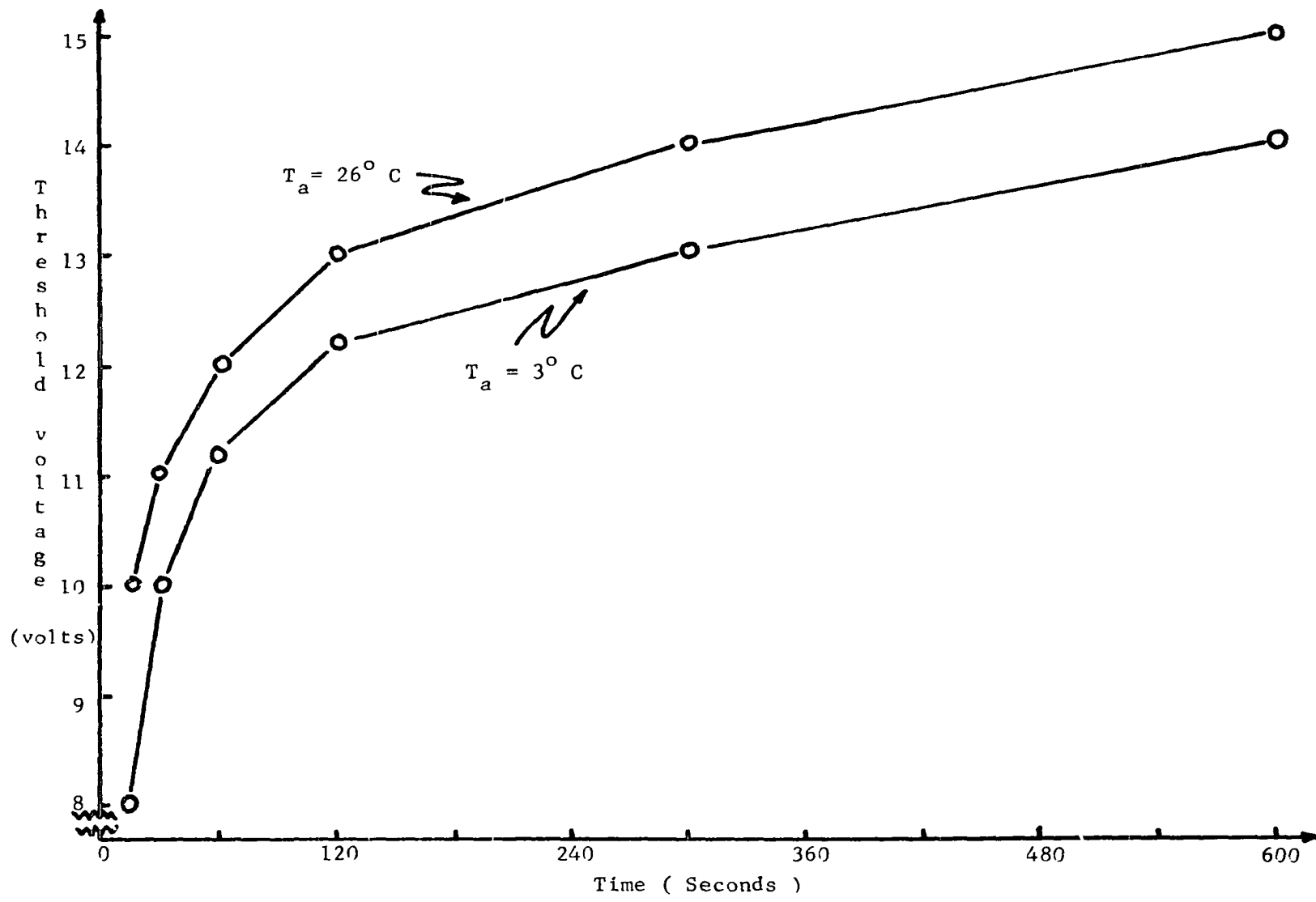
With these assumptions in mind, a study of the fields within the material was conducted. It was shown that as the ionic field increased with time, the applied field required to reverse the polarization also increased with time. This variation is consistent with the observed experimental results of the preceding chapter.

The threshold growth rate was examined as a function of ambient temperature. It was noted that the threshold growth rate decreased for decreasing temperature. Thus, this author concludes that ions are the source of the internal bias field. This conclusion is based on the fact that ion migration is slower for decreasing temperature and correspondingly this would result in a slower threshold growth rate.

Table 5. Threshold voltage as a function of elapsed time following the polarization of a bismuth titanate single crystal for two ambient temperature conditions.

Elapsed time (seconds)	Threshold (volts) $T_a = 3^{\circ}\text{C}$	Threshold (volts) $T_a = 26^{\circ}\text{C}$
15	8	10
30	10	11
45	10.8	-
60	11.2	12
120	12.2	13
300	13	14
600	14	15

Figure 20. Growth of threshold voltage following polarization of a bismuth titanate single crystal for two ambient temperatures.



DOMAIN DYNAMICS

General Comments

Fousek and Janovec (48) have shown that it is possible to derive the orientations of domain walls in any ferroelectric if (a) the orientations of the possible polarization vectors are known and (b) the point group symmetry of the paraelectric phase is known. Considering the paraelectric point symmetry of $4/mmm$ as was determined by Aizu (44) and the four possible orientations of the polarization vector,¹⁵ Cummins and Cross (42) established eighteen possible domain wall configurations. These eighteen wall configurations are illustrated in Figure 21 a-r. The polarization directions which are shown on the "monoclinic cells"¹⁶ are given in terms of the uvw indices of the tetragonal paraelectric phase.

Using optical techniques Cummins and Cross (42) were able to observe the various domain walls in virgin crystals and in crystals to which electric fields had been applied. They were able to observe domain walls corresponding to those illustrated in Figure 21 c-r. The possibilities illustrated in Figure 21 a-b were not observed since they represent anti-parallel walls which are not optically distinguishable with the technique utilized. From their investigation of virgin crystals they found stable

¹⁵The polarization vector is perpendicular to one of the four fold axes of the original paraelectric state. Therefore, considering both axes there are eight possible vector directions.

¹⁶The cells are shown in a tetragonal form. To truly represent the monoclinic situation, a slight tilting of the cell should be shown.

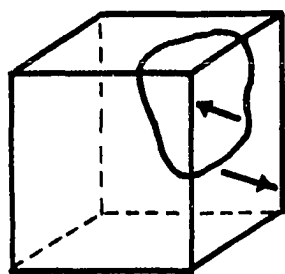
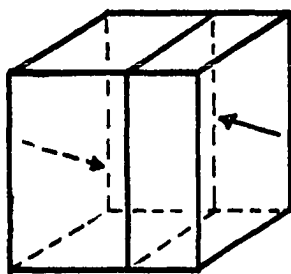
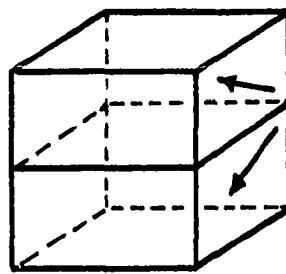
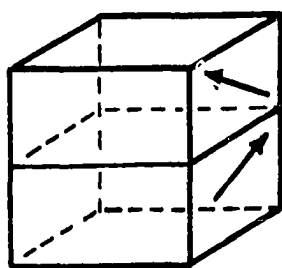
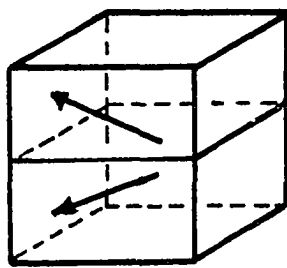
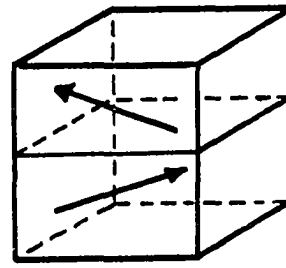
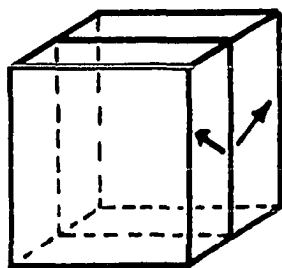
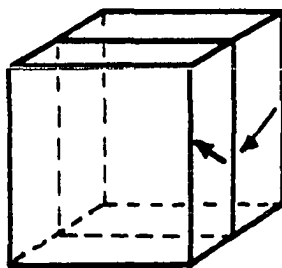
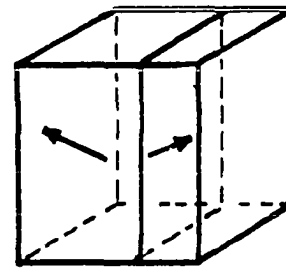
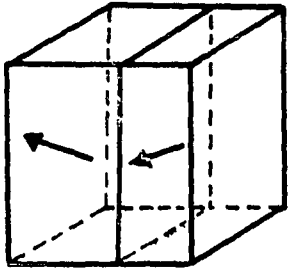
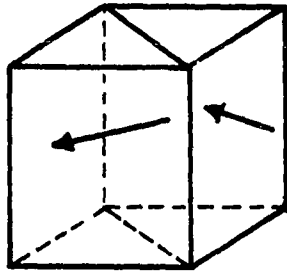
a) $uw \bar{u}\bar{w}$ b) $uw \bar{u}\bar{w}$ c) $uw u\bar{w}$ d) $uw \bar{u}\bar{w}$ e) $u\bar{w} u\bar{w}$ f) $u\bar{w} \bar{u}\bar{w}$ g) $uw \bar{u}\bar{w}$ h) $uw u\bar{w}$ i) $u\bar{w} \bar{u}\bar{w}$

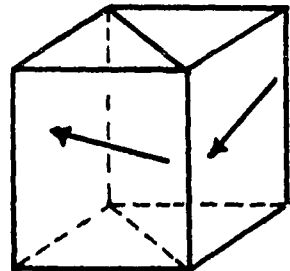
Figure 21. Domain wall possibilities in bismuth titanate.



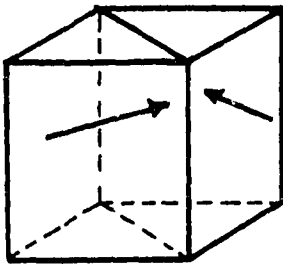
j) $u\bar{u}w \quad u\bar{u}\bar{w}$



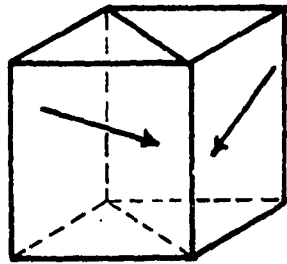
k) $u\bar{u}w \quad u\bar{u}\bar{w}$



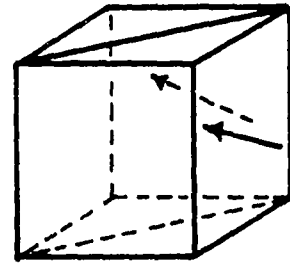
l) $u\bar{u}w \quad u\bar{u}\bar{w}$



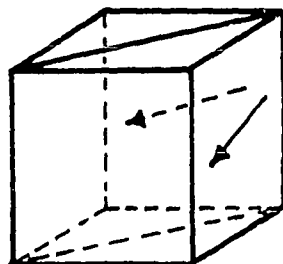
m) $u\bar{u}w \quad \bar{u}\bar{u}w$



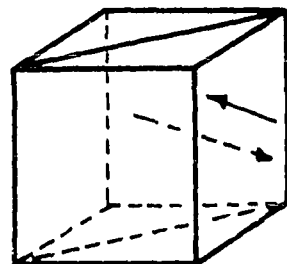
n) $\bar{u}\bar{u}\bar{w} \quad u\bar{u}\bar{w}$



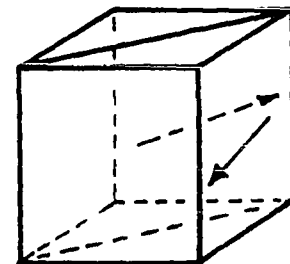
o) $u\bar{u}w \quad u\bar{u}\bar{w}$



p) $u\bar{u}\bar{w} \quad u\bar{u}\bar{w}$



q) $u\bar{u}w \quad \bar{u}\bar{u}\bar{w}$



r) $u\bar{u}\bar{w} \quad \bar{u}\bar{u}w$

Figure 21. (Continued)

walls parallel to the a-b plane (Figure 21 c-f) and stable 90 degree walls (Figure 21 k-r). In crystals which were partially switched due to the application of electric fields, they found walls parallel to the b-c plane (Figure 21 g-j). Their experimental results verified the assumed point symmetry of $4/mmm$ and the ferroelectric species classification of $F4/mmm$ (4) A2.

Domain wall Formation

A point of primary concern is the manner in which the various polarization regions combine to form the possible domain wall configurations. It is of interest to determine whether the regions with their respective polarization directions fit together with or without stress. This can be accomplished by considering the four basic monoclinic cell forms shown in Figure 21 and then by considering the manner in which they must combine to form the various wall configurations that Cummins and Cross (42) found to exist in this material. The four basic monoclinic cell forms which are shown in Figure 22 can be described mathematically as follows:

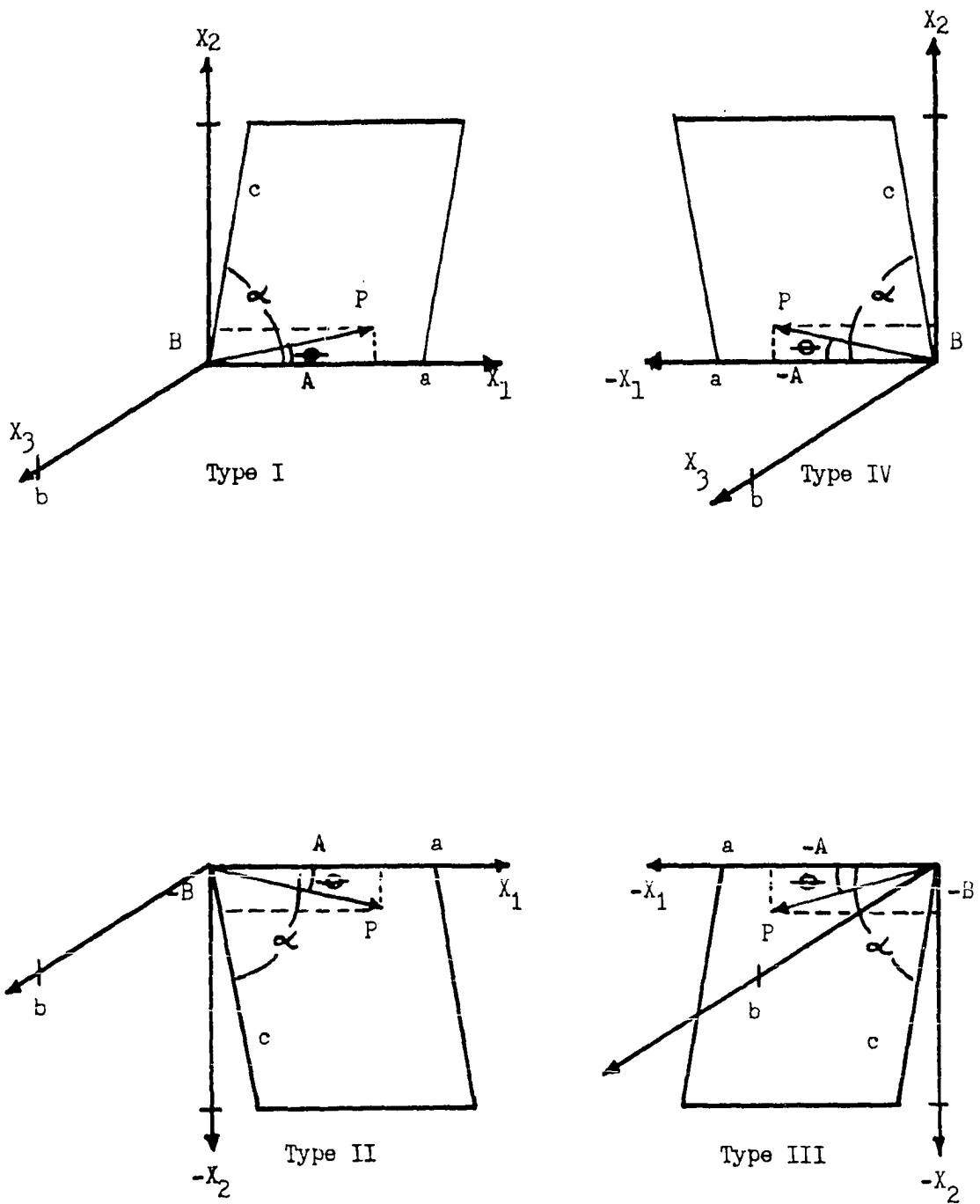


Figure 22. Monoclinic cell forms showing four possible polarization orientations.

a) Type I -

$$\bar{P} = \begin{vmatrix} A \\ B \\ 0 \end{vmatrix} \quad \bar{a} = \begin{vmatrix} a \\ 0 \\ 0 \end{vmatrix} \quad \bar{b} = \begin{vmatrix} 0 \\ 0 \\ b \end{vmatrix} \quad \bar{c} = \begin{vmatrix} c \cos \alpha \\ c \sin \alpha \\ 0 \end{vmatrix}$$

b) Type II -

$$\bar{P} = \begin{vmatrix} A \\ -B \\ 0 \end{vmatrix} \quad \bar{a} = \begin{vmatrix} a \\ 0 \\ 0 \end{vmatrix} \quad \bar{b} = \begin{vmatrix} 0 \\ 0 \\ b \end{vmatrix} \quad \bar{c} = \begin{vmatrix} c \cos \alpha \\ -c \sin \alpha \\ 0 \end{vmatrix}$$

c) Type III -

$$\bar{P} = \begin{vmatrix} -A \\ -B \\ 0 \end{vmatrix} \quad \bar{a} = \begin{vmatrix} -a \\ 0 \\ 0 \end{vmatrix} \quad \bar{b} = \begin{vmatrix} 0 \\ 0 \\ b \end{vmatrix} \quad \bar{c} = \begin{vmatrix} -c \cos \alpha \\ -c \sin \alpha \\ 0 \end{vmatrix}$$

d) Type IV -

$$\bar{P} = \begin{vmatrix} -A \\ B \\ 0 \end{vmatrix} \quad \bar{a} = \begin{vmatrix} -a \\ 0 \\ 0 \end{vmatrix} \quad \bar{b} = \begin{vmatrix} 0 \\ 0 \\ b \end{vmatrix} \quad \bar{c} = \begin{vmatrix} -c \cos \alpha \\ c \sin \alpha \\ 0 \end{vmatrix}$$

A 90 degree rotation about the axis X_2 will yield four more possibilities and thus will allow a complete description of all the possible wall configurations in this material. A simple representation of the original system and the rotated system is illustrated in Figure 23a and Figure 23b, respectively.

The 180° domain wall possibilities are illustrated in Figure 21 a-j. Of these possibilities it can be shown that those represented by Figure 21 a-f correspond to what can be considered as "stress free" type walls

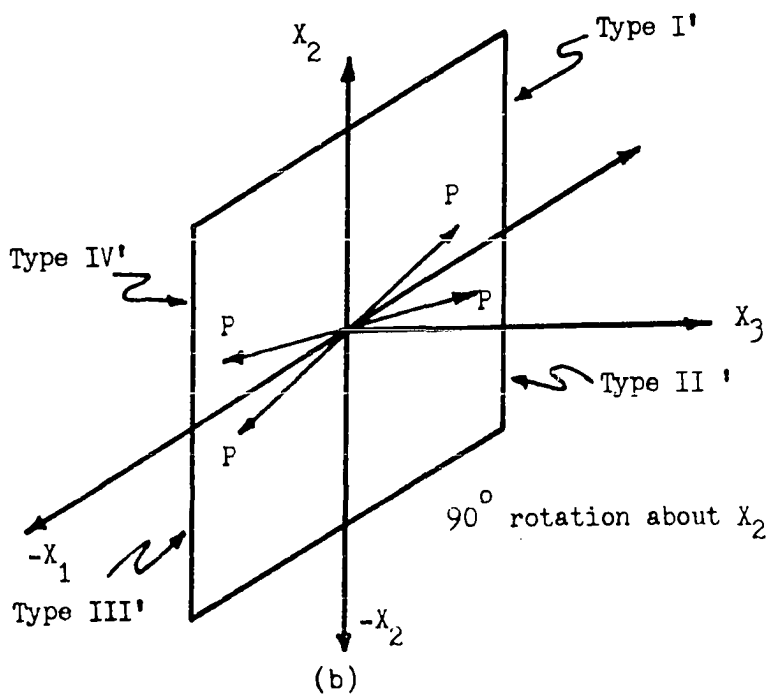
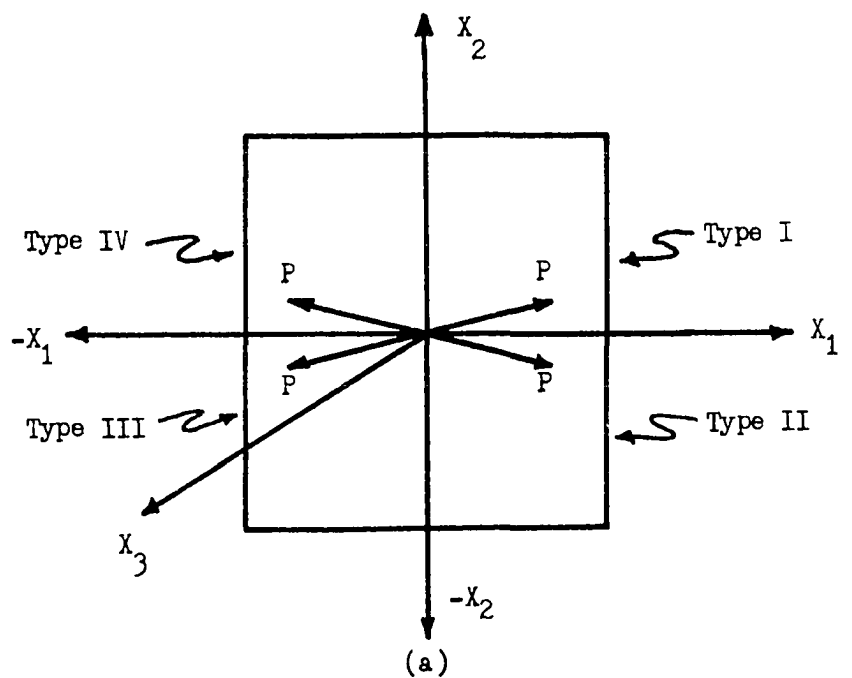


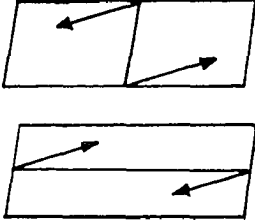
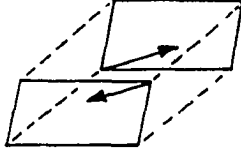
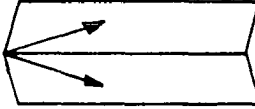
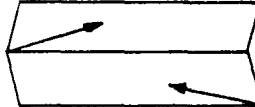
Figure 23. Simple representation of (a) the four types of "monoclinic" cell forms and (b) the four types derived from a 90° rotation about X_2 .

in that the respective monoclinic cells can be matched together in a stress free manner. To illustrate how these combinations are accomplished reference is made to Table 6 which gives the allowable wall configuration, the formation procedure required, and an illustration of the resulting configuration. Note in each case that the monoclinic cells combine in a stress free manner. These basic wall configurations are present in virgin crystals according to Cummins and Cross (42).

It is of interest to note that the remaining four 180° domain wall possibilities as are shown in Figure 21 g-j do not represent stress free wall combinations. The required combination of monoclinic cells cannot be accomplished in a stress free manner and thus for these wall combinations to exist there must be a stress distribution. It is expected that a wall of this nature is not smooth, but is irregular or jagged due to the stress distribution along the wall. This assumption is substantiated to some extent by a photomicrograph of a virgin crystal taken by Cummins and Cross (42) which showed a rather jagged domain wall for a situation similar to the combination shown in Figure 21 i.¹⁷ Cummins and Cross (42) noted these type walls were present in crystals which were partially switched due to the application of electric fields. This indicates the presence of domain wall stress conditions during the reversal of polarization by the application of an external field.

¹⁷Domain wall stress conditions must exist in the virgin crystal if these type walls are present.

Table 6. Methods for forming 180° stress free wall combinations in virgin $\text{Bi}_4\text{Ti}_3\text{O}_{12}$ single crystals.

Allowable Wall Configuration	Formation Procedure	Illustration
a. Figure 20a	<p>Translation of III in $+X_2$ direction: matched in plane formed by b and c.</p> <p>Combination of I and III matched at $X_2 = 0$.</p>	
b. Figure 20b	<p>Translation of III in $+X_1$ direction and then $+X_2$ direction. Combined at $X_3 = 0$.</p>	
c. Figure 20c	<p>Combination of I and II matched at $X_2 = 0$.</p>	
d. Figure 20d	<p>Translation of IV in $-X_2$ direction: Combined with I at $X_2 = 0$.</p>	
e. Figure 20e	<p>Requires 90° rotation of 4 basic types. Combined in manner similar to c above.</p>	<p>Same as c above.</p>
f. Figure 20f	<p>Requires 90° rotation of 4 basic types. Combined in manner similar to d above.</p>	<p>Same as d above.</p>

The 90° domain walls which are shown in Figure 21 k-r are present in the virgin crystals. These walls are the result of 90° twins which form during crystal growth.¹⁸ The twinning in the virgin crystals is a result of the four possible spontaneous polarization directions which can be present in this material. It is possible to form the 90° type walls in a stress free fashion. However, the combination technique for forming the 90° type walls is somewhat more complicated than the technique utilized in forming the 180° type walls. First, the formation requires the cell lengths as are shown in Figure 22 to be equal in length and secondly the combinations must be made along specific diagonal planes. The necessary formation procedures for the allowable wall configurations are listed in Table 7, and the corresponding illustration of each combination is shown in Figure 24 a-h. It should be noted though that these walls are of little concern when considering polarization reversal along the c axis, but are of primary concern when considering polarization reversal along the b axis.

Polarization Reversal Analysis

Hamilton (41) using x-ray techniques to investigate the threshold field effect in this material noted that distinct rearrangement of the crystallographic structure occurred as the polarization was reversed from one saturation state to the opposite saturation state. A general shift

¹⁸Pulvari (32) annealed the crystals to remove this 90° type twinning. See Appendix A.

Table 7. Methods for forming 90° stress free wall combinations in $\text{Bi}_4\text{Ti}_3\text{O}_{12}$ single crystals using "monoclinic cells" with $\alpha = 90^\circ$ and with restriction $a=b$.

Allowable Wall Configuration	Formation Procedure
Figure 2lm	Translation of I' in $+X_3$ direction. Combined with I along a diagonal plane passing thru a and b of I.
Figure 2ln	Translation of III' in $+X_2$ direction. Combined with I along a diagonal plane passing thru a and b of I.
Figure 2lk	Translation of II in $+X_2$ direction. Combined with IV' along diagonal plane passing thru a and b of II.
Figure 2ll	Translation of II' in $+X_2$ and then $+X_3$ direction. Combined with translation of II in $+X_2$ direction along diagonal plane passing thru a and b of II.
Figure 2lq	Combination of I with IV' along diagonal plane passing thru origin and opposite corner of I.
Figure 2lr	Translation of II' in $+X_2$ direction and then $+X_3$ direction. Combined with I along diagonal plane passing thru origin and opposite corner of I.
Figure 2lo	Translation of III' in $+X_2$ direction. Combined with translation of II in $+X_2$ direction along diagonal plane passing thru origin and opposite corner of II.
Figure 2lp	Translation of I' in $+X_2$ direction. Combined with translation of II in $+X_2$ direction along diagonal plane passing thru origin and opposite corner of II.

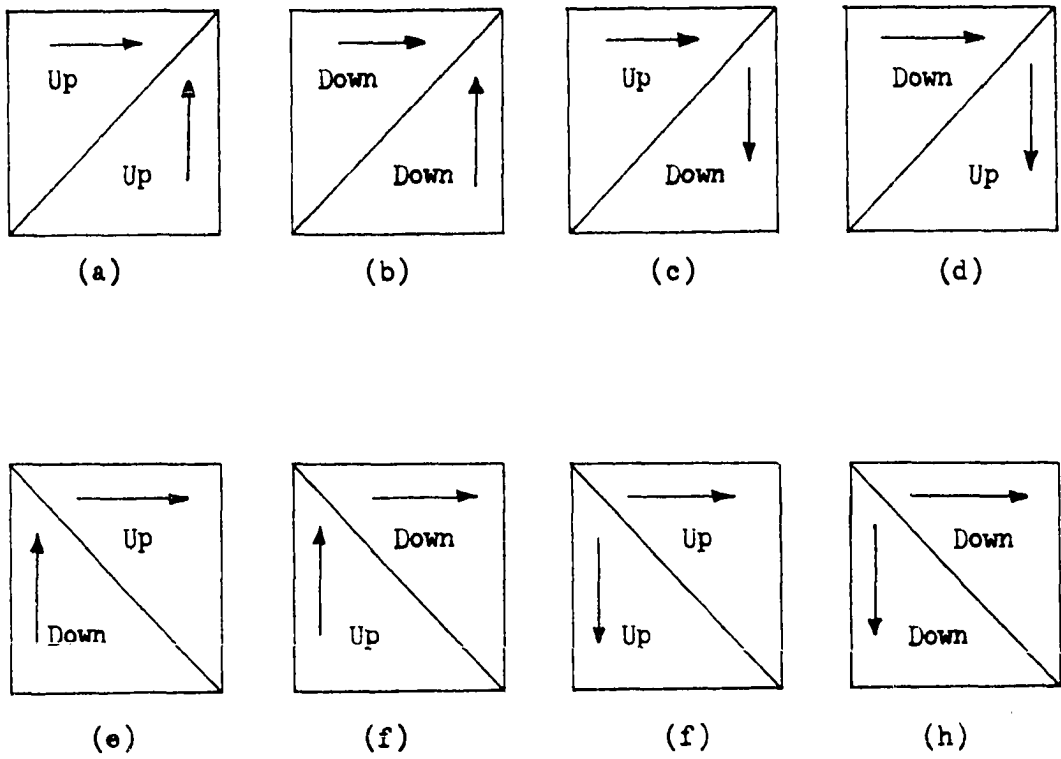


Figure 24. Combination techniques for formation of 90° wall possibilities.

in atomic positions was expected, but in this instance Hamilton (41) found a remanent structural rearrangement of the unit cell resulted. Cummins and Cross (42) using optical techniques to study polarization reversal in these crystals noted that switching occurred by a unique rocking of the large polarization, P_s , through a small angle.¹⁹ Since the polarization P_s must lie along only one direction with respect to the monoclinic axes, they concluded that a change in the direction of the monoclinic " β " was necessary to explain the reversal.

Considering the results of Hamilton (41) and Cummins and Cross (42), it can be concluded that reversal from one saturation state to the other requires a simple re-orientation of the typical monoclinic cell. To demonstrate this reference is made to Figure 25a which shows a typical monoclinic cell and one possible polarization orientation while Figure 25b shows the same cell after reversal to the opposite state. The c component of the polarization reverses while the horizontal component remains the same. To account for these polarization directions the monoclinic " β " of the unit cell must change as is noted in Figure 25.

In general, for ordinary ferroelectrics the mechanism of polarization reversal from one saturation state to the other saturation state usually involves four basic steps. A description of this procedure is given below:

¹⁹The polarization P_s makes an angle of 4.5° with respect to the a-b plane and thus P_s moves through an angle of 9° when switched from one saturation state to the other saturation state.

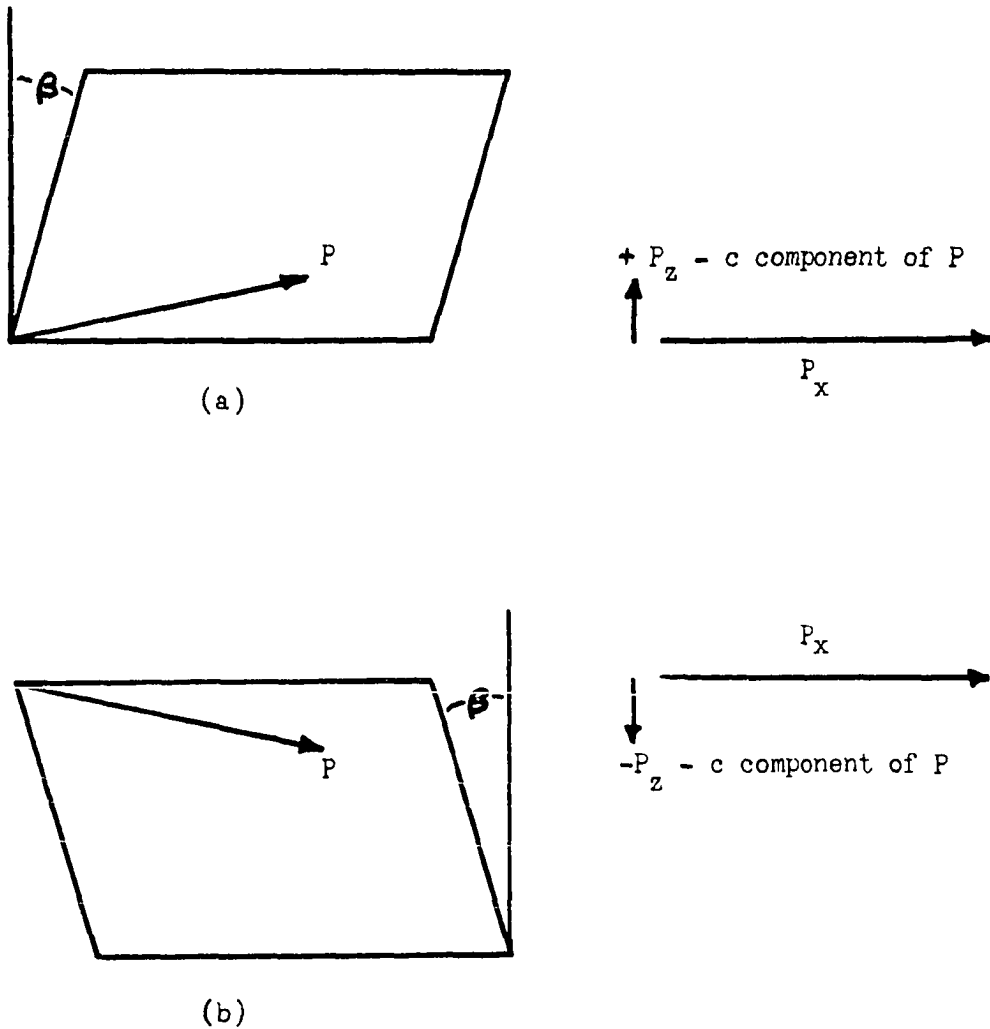


Figure 25. Illustration of (a) a typical monoclinic cell and the corresponding polarization components and (b) a re-oriented monoclinic cell and the corresponding polarization components which result from a reversal of the polarization.

- a) First new domains are nucleated through the application of an external field.
- b) These new domains then grow through the crystal in a forward manner.
- c) The newly formed domains grow sideways through the crystal.
- d) The domains coalesce thus leaving the polarization of the crystal reversed from its original saturation state.

An illustration of these steps is given in Figure 26 a-f. In Figure 26a, the crystal polarization is in a saturated state. The application of a reversing field causes new domains to nucleate as is shown in Figure 26b. These domains grow in a forward fashion as is shown in Figure 26c, until they grow through the crystal as is shown in Figure 26d. After having grown through the crystal, the domain walls start to move sideways²⁰ as is shown in Figure 26e. While these domains grow, new domains are nucleated and begin a similar growth. Sideways expansion of the domains continues until the new domains coalesce thus leaving the polarization of the crystal in the opposite saturation state as is shown in Figure 26f.

Bismuth titanate single crystals are quite unique in that they are "mica-like" in structure, i.e. the crystals possess a layered structure. (For a complete description of their physical appearance, reference is made to Appendix A). The layers, which are parallel to the crystal plate

²⁰Miller and Weinreich (49) in studying sideways expansion of domains in BaTiO_3 found the nucleation probability to be larger next to an existing wall. Nucleation next to an existing wall gives the effect of sideways expansion of the domain.

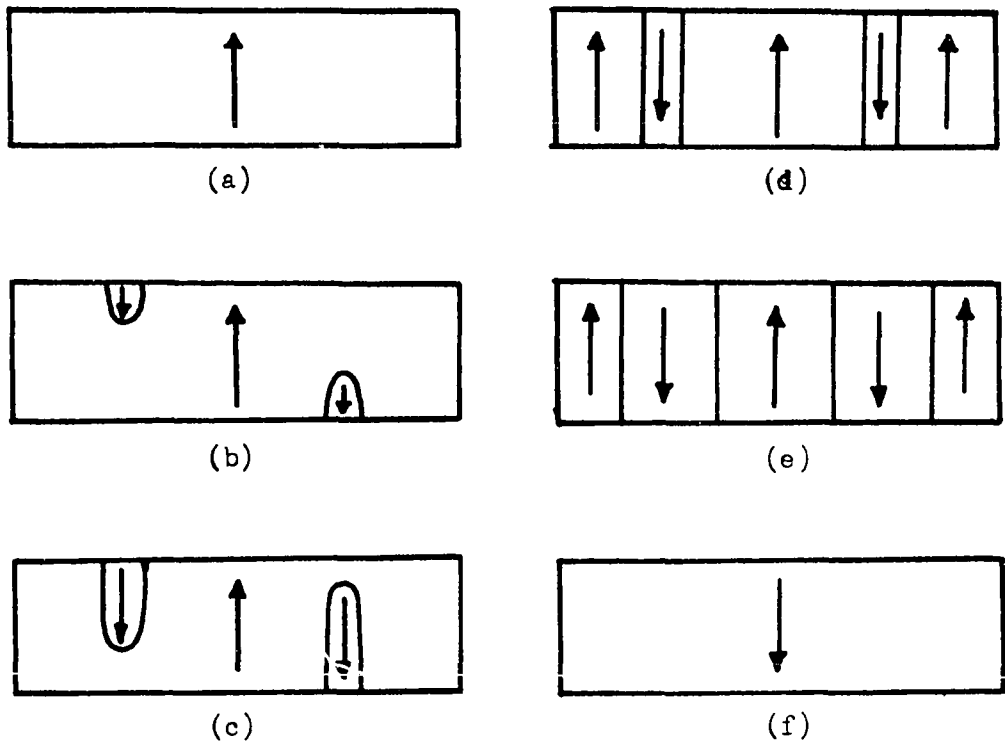


Figure 26. Typical forward and sideways growth of domains in ferroelectrics.

surfaces, are approximately 4000 \AA thick according to McDonnell (29). Therefore, a crystal of thickness $d = 4$ mils would be composed of approximately 25^4 such layers. Considering this "mica-like" structure, the mechanism of polarization reversal in the crystal must be somewhat different than that described in the previous paragraph which pertained to "bulk-like" crystals. Cummins and Cross (42) noted switching in this material to occur by nucleation of new domains and by apparent wall motion, but they did not examine the exact process of reversal. Considering their observations and the structure of this material, it is possible to theorize about the manner in which switching along the c axis occurs in this material. It seems appropriate to assume that the four basic steps -- nucleation, forward domain growth, sideways domain growth, and domain coalescence -- are still involved, but these processes occur within the individual layers. Speaking strictly from a theoretical standpoint, this author offers the following steps as a possible explanation of the reversal process:

- a) Once the apparent threshold field is overcome, nucleation probably takes place at the surfaces in the outer layers.
- b) Considering one such layer, the nucleated domains would grow quite rapidly through the thin layer.
- c) Sideways expansion would follow once the domains were through the layer.
- d) Additional nucleation and growth would occur while the initial domains grow. This nucleation is probably enhanced by an increase in the field in the unswitched region of

- d) the layer. (Nucleation next to an existing reversed domain could explain the sideways expansion noted in (c) above.)
- e) Reversal within a layer would also tend to alter the field intensity in the inner layers. Thus, while the process of reversal occurs in the outer layers, nucleation would begin in the inner layers with a similar growth process occurring.
- f) Eventually, coalescence of domains would occur in all the layers and the crystal polarization would be completely reversed.

The previous description was offered to provide insight into how reversal might be accomplished. Verification of this proposed reversal process represents a problem of such magnitude that this author suggests that the topic be treated in a separate research investigation.

In crystals that were partially switched due to the application of external fields, Cummins and Cross (42) noted the presence of domain walls corresponding to the types shown in Figure 21 g-j. The types shown in Figure 21g and Figure 21i are similar and thus will be referred to as "A" walls by this author. Likewise those shown in Figure 21h and Figure 21j are similar and thus will be referred to as "B" walls. In considering polarization reversal within a region, it was previously noted that this was accomplished by a reversal of the c component of the polarization with the horizontal component remaining the same. Therefore, considering this fact, it can be concluded that the "A" walls do not relate to the situation in which polarization is being reversed within a region. As was previously mentioned these "A" type walls were noted to be present in virgin crystals

as well as in crystals which were partially switched due to the application of external fields. It is anticipated that these "A" walls do not move, but remain essentially stationary during reversal. While polarization reversal is occurring, it is expected that the stress distribution along this type of wall changes, and this results in a slight modification of the wall shape.

It is evident that "B" walls are related to the situation in which polarization is being reversed within a region since the c components on either side of such a wall are opposite in sign while the respective horizontal components are of the same sign. It is anticipated that these "B" walls appear within a region after forward growth of nucleated domains is completed and that these "B" domain walls apparently move sideways through the region until they coalesce with similar domains thus leaving the polarization completely reversed.

To illustrate typically the anticipated reversal process and to demonstrate the roles that the "A" and "B" walls play, reference is made to the sequence shown in Figure 27 a-d which shows in a theoretical sense how polarization reversal might be accomplished within a single layer of this type of material. In Figure 27a the polarization in each region is in the same saturation state, and these regions are separated by an "A" wall. After the apparent threshold field effect has been overcome, the applied field causes nucleation to occur within the layer and the new domains grow through the crystal as is shown in Figure 27b. The "B" walls apparently move sideways (possibly the result of nucleation next to an existing domain) as is shown in Figure 27c, and eventually the polariza-

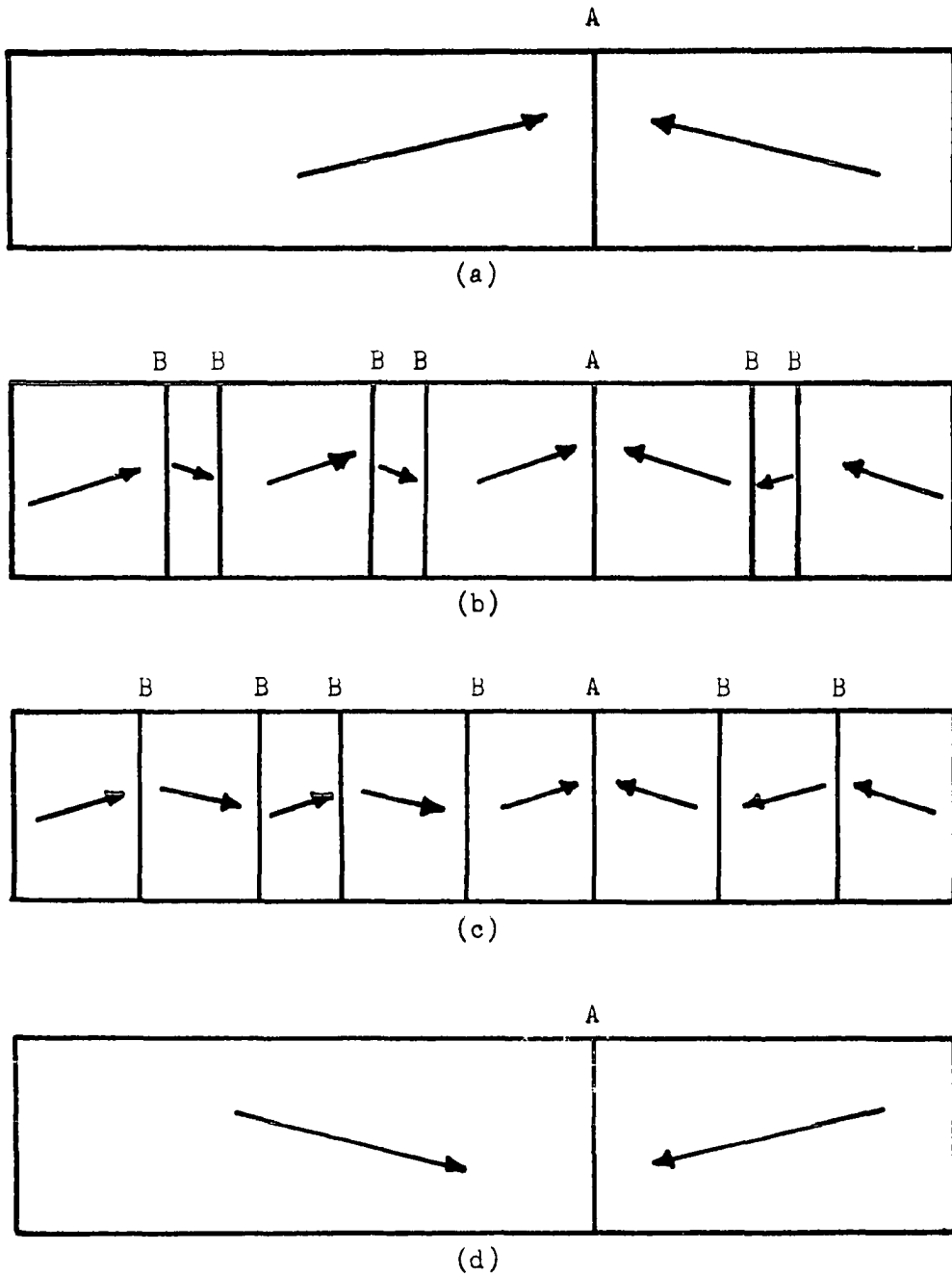


Figure 27. Theoretical forward and sideways growth of domains in a single layer of the ferroelectric bismuth titanate.

tion in each region is completely reversed as is shown in Figure 27d. As is evident in this example, the "A" walls remain essentially stationary while the "B" walls apparently move.

It is of interest to note that there is a stress or more precisely a stress distribution associated with both "A" and "B" walls.²¹ During the process of polarization reversal there is the appearance of stress distributions associated with "B" walls, and there is a change in stress distributions associated with "A" walls. This author considers the stress distributions that occur during the reversal process to be directly related to the cracking of the crystals which was experimentally noted and considers this cracking to be the physical origin of the nonrecoverable decay which occurred in the crystals after repeated switching.

Conclusions

In this chapter a study was made of the 18 possible domain wall configurations of bismuth titanate which has a symmetry of monoclinic point group m . The manner in which unit monoclinic cells with their respective polarizations must combine in order to form the various wall configurations was investigated. It was noted that the 180° domain walls which are present during reversal along the c axis could not be formed in a stress

²¹The "A" and "B" walls should not be smooth in nature but should be rather irregular or jagged because of stress distribution. The walls shown in Figure 27 a-d are shown as smooth walls merely for simple demonstration purposes.

free fashion. A stress distribution must be associated with these walls.

A theoretical study of the reversal process in this material was conducted. The roles of the above mentioned 180° walls in the reversal process were examined. During reversal the stress distributions associated with these walls must change. This author considers this change in stress distribution to be responsible for sample cracking and correspondly for the nonrecoverable decay in reversible polarization exhibited by some test samples.

COMMENTS

The goals of this author were (a) to perform an original investigation of polarization reversal in bismuth titanate, (b) to examine in detail the threshold field phenomenon, (c) to determine any limitations that might hamper device application, and (d) to examine the mechanism associated with polarization reversal. In the opinion of this author these goals were successfully achieved. A final summary or conclusion chapter is not presented at this point since in the development of the topic the author has presented major summaries at the end of each chapter.

BIBLIOGRAPHY

1. Wert, C. A. and Thomson, R. M. Physics of solids. 1st ed. New York, New York, McGraw-Hill Book Co., Inc. 1964.
2. Levy, R. A. Principles of solid state physics. 1st ed. New York, New York, Academic Press. 1968.
3. Beam, W. R. Electronics of solids. 1st ed. New York, New York, McGraw-Hill Book Co., Inc. 1965.
4. Nye, J. F. Physical properties of crystals. 1st ed. London, England, Oxford-at the Clarendon Press. 1964.
5. Kittel, C. Introduction to solid state physics. 3rd ed. New York, New York, John Wiley and Sons, Inc. 1966.
6. Dekker, A. J. Solid state physics. 4th ed. Englewood Cliffs, New Jersey, Prentice Hall, Inc. 1960.
7. Elliott, R. S. Electromagnetics. 1st ed. New York, New York, McGraw-Hill Book Co., Inc. 1966.
8. Wang, S. Solid state electronics. 1st ed. New York, New York, McGraw-Hill Book Co., Inc. 1966.
9. Jaynes, E. T. Ferroelectricity. 1st ed. Princeton, New Jersey, Princeton University Press. 1953.
10. Jona, F. and Shirane, G. Ferroelectric crystals. 1st. ed. New York, New York, The Macmillan Company. 1962.
11. Fatuzzo, E. and Merz, W. J. Ferroelectricity. 1st ed. New York, New York, John Wiley and Sons, Inc. 1967.
12. Merz, W. J. Domain formation and domain wall motions. Physical Review 95, No. 3: 690-698. August 1954.
13. Fatuzzo, E. and Merz, W. J. Switching mechanism in triglycine sulfate. Physical Review 116, No. 1: 61-68. October 1959.
14. Wieder, H. H. Model for switching and polarization reversal in colemanite. Journal of Applied Physics 31, No. 1: 180-187. January 1960.
15. Wieder, H. H. Ferroelectric properties of colemanite. Journal of Applied Physics 30, No. 7: 1010-1018. July 1959.

16. Pulvari, C. F. Ferrielectrics as a possible computer element. U. S. Department of Commerce Technical Documentary Report No. ASD TDR 61-331. October 1961.
17. Pulvari, C. F. Ferrielectricity. *Physical Review* 120, No. 3: 1670-1673. December 1960.
18. Cross, L. E. A thermodynamic treatment of ferroelectricity and anti-ferroelectricity in pseudo-cubic dielectrics. *Philosophical Magazine* 1, No. 1: 76-92. January 1956.
19. Kanzig, W. Solid state physics. Volume 4. New York, New York, Academic Press, Inc. 1957.
20. Goldsmith, G. J. and White, G. J. Ferroelectric behavior of thiourea. *Journal of Chemical Physics* 31, No. 5: 1175-1187. November 1959.
21. Miller, R. C., Wood, E. A., Remeika, J. P., and Savage, A. $\text{Na}(\text{Nb}_{1-x}\text{V}_x)\text{O}_3$ system and ferrielectricity. *Journal of Applied Physics* 33, No. 5: 1623-1630. May 1962.
22. Shuvalov, L. A. and Sonin, A. S. The crystallography of anti-ferroelectrics. *Soviet Physics - Crystallography* 6, No. 3: 258-262. November 1961.
23. Pulvari, C. F. Progress in solid state chemistry. Volume 1. New York, New York, Pergamon Press, Inc. 1964.
24. Aurivillius, B. Mixed bismuth oxides with layer lattices; II structure of $\text{Bi}_4\text{Ti}_3\text{O}_{12}$. *Arkiv for Kemi* 1, No. 58: 499-512. 1949.
25. Subbarao, B. C. Ferroelectricity in bismuth titanate and its solid solutions. *Physical Review* 122, No. 3: 804-807. May 1961.
26. Van Uitert, L. G. and Egerton, L. Bismuth titanate. A Ferroelectric. *Journal of Applied Physics* 32, No. 5: 959. May 1961.
27. Fang, P. H. and Fatuzzo, E. Switching properties in ferroelectrics of the family $\text{Bi}_4\text{Ba}_{m-2}\text{Ti}_{m+1}\text{O}_{3(m+2)}$. *Physical Society of Japan Journal* 17, No. 1: 238. January 1962.
28. Fang, P. H., Robbins, C. R., and Aurivillius, B. Ferroelectricity in the compound $\text{Bi}_4\text{Ti}_3\text{O}_{12}$. *Physical Review* 126, No. 3: 892. May 1962.

29. McDonnell, F. E. Domain dynamics and threshold switching phenomena in ferrielectrics. Unpublished Ph.D. thesis. Washington, D.C., Library, The Catholic University of America. 1963.
30. Pulvari, C. F. Ferrielectrics and their applications in solid-state devices as an adaptive control. IEEE Transactions on Military Electronics, No. 2 and No. 3: 254-260. April-July 1963.
31. Tambovtsev, D. A., Skorikov, V. M., and Zheludev, I. S. Production of bismuth titanate single crystals and some of their properties. Soviet Physics - Crystallography 8, No. 6: 713-716. May-June 1964.
32. Pulvari, C. F. Mixed bismuth oxide (MBO) type ferrielectrics. Department of Commerce Technical Documentary Report No. AL TDR 64-124. May 1964.
33. Cummins, S. E. Effects of constant d.c. fields on the hysteresis loops of ferroelectric $\text{Bi}_4\text{Ti}_3\text{O}_{12}$ crystals. Journal of Applied Physics 35, No. 10: 3045-3046. October 1964.
34. Cummins, S. E. Switching behavior of ferroelectric $\text{Bi}_4\text{Ti}_3\text{O}_{12}$. Journal of Applied Physics 36, No. 6: 1958-1962. June 1965.
35. Pulvari, C. F. and de la Paz, A. S. Phenomenological theory of polarization reversal in ferrielectric $\text{Bi}_4\text{Ti}_3\text{O}_{12}$ single crystals. Journal of Applied Physics 37, No. 4: 1754-1763.
36. Pulvari, C. F. and Kuebler, W. Phenomenological theory of polarization reversal in BaTiO_3 single crystals. Journal of Applied Physics 29, No. 9: 1315-1321. September 1958.
37. Cummins, S. E. Ferroelectric domains in $\text{Bi}_4\text{Ti}_3\text{O}_{12}$ single crystals. Journal of Applied Physics 37, No. 6: 2510. May 1966.
38. Cummins, S. E. and Cross, L. E. Crystal symmetry, optical properties, and ferroelectric polarization of $\text{Bi}_4\text{Ti}_3\text{O}_{12}$ single crystals. Applied Physics Letters 10, No. 1: 14-16. January 1967.
39. Cummins, S. E. A new optically read ferroelectric memory. IEEE Proceedings 55, No. 8: 1536-1537. August 1967.
40. Cummins, S. E. A new bistable ferroelectric light gate or display element. IEEE Proceedings 55, No. 8: 1537-1538. August 1967.

41. Hamilton, D. Existence and origin of a polarization threshold field in bismuth titanate. *Journal of Applied Physics* 39, No. 1: 10-12. January 1967.
42. Cummins, S. E. and Cross, L. E. Electrical and optical properties of ferroelectric $\text{Bi}_4\text{Ti}_3\text{O}_{12}$ single crystals. *Journal of Applied Physics* 39, No. 5: 2268-2274. April 1968.
43. Cross, L. E. and Pohanka, R. C. A thermodynamic analysis of ferroelectricity in bismuth titanate. *Journal of Applied Physics* 39, No. 8: 3992-3995. July 1968.
44. Aizu, K. Possible species of ferroelectrics. *Physical Review* 146, No. 2: 423-429. June 1966.
45. Merz, W. J. and Anderson, J. R. Ferroelectric storage devices. *Bell Laboratory Record* 33: 335-341. September 1955.
46. Williams, Richard. Surface layer and decay of the switching properties of barium titanate. *Journal of Physics and Chemistry of Solids* 26, No. 2: 399-405. February 1965.
47. Taylor, G. W. Electrical properties of niobium-doped ferroelectric $\text{Pb}(\text{Zr}, \text{Sn}, \text{Ti})\text{O}_3$ ceramics. *Journal of Applied Physics* 38, No. 12: 4697-4706. November 1967.
48. Fousek, J. and Janovec, V. Orientation of domain walls in ferroelectrics. *American Physical Society Bulletin* 12, No. 6: 902. September 1967.
49. Miller, R. C. and Weinreich, G. Mechanism for the sidewise motion of 180° domain walls in barium titanate. *Physical Review* 117, No. 6: 1460-1466. March 1960.
50. Remaika, J. P. A method for growing barium titanate single crystals. *American Chemical Society Journal* 76, No. 3: 940-941. February 1954.
51. Merz, W. J. The electrical and optical behavior of BaTiO_3 single domain crystals. *Physical Review* 76, No. 8: 1221-1225. October 1949.
52. Sawyer, C. and Tower, C. Rochelle salt as a dielectric. *Physical Review* 35: 269-273. February 1930.

ACKNOWLEDGMENTS

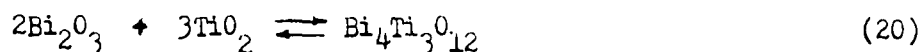
The author wishes to thank Dr. A. V. Pohm for suggesting the topic, for providing the support through the Solid State Affiliates Program, and for guiding the candidate in this research endeavor. The author also wishes to thank Dr. George Koerber for his many suggestions, for his helpful discussions and for reading the manuscript. The author also wishes to thank the Engineering Research Institute, the administrating agent of the Solid State Affiliates Program, for its helpfulness in locating and providing test equipment. The author wishes to acknowledge the participating corporations who were responsible for the funding of the program.

APPENDIX A: GROWTH TECHNIQUES FOR BISMUTH TITANATE

SINGLE CRYSTALS

General Techniques

Bismuth titanate is formed according to the equation



The reaction in the formation of single crystals takes place in the neighborhood of 1000°C . The basic methods utilized in growing these single crystals of bismuth titanate have been described by Van Uitert and Egerton (26), Pulvari (32), Cummins and Cross (42), and Tambovtsev, et al. (31). The general steps in each process are essentially the same. These steps are as follows:

- a) The chemical constituents, bismuth trioxide and titanium dioxide, are mixed thoroughly.
- b) The mixture is packed into a platinum crucible.
- c) The crucible and its contents are heated and a melt is formed.
- d) The melt is cooled and crystallization takes place.
- e) The crystals are then separated from the melt.

Each method differs somewhat and in order to present the specific details these basic methods are described below:

1) Method of Van Uitert and Egerton

Van Uitert and Egerton (26) utilized 100 grams of Bi_2O_3 and

5 grams of TiO_2 . The chemical ingredients were melted in a platinum crucible at a temperature of $1200^{\circ}C$. The melt was slowly cooled. On cooling, sheet like crystals running the width of the crucible were formed. The sheets were separated by intervening layers of Bi_2O_3 . These layers, however, were dissolved in a strong mineral acid, and the crystals were removed from the mixture. The resulting crystals were clear and slightly grayish in color, and were between 2×10^{-3} inches and 4×10^{-3} inches in thickness.

2) Method of Tambovtsev, Skorikov, and Zheludev

Tambovtsev, et al. (31) did not state the amount of each chemical constituent that was utilized. They did however give the heating and cooling rate that they used in the crystallization procedure. They utilized a heating rate of $40^{\circ}C$ /hour. The melt that occurred was held at a temperature greater than $1000^{\circ}C$ for a period of 24 hours. It was then cooled at a rate of $5^{\circ}C$ /hour. The crystals were then separated from the solvent, Bi_2O_3 , by use of a strong mineral acid. They concluded that the size of the crystals were limited mainly by the diameter of the crucible. The crystals that they grew formed in platelets which could be split like mica. The crystals were transparent with a slightly yellowish color, and they were between 4×10^{-3} inches and 20×10^{-3} inches in thickness.

3) Method of Pulvari

Cummins and Cross (42) described in detail a technique attributable to Pulvari (32). This method is referred to as the modified flux method.²² It called for a mixture of 4 parts TiO_2 and 96 parts Bi_2O_3 , by weight. The ingredients were ball milled and packed into a platinum crucible. The crucible was then heated to about $1100^\circ C$ and held at this temperature for about 16 hours. The melt was then cooled at a programmed rate of $10^\circ C/hour$ down to $940^\circ C$. At this point the excess flux was poured off. The crucible was then placed back in the furnace and was cooled with the power off to near room temperature. The remaining crystals were removed quite easily since most of the flux was poured off. After removal, the crystals were placed on a platinum wire grid and annealed by heating to $900^\circ C$. The crystals were cooled at a rate of $350^\circ C/hour$ - the furnace cooling rate. This annealing removed most of the 90 - degree - type of twinning present in the virgin crystals.

²²The pouring technique was originally utilized by Remeika (50) in growing barium titanate crystals.

Specific Technique

As was previously mentioned the crystals utilized in this investigation were grown by C. F. Pulvari and were purchased from the Electrocrystal Corporation. The crystals were packaged in a T O-5 can and were electroded as shown in Figure 3. A decision was made to grow a batch of these crystals so as to allow this author (a) to gain insight into the physical problems involved in growing these crystals, (b) to make a study of the physical nature of the virgin crystals, and (c) to make a study of the electrical properties of the virgin crystals.

The procedure utilized by this author in the growth of single crystals of bismuth titanate is outlined below:

- a) Bismuth trioxide (40 grams) and titanium dioxide (2 grams) were mixed and packed into a platinum crucible.
- b) The crucible and its contents were brought slowly up to a temperature of 932°C .
- c) The power to the furnace was then increased. (This yielded an approximate heating rate of $55^{\circ}\text{C}/\text{hour}$.)
- d) The crucible and its contents were then held at approximately 1100°C for a period of 18.5 hours.
- e) The power to the furnace was then decreased at specific time intervals. (This reduction yielded a cooling rate of approximately $7^{\circ}\text{C}/\text{hour}$.)
- f) The power to the furnace was then shut off after a temperature of 923°C was achieved, and the crucible and its contents

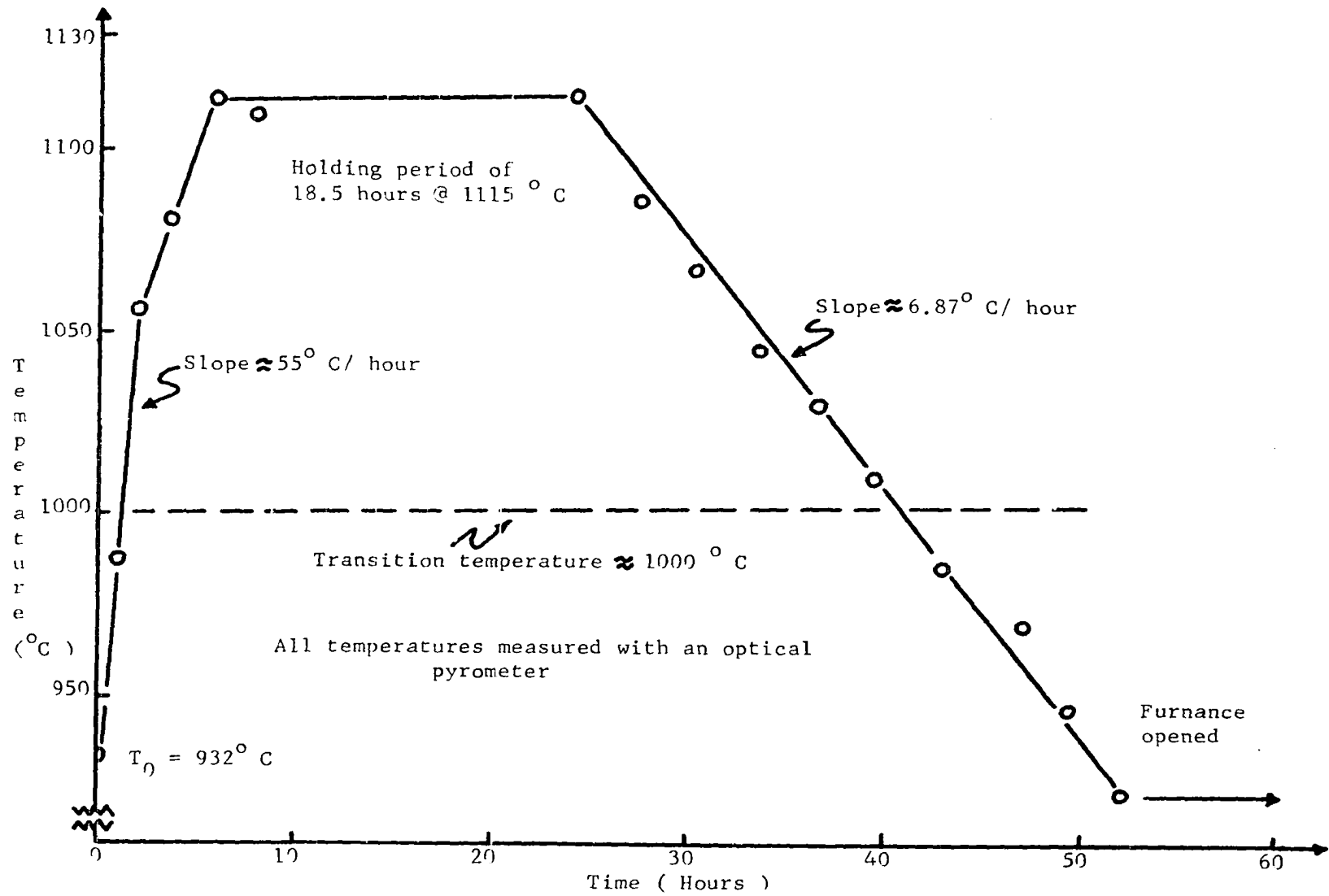
were allowed to cool in the furnace to a temperature of 40°C. The crucible was then removed from the furnace and was allowed to cool to room temperature. (A graphical representation of the described steps (a) through (f) is shown in Figure 28.

- g) Hydrochloric acid was then added in order to dissolve the intervening layers of solvent. After a prolonged soaking it was possible to remove the crystals from the melt.

The crystals obtained by this growth technique were in the form of platelets which were transparent but slightly yellow in tint. The thicker crystals could be split much like mica thus yielding thinner crystals with smoother surfaces. The best crystals retrievable were approximately .1 of a square inch in area and were between 6×10^{-3} inches and 12×10^{-3} inches in thickness. Additional batches were grown with the chemical constituents in the same ratio, but with faster rates of cooling. The resulting crystals were much thinner and smaller in area thus making them quite difficult to handle. It was thus concluded that the cooling rate governed the size of the crystals obtainable.

The modified flux technique was tried, but this author was unable to successfully remove the crucible and pour off the excess flux during the critical period of crystal formation. In each case the formation had already taken place and the flux was not liquid in nature. Exposing the melt to the atmosphere caused cracking of the surface layer of the melt. Since this author was capable of acquiring good crystals by splitting those obtained by the slow cooling method, no additional time was spent

Figure 28. Crystal growth temperature chart.



in trying to determine the optimum conditions necessary for successful crystal growth by the modified flux technique. Considering the quality of the crystals obtained, the growth technique utilized was considered by this author to be a success.

Characteristics Of Grown Crystals

A number of good quality crystals were selected from the yield and were electroded as illustrated in Figure 29a. In order to examine the switching characteristics of a test crystal, a 1 K ohm resistor was placed in series and the combination was driven with a transformer output as illustrated in Figure 29b. At first, the resulting current waveform did not show any "spikes" - the presence of which indicates polarization reversal. However, after several minutes of cycling the "spikes" began to appear. A typical current response along with the driving voltage is shown in Figure 30a. This unusual effect corresponds to hysteresis appearing after continued cycling of a material which initially showed a lack of hysteresis.

To observe the hysteresis loop, a scheme as is described in Appendix B was employed. It was observed that the loops did not begin to open until the crystals were cycled for a period of several minutes and that with continued cycling the loops soon opened fully. Utilizing the scheme of Appendix B, the hysteresis loop for the situation shown in Figure 30a was observed. The loop is shown in Figure 30b. Two additional steady state hysteresis loops are shown in Figure 31. Note that the upper loop is nearly symmetrical while the lower loop shows a shift along the field

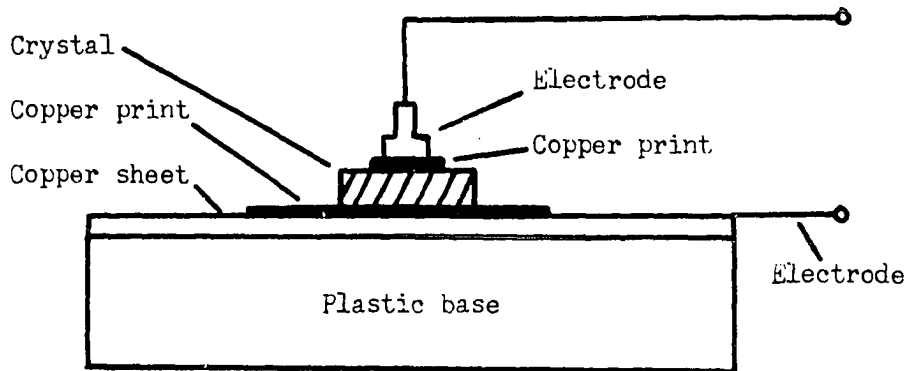


Figure 29a. Diagram of electroding scheme.

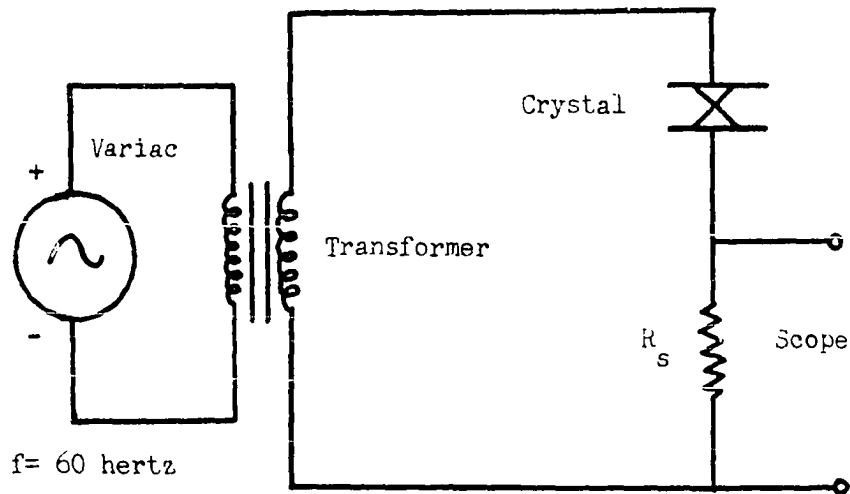


Figure 29b. Test circuitry for examination of the response of a crystal to sinusoidal excitation.

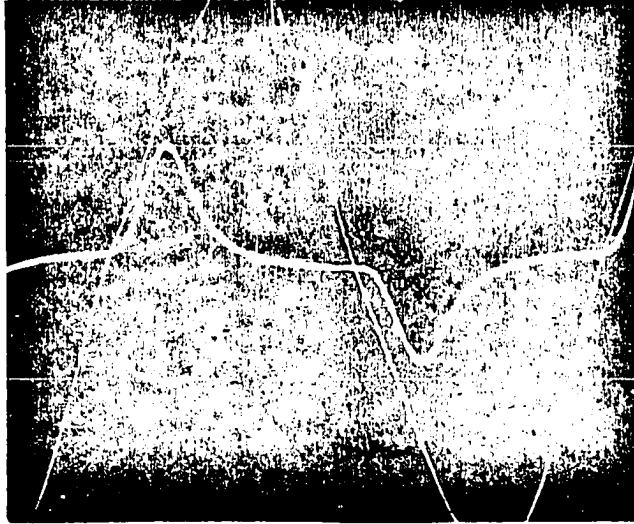


Figure 30a. Typical current response of a test crystal due to sinusoidal excitation. Scales: Time - 2ms/cm; Current - 100×10^{-6} amps/cm; Voltage - 100 volts/cm.

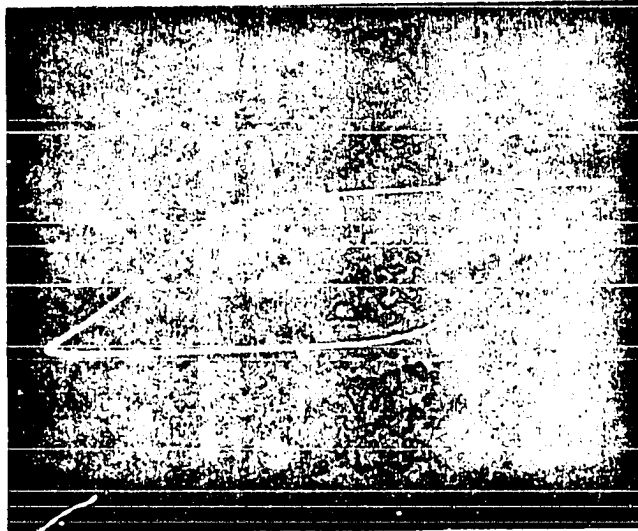


Figure 30b. Hysteresis loop derived from tracing voltage output of integrator versus applied voltage for the situation shown in Figure 29a. Scales: Horizontal - 100 volts/cm; Vertical - 5 volts/cm.

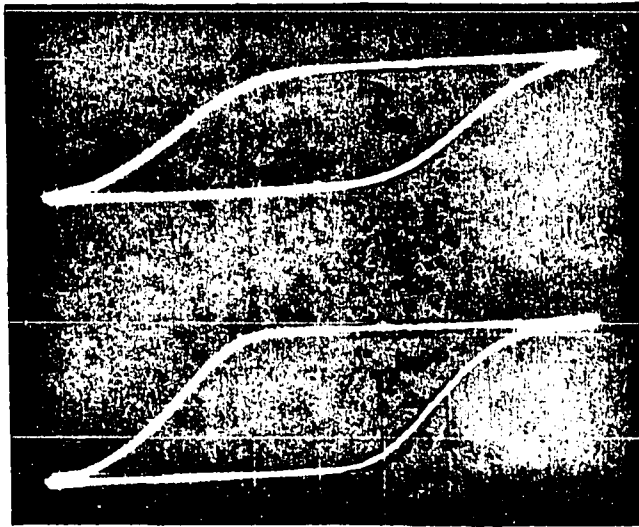


Figure 31. Typical hysteresis loops derived from tracing voltage output of integrator versus applied voltage for two bismuth titanate single crystals. Scales: Same as Figure 30b.

axis thus indicating a fixed internal bias is present.

This effect of the opening of the loop following cycling was first noted by Merz (51) in his examination of single domain crystals of BaTiO_3 . He attributed this effect to macroscopic domain clamping. In his investigation he found that the loops opened faster if the crystals were heated. Pulvari (32) noted that the loops of bismuth titanate also opened faster if the crystals were heated. Cummins (34) speculated that just as was the case with barium titanate the lack of hysteresis might be due to macroscopic domain clamping, but he also suggested that the opening of a loop might depend upon relocation of compensating charge which occurs faster at higher temperatures due to the increase in conductivity.

It is possible to calculate from the hysteresis loop the magnitude of the z component of the polarization. For example, consider the lower loop shown in Figure 31. For this situation the series resistance for the test circuit in Appendix B was 500 ohms, and the electrode diameter was measured as 1/8 inch. The amount of charge switched when the polarization reverses can be determined by measuring the corresponding change in output voltage from the hysteresis loop and using this value in Equation 33. The amount of charge reversed is equal to $2P_zA$. For this example the value of the z component of the polarization was determined to be $3.75 \text{ coulombs/cm}^2$. This value compares favorably with the value of 4 coulombs/cm^2 reported by Cummins and Cross (42).

The purpose for the growth of these crystals was considered to be achieved. However, it was decided to proceed one step further and ob-

serve the switching characteristic of a typical grown crystal. First, a crystal was selected from the yield and electroded in a fashion similar to that shown in Figure 29a. It was then cycled with a sine wave of voltage until the loop was fully opened. The test crystal was then polarized and immediately interrogated. The resulting current versus applied voltage response yielded a threshold level of 100 volts - a reasonable value considering the thickness of the crystal being tested. To check for the possible formation of an internal bias field, the crystal was again polarized but was allowed a stabilization period of 10 minutes prior to interrogation. The interrogation response of current versus applied voltage yielded a new threshold value of 150 volts. Thus, the characteristic of a threshold switching field and the characteristic of the formation of an internal bias field following polarization compare favorably with the identical characteristics for the purchased crystals.

APPENDIX B: HYSTERESIS LOOP ANALYSIS
OF FERROELECTRICS

Standard Procedure

A most common method for measuring the saturation polarization P_s , and for observing the hysteresis loop of a dielectric is to use some modification of the standard circuit presented by Sawyer and Tower (52) and shown in Figure 32. The magnitude of the capacitance of the linear condenser is selected to be large compared to the crystal capacitor. The linear capacitor must also have a low leakage, and it must be large in magnitude compared to the crystal capacitance. Therefore, the voltage along the horizontal axis represents the applied voltage to the crystal under test. As the crystal is cycled, the polarization reverses and this reversal corresponds to a change in charge of $2P_sA$. This change in charge produces a change in voltage of $\Delta V = \frac{2P_sA}{C_0}$ across the linear condenser C_0 . This voltage is applied to the vertical plates of the oscilloscope. Thus, the polarization can be related to the intercept along the vertical axis, and the coercive field can be related to the intercept along the horizontal axis. The frequency is a variable, but the loops are generally observed at a frequency of 60 hertz.

Loop Display Using An Operational Amplifier

The hysteresis loops displayed throughout this investigation were obtained, not by the standard technique explained in the previous section

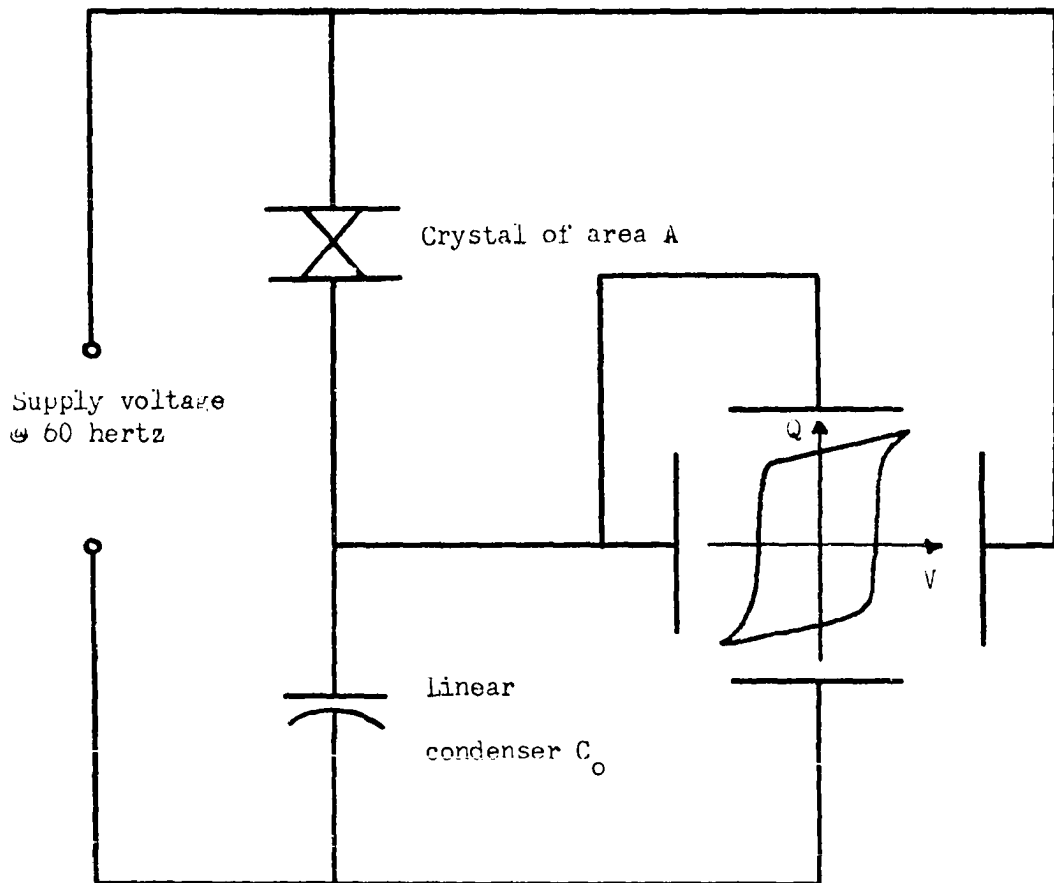


Figure 32. Sawyer and Tower (52) circuit for displaying the hysteresis loop of a ferroelectric crystal.

but by a technique devised by this author. The technique requires the use of an operational amplifier. The operational amplifier, an Analog III, used in this situation is a low cost device. The circuit diagram of the equipment used to observe the hysteresis loops is shown in Figure 33.

To understand the operation first consider the connections of the impedances as shown in Figure 33. The gain for such a connection is given by

$$G = \frac{e_o}{e_i} = \frac{Z_i + Z_f}{Z_i} \quad (21)$$

With

$$Z_i = R_1 \quad (22)$$

and

$$Z_2 = R_2 \parallel \frac{1}{sC} \quad (23)$$

the gain expression can be written as

$$G = \frac{\frac{R_1 + R_2}{R_1} + sC_2R_2}{1 + sC_2R_2} \quad (24)$$

Now letting $s = j\omega$ the gain expression becomes

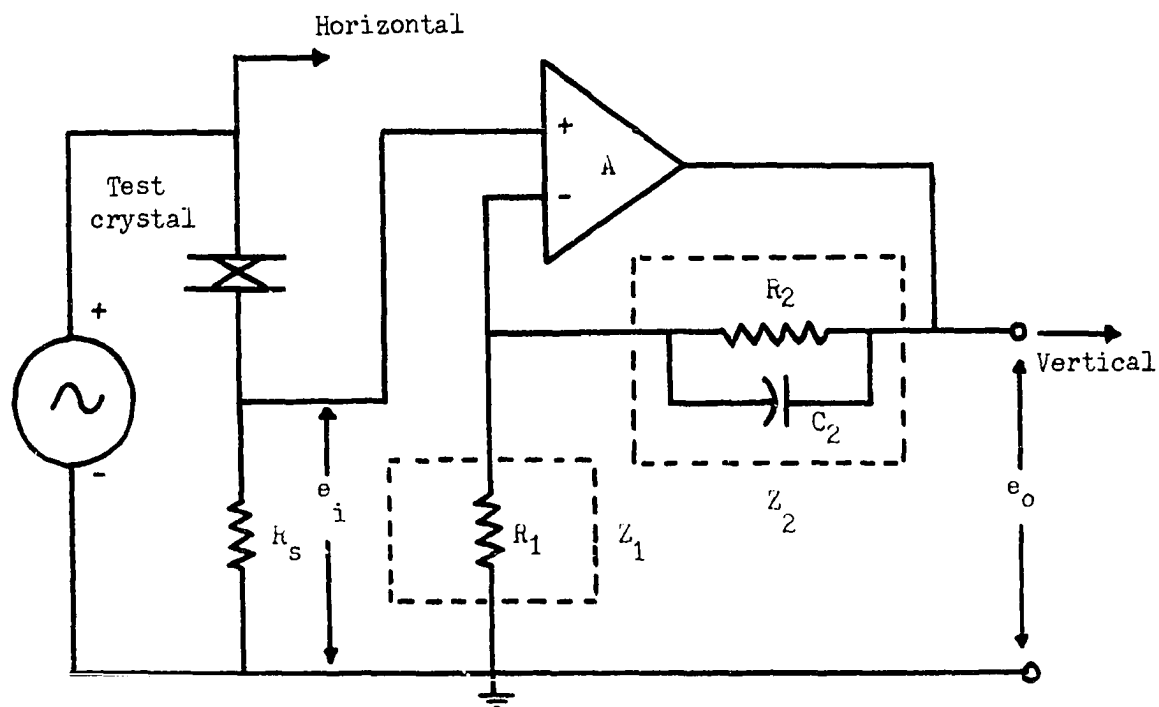


Figure 33. An integrating circuit for displaying the hysteresis loop of a ferroelectric crystal.

$$G = \frac{\frac{R_1 + R_2}{R_1} + j\omega C_2 R_2}{1 + j\omega C_2 R_2} \quad (25)$$

Assuming

$$1 \ll \left| j\omega C_2 R_2 \right| \ll \frac{R_1 + R_2}{R_1} \quad (26)$$

the gain expression becomes

$$G = \frac{R_1 + R_2}{j\omega R_1 R_2 C_2} \quad (27)$$

which can be written as

$$G = \frac{R_1 + R_2}{C_2 R_1 R_2} \frac{1}{j\omega} \quad (28)$$

Thus integration is possible if the conditions in Equation 26 are met.

For a typical set of values consider $R_1 = 1K$, $R_2 = 10 \times 10^6$,
 $C_2 = .03 \times 10^{-6}$, $R_s = 10K$, and $\omega = 377$.

Then

$$1 \ll \left| j 113.1 \right| \ll 10,001 \quad (29)$$

and

$$G = \frac{e_o}{e_i} = 33,336 \frac{1}{j\omega} . \quad (30)$$

Now

$$e_o = 33.336 \times 10^3 \int e_{in} dt . \quad (31)$$

but

$$e_{in} = i R_s , \quad (32)$$

so

$$e_o = 33.336 \times 10^3 R_s \int i dt . \quad (33)$$

The integral in Equation 33 of course represents the charge switched, and thus the output voltage of the operational amplifier is proportional to the charge switched. The output can be placed on the vertical axis of an oscilloscope, and the applied voltage on the horizontal axis with the resulting trace being a charge versus voltage plot. From the displayed loop it is possible then to relate the intercept along the vertical axis to the polarization and to relate the intercept along the horizontal axis to the coercive field.

Using (a) the relationship

$$A(e_{in} = e_x) = e_o . \quad (34)$$

(b) the relationship

$$e_o = \frac{Z_i + Z_f}{Z_i} e_{in} \quad (35)$$

and (c) the nodal expression

$$i = e_x \left(\frac{1}{Z_i} + \frac{1}{Z_f} \right) - \frac{e_o}{Z_f} \quad (36)$$

it can be shown that the input impedance is given by

$$Z_{in} = - \frac{A Z_i^2 Z_f}{(Z_i + Z_f)^2} \quad (37)$$

Utilizing the assumed values for Z_i and Z_f the impedance expression reduces to

$$Z_{in} = -j 10.31 A \quad (38)$$

A is the open loop gain which is approximately 30,000 for this operational amplifier. Therefore the input impedance is highly capacitive in nature, and its reactance is extremely high so that when paralleled with the series resistance of $R_s = 10K$ no loading effect is noted.

It is concluded that these are two attractive features if this type

of arrangement is employed in displaying hysteresis loops of dielectrics.

These features are as follows:

a) Sensitivity -

The output voltage is related to the charge switched, $\int i dt$, by a high gain constant. Thus, a relatively small change in charge results in a considerably large change in output voltage.

b) High input impedance -

The input impedance is extremely high for this connection and thus the measurement technique does not result in any loading of the test circuit.